Addis Ababa University
Addis Ababa Institute of Technology
School of Mechanical and Industrial Engineering

Simulation and Experimental Investigation of Continuous Biochar Production from Flower Waste

By

Geremew Nigussie

Msc Thesis

A thesis Submitted to Addis Ababa University Institute of Technology School of Mechanical and Industrial Engineering in partial Fulfilment of the Requirements for the Degree of Masters of Science in Thermal Engineering

October 2018

Addis Ababa, Ethiopia

Addis Ababa University
Addis Ababa Institute of Technology
School of Mechanical and Industrial Engineering

Simulation and Experimental Investigation of Continuous Biochar Production from Flower Waste

By

Geremew Nigussie

Approved by Board of Examiners

Dr.Ing Wondwossen Bogale		
Advisor,	Date	Signature
Dr. Abdulkadir Aman		
Thermal Engineering Chair	Date	Signature
Dr. Kamil Dino		
Internal Examiner,	Date	Signature
Dr. Ing Demiss Alemu		
External Examiner,	Date	Signature
Dr. Yilma Taddese		
Dean of SMIE,	Date	Signature
Dr. Ermias Tasfaye		
Director of Post Graduate Program,	Date	Signature

Declaration

I, the undersigned, declare that this thesis entitled *"Simulation and Experimental Investigation of continuous biochar production from flower waste"* is my original work under School of Mechanical and Industrial Engineering, AAiT, and has not been submitted by any other person for an award of a degree in this or any other University, and that all resources of materials used for this thesis have been duly acknowledged and a list of references is given.

Name:

Geremew Nigussie Bedada _____ _____

Signature Date

This thesis has been submitted to the Addis Ababa University with my approval as the University Advisor.

Advisor:

Dr.Ing Wondwossen Bogale _____ _____

Signature Date

Table of Contents

List of figures

List of tables

Lists of acronym, symbols, units and abbreviation

$\bar{\sigma}_1$	Stress acting in the arch at
ΔP_r	Pressure gradient
ρ_b	Bulk density of the biomass
g	Acceleration due to gravity
a	Acceleration
a_c	Convergence components
a_v	Component due to velocity increase
B	Hopper opening
$B_{\min}$	Minimum hopper opening
ff	Flow factor
FF	Failure function
ff_a	Actual flow factor
V	Discharge velocity of flower waste
V_a	Average terminal velocity
m_c	Constant value for different geometry
L	Slant height of hopper
S_1	Circumferences of the upper diameter
S_2	Circumferences of the opening diameter
P_d	Diameteral pitch
N	Number of gear teeth

m	Number of Module of gear
V_p	Pitch line velocity of gear
VR	Velocity ratio
N_1	Input speed from motor
N_2	Output speed on pulley
(2β)	Angle for V-belt
ρ_{bm}	Density of belt material
$(\sigma_{all,belt})$	Allowable stress for belt material
$x_{\max}$	Maximum centre distance of belt
D	Diameter of larger pulley
d	Diameter of smaller pulley
α	Coefficient of friction in belt selection
θ_1	Angle of contact on small pulley
θ_2	Angle of contact on larger pulley
μ	Coefficient of friction for belt material
V_b	Velocity of belt
m_b	Mass of belt material
F_c	Centrifugal force for belt
$R\delta\theta$	Small element length for belt design
T_c	Tension in the belt due to centrifugal effect
T	Total tension in the belt

T_1	Tension 1 in belt
T_2	Tension 2 in belt
MPa	Mega Pascal
KW	Kilowatt
τ_{all}	Allowable shear stress
T_t	Torque transmitted by shaft
W_f	Weight of the flight
W_p	Weight of pulley
W_{df}	Vertical load on the pulley from belt and pulley
F_y	Y components forces
M	Bending moment
T_e	Equivalent twisting moment
d_s	Diameter of the shaft
B_p	Width of the pulley
t	Thickness of the pulley
C_o	Static load on bearing
C	Dynamic load
W_e	Equivalent radial load
W_R	Radial load
W_A	Axial load

Y_o	Radial load factor
X_o	Axial load factor
L	Rating (or service) life of ball bearing
(L_H)	Life working hours
V_o	Volume of outer reactor
V_i	Volume of inner reactor
d_i	Diameter of inner reactor
d_o	Diameter of outer reactor
r_i	Radius of inner reactor
r_0	Radius of outer reactor
L_i	Length of inner reactor
L_o	Length of outer reactor
$V_{\max,gas}$	The maximum volume of the gas
$M_{flower.Wast}$	The mass of flower waste
C	Radial clearance between screw and tubing
D	Screw diameter
D_c	Shaft diameter
P_s	The screw pitch
t_s	Thickness of the screw flight
ω	Angular velocity

V_{cs}	Conveyor speed
n_{sc}	Revolutions per minute of screw (screw rotating speed)
p_s	Is screw pitch
GPa	Giga Pascal
kg	Kilogram

Acknowledgement

First of all my gratitude goes to the Almighty God for his positive will and help. Second I would like to thank my advisor Dr.Ing Wondwossen Bogale, for giving me the opportunity to conduct this research work under his supervision. His excellent guidance, follow-up and advice throughout all phases of my research activities motivated me in my efforts.

I also express my deep appreciation to individuals and organization that helped me through my work, to Addis Ababa University Chemistry Department and Geological Survey of Ethiopia for their crucial help during laboratory test on flower waste characterization.

I am especially indebted to express my special thanks to all Addis Ababa Institute of Technology Workshop workers for their technical support.

Finally, special thanks to all my friends who have supported and encouraged me.

Abstract

Pyrolysis plays a major role in investigation of continuous biochar production from flower waste. It is a thermal decomposition processes that occurs at moderate temperatures in which the biomass is slowly heated in the absence of oxygen or air to produce biochar.

Once the flower have been harvested its waste is usually thrown away without consideration for other uses. Freesia Ethiopia Plc. is one of the flower producer in Ethiopia located in Sululta. It produces approximately 700kg waste per day. This waste is thrown away to the field without considering for other use. As fossil fuel is depleting, there is an urgent need to exploit any type of biomass as renewable sources by converting them to various forms of green fuels such as biochar.

The main objective of this research is to use simulation and experimental investigation of continuous biochar production from flower waste. The simulation is done by modelling two reactors the inner and outer and simulating the temperature distribution along the length of the reactor and energy flows through them.

The overall methods used for this research paper is described as follows. First feed stock collection, preparation, its ultimate and proximate analysis i.e. characterization has been performed. Second, the three dimensions of the reactor with the screw conveyor is modelled using CATIA software and then imported in COMSOL5.0. Then after temperature profile along the length of reactor has been simulated to study temperature distribution. Subsequently, heat flux were added to investigate the temperature profile on the reactor and product yields. Finally, manufacturing and experimental investigation was conducted. Using slow pyrolysis process great biochar yields could be produced for the experiment conducted with the pyrolysis temperature of 293^{o}C to 773 ^{o}C at heating rate of 50 ^{o}C/min. An original screw reactor machine which has a capacity to produce 470 kg biochar per day in continuous operating mode was designed, manufactured and tested. This findings support the potential to prepare biochar from flower waste by slow pyrolysis processes.

Key words

Slow pyrolysis, Biochar, screw reactors

1. Chapter 1: Introduction

1.1. Background of the research

Biomass is a very abundant, various and inexpensive resource in the world. It is considered as one of the most plenty and well-utilized sources of renewable energy. Compared to fossil fuels, energy obtained from biomass has been paid a great deal of attention in recent years due to the problem of environment pollution and energy shortage. As a result it is an important renewable source contributing to the world's budget, sustainably and energy security. In developing countries, the use of biomass is of high interest as these countries have economy largely based on agriculture and forestry [1].

The agricultural sector generates an abundance of agricultural wastes such as wheat and barley straw, coffee husks, flower waste, maize straw; corn straw while much research has been carried out to utilize agricultural wastes for value-added products, its continuous production is not well-known. This wastes are handled in Ethiopia as something that causes problems. Here most of the agricultural waste is returned to the field as much to maintain land fertility. As fossil fuel is reducing, there is a crucial need to exploit any type of biomass as renewable sources by converting them to various useful forms of green fuels. Technologies to transform biomass into bioenergy vary from normal combustion to thermal processes requiring higher temperature and pressure such as pyrolysis and gasification. The thermochemical conversion of biomass includes combustion, liquefaction, gasification and pyrolysis.

Pyrolysis is a thermal decomposition processes that occurs at moderate temperatures in which the biomass is rapidly heated in the absence of oxygen or air to produce biochar and gases. It is one of the most recent renewable energy processes and promises high yields of biochar with a minimum of condensable bio-oil and gases if it is carefully controlled. The yields and composition of end products of pyrolysis are extremely dependent on types of biomass, chemical and structural compositions of biomass and other physical parameters such as temperature, heating rates, pyrolysis mode, reactor type, particle size and others.

Biochar, a by-product of biomass pyrolysis for energy, is being supported for its potential large-scale and low-cost carbon sequestration in soil. Much of the knowledge regarding Biochar drives from studies of Terra Preta soils in the Amazonian basin [2], where Biochar –like materials appear to have substantially altered soil physical and chemical properties and lead to long lasting carbon storage and improved crop production. It is produced by biomass pyrolysis,

a process whereby organic substances are broken down at a temperatures ranging from 350˚C to 1000˚C in a low oxygen thermal process.

Biochar has recently received significant attention in research because it is carbon rich and resistant to biodegradation [3]. Biochar production from flower waste is generated in continuous feeding and discharging in to biochar plants through a process called pyrolysis occurring in the reactor. Flower wastes will create significant waste management problems unless properly managed. However, there are not well-established methods to manage the waste generated during the processing of flower harvesting in Ethiopia. Pyrolysis can be an attractive option not only for the management of flower wastes but also producing renewable energy in the form of solid biochar. This study investigates continuous biochar production from flower wastes by using pyrolysis technology. The end product is biochar which is a mixture of minimum bio-oil and gases. Biochar is a useful renewable energy source. However, there has no report on applying continuous biochar production from flower wastes.

In this paper, continuous biochar production from flower waste is a technology which owns many attentions in the world will be discussed. The agricultural waste which is accumulated every-year in Ethiopia is around 85% and its disposal is very difficult [1]. To make use of the agricultural wastes effectively and economically favourable, an alternative method of the producing biochar is the pyrolysis.

Flower waste is continuously fed from the feed hopper by the help of screw feeder into a cylindrical inner reactor. The waste is then heated indirectly from combustion chamber and pyrolyzed to produce biochar. The produced biochar is removed from the inner reactor by screw conveyor.

1.2. Relevance of the research

The continuous biochar production process is energy efficient and gives an even production of the products pyrolysis gas and biochar [4]. The most benefit of this technology is that operating the pyrolysis plant takes very little effort. It is easy to produce heat, biochar and the plant does not need to cool down in order to take in more material. The advantage of produced biochar from flower waste is ,it offers not only an attractive solution for reducing air pollution from open burning of this waste, but also as fuel for cooking and heating as it burns without either smoke or flame. Production of biochar from flower waste in general, has a potential to be used as alternative fuel.

1.3. Advangates and drawback of the technology

1.3.1. Advantage of the technology

The most benefit of this technology is that operating the pyrolysis plant takes very little effort. They are easy to design and manufacture, and there is no need to use inert carrier gas [5]. It is easy to produce heat, biochar and the plant does not need to cool down in order to take in more material.

1.3.2. Drawback of the technology

Compared to others types of reactor, plugging risks, moving in hot zone and heat transfer at large scales are major drawbacks.

- Mechanics of conveying and mixing are found to complex system
- Expensive more than batch type reactor.

1.4. Important pyrolysis process parameters

The thermo-chemical decomposition of biomass in inert atmosphere is dependent on various process parameters such as temperature, mass flow, type and particle size, pressure, moisture content [6]. Below some of these important process parameters are briefly discussed.

1.4.1. Temperature

The top temperature has a direct effect on the carbon production and the biochar characteristics. Higher temperature gives less biochar in all types of pyrolysis reactions. With a higher temperature you can imagine that the more volatile material is forced out of the biomass and therefore the amounts of biochar decreases. On the other hand the level of carbon in the char increases [4].

1.4.2. Mass flow (feed flow rate)

The mass flow of material input, char and pyrolysis gas out put in the pyrolysis process together with the reactor temperature affect the heat transfer rate [4].

The heat transfer rate means how quickly heat moves through the material and thereby starts the pyrolysis process in every particle. The gas flow rate in the reactor is the speed of which the pyrolysis gas flows out of the pyrolysis plant. The gas flow rate affects biochar production. Low gas flow rates give a larger biochar production and is refered to as slow pyrolysis while high gas flow rates are referred to as fast pyrolysis.

1.4.3. Particle size

The size of the particles in the material is adjusted depending on what kind of char you want to produce and it also affects the heat transfer rate in the biomass. Larger particles give more char and small particles give more bio oil. The size of the flower waste has been reduced by making use of jaw crusher for this research.

1.4.4. Pressure

High pressure increases the gas flow rate in and on the surface of the particles, which give a secondary carbonization. For this study pressure was kept constant.

1.4.5. Moisture content

The moisture content in the material can have different effects on the production of biochar and pyrolysis gas depending on the enviroment in the reactor. Under pressure the process gives more biochar if the moisture content is low. The moisture content affects the biochar final characterics. By regulate the moisture content you can produce active carbon which has specific structural characteristics. The collected flower waste dried to remove the moisture content and its content is measured while the experiment was conducted.

1.6. Delimitation

To achieve an advanced process for improving product yields from pyrolysis of selected biomass, flower waste, in-depth investigations on heating methods are needed. Handling three phases of material i.e. including multiphase using COMSOL 5.0 software was not achieved due to computer limitation.

1.7. Problem statement

The agricultural sector generates an abundance of agricultural biomass such as wheat and barley straw, coffee husks, leaves, chat waste, manures and woods, while much research has been carried out to utilize agricultural biomass for value-added products, its continuous production is not well-known. Most Ethiopian farmers, after yields have been harvested, and further processed into other products, the waste is usually thrown away without consideration for other uses. Freesia Ethiopia Plc. is one of the flower producer in Ethiopia located in Sululta. The company produces approximately 700kg flower wastes per day. Here the flower waste was collected at one place and it will be burned without consideration for the other uses. These wastes can also be processed into other forms so they become useful as well. Solids waste management or waste minimization is encouraged to ensure that the environment is not polluted. Most of the agricultural waste is returned to the field as much to maintain land

fertility. As fossil fuel is reducing, there is a crucial need to exploit any type of biomass as renewable sources by converting them to various forms of green fuels such as biochar. Technologies to transform biomass into biochar vary from normal combustion to thermal processes requiring higher temperature and pressure such as pyrolysis. Therefore, continuous biochar production from flower waste is found to be best alternative for all stated problems.

1.8. Objectives

1.8.1. The main objective

The main objective of this research is simulation and experimental investigation of continuous production of biochar from flower waste.

1.8.2. Specific objective

The purpose of this research is to produce biochar by continuous production mode from flower waste. This is done by designing two reactors the inner and outer and simulating the temperature profile and energy flows through them. In doing so the following points are emphasized as specific objectives.

1. Feed stock characterization and its analysis.
2. Design of components and size of the reactors.
3. Heat transfer analysis on the screw reactors.
4. Simulation using COMSOL 5.1.
5. Manufacturing of prototype.
6. Experimental investigation.

1.9. Scope of Study

This thesis work is to use simulation and experimental investigation of continuous biochar production from flower waste. The heat transfer analysis on the reactor analysed experimentally and by simulation tools. Cooling mechanisms during biochar production was not included in this thesis work.

1.10. Thesis Organization

This study deals simulation and experimental investigation of continuous biochar production from flower waste. It has eight chapters. The chapters are organized as follows: Chapter two discusses existing literatures on previous work on pyrolysis in general and specifically slow pyrolysis. Chapter three presents' methods and material needed. Chapter four tells design of components for continuous biochar production machine. Chapter five discusses heat transfer analysis on reactors and modelling the flower waste pyrolysis. Chapter six tells experimental investigations. Chapter seven discusses the results and discussions. Chapter eight concludes with a summary and recommendation for future work.

2. Chapter 2: Literature Review

2.1. Literature on definition of biochar

The International Biochar Initiative (IBI) defines Biochar as the carbon rich when biomass, such as wood, manure or leaves, is heated with little or no available oxygen produced with the intent to be applied to soil as a means to improve soil health, to filter and retain nutrients from permeating soil water, and to provide carbon storage [7].

It can be also defined as; biochar is the carbon rich product obtained when biomass, such as agricultural wastes, is heated with little or no available air [8].

Biochar is defined as the solid carbon reach product that continuously produced when biomass such as agricultural wastes are heated in an oxygen deficit system. Biochar is created during pyrolysis and to a minor extent from gasification and imperfect combustion processes. Biochar can be applied to soil as a means to improve soil health, to filter and retain nutrients from percolating soil water. It is claimed to provide a means sequester and remove carbon from the atmosphere when applied as a soil amendment that stores carbon and reduces emission from soils of strong greenhouse gases such as nitrous oxide and methane [9].

2.2. Literatures on Advantages of Biochar

Biochar reduces climate change caused by emissions CO_2 and other greenhouse gases. Biochar is a way for carbon to be drawn from the atmosphere and is a solution to reducing the global impact of farming and in reducing the impact from all agricultural waste.

In general, the popular value of Biochar produced discussed is 1. Soil improvement 2. Carbon sequestration, 3. Carbon-neutral energy production 4. Waste management and 5. Water quality production through more efficient nutrient utilization [10].

2.3. Literature reviews on the Topic:

Mathieu et al., 2013: they studied Authermal *and allothermal Pyrolysis in a continuous fixed bed reactor.* The objective of their study was;1)To develop a new original fixed bed reactor at pilot scale to investigate continuous fixed bed pyrolysis either in allothermal or Authermal operation mode. 2) To study the influence of an oxidizing atmosphere on the thermal behaviour of a fixed bed designed for wood chips. 3) To measure the yield and composition of char, permanent gases, and condensable products at the outlet of the pyrolysis fixed bed, in two operating modes. The main conclusion during Authermal pyrolysis in a fixed bed conditions, the presence of oxygen promotes oxidation of volatile matter and cracking reactions, thereby

increasing production of pyrolysis water and parameter gases. They observed a significant increase in yields of CO_2 and CO, while the yield of char remained comparable to that in allothermal experiment. Heat comes from outside the fixed be (wall heating, hot exhaust gases), pyrolysis is called *allothermal.* When heat is generated by partial oxidation the wood itself, pyrolysis is called *autothermal* (or oxidative) [10].

Thiago et al., 2014: they studied *mass and energy balance of the carbonization of babassu nutshell as affected by temperature* in which the objective of their work was to evaluate the carbonization yield of babassu nutshell as affected by final temperature, as well as energy losses involved in the process. Despite the considerable supply of babassu nut and the demand for charcoal from iron industries in the North and Northeast of Brazil, there are few studies related to the feasibility in the use of this raw material for that purpose [11].

Abhishek et al., 2015: *they studied biomass Pyrolysis-a review of modelling, process parameters and catalytic studies*. The main aim of their review was to identify knowledge gabs for further research and opportunities for integration of biomass pyrolysis models of disparate scales. Models for the hydrodynamic behaviour of particles in pyrolysis, and their interaction with the reactive flow and the effect on the performance of the reactors have also critically analysed. The operation of a pyrolysis process depends on several parameters such as the feedstock and reactor conditions that lead to the formation of products in different proportions. The review discusses the kinetics, particle, reactor scale models for studying biomass pyrolysis and focuses on the effect of important parameters such as temperature, particle size, and density on the biomass degradation mechanisms. Phenomenological as well as CFD models have been used to study the biomass pyrolysis in various reactor configurations for analysing the effect of process parameters on the reactor hydrodynamics and the product yields. Therefore, more research and development effort is needed to design industrial – scale pyrolysis reactors [6].

Muhammad et al., 2016; *they studied on Co-production of Biochar, bio-oil and syngas from halophyte grass (Achnatherum splendens L) under three different pyrolysis temperatures* to investigate the characteristics of Biochar, bio-oil and syngas. The objective of this study was 1) to investigate the effect of pyrolysis temperature on the production of Biochar, bio-oil and syngas. 2) Determine the properties of the Biochar, bio-oil and syngas, 3) and evaluate their potential as an energy source or soil amendment. Achnatherum splendens L is a natural perennial halophytic grass with high resistance to drought, cold, alkali and salt and has enormous roots and high above ground biomass and cellulose but low lignin content. Biochar

is a by-product of biomass pyrolysis and usually characterized as rich in recalcitrant C, with a large surface area, and diverse groups [12].

Muhammad et al., 2016; The authors indicated that further studies were required to optimize the conditions to produce a biochar with unique properties and increase the potential to adsorb contaminants and sequester C. The pyrolysis process was conducted at 300,500 and 700˚C for a 2hour residence time in a fixed – bed pyrolysis system under a pure nitrogen atmosphere. The systems consists of pyrolyzer, a condenser, a bio-oil trap, a coolant circuiting unit, a heater controller, a data logger, and carrier gas supply. The pyrolyzer was composed of an electric heater and stainless steel reactor with an inner diameter 80mm and height of 1.3m. Heating values were determined by bomb calorimetry. To summarize their study indicate Biochar yield from pyrolysis of Splendens L. decreased and syngas yield increased as pyrolysis temperature was increased. Maximum bio-oil yield was obtained at 500 ˚C. These preliminary results show that A. splendens L. biomass is useful for producing Biochar and bioenergy [13].

Gao et al., 2015; they studied *Continuous pyrolysis of pine sawdust at different pyrolysis temperatures and solid residence times* was performed with a screw reactor to investigate the influence of pyrolysis temperature and solid residence time on products and energy distribution. CO was the dominating composition at pyrolysis temperature between 600 and 900 ˚C with solid residence time ranging from 3 to 7 min. The combustion kinetics of Biochar had been analysed by thermo gravimetric (TG). The results of gas chromatograph showed that CO is the main component in produced gas, and the maximum gas yield of 54.5% was obtained at temperature of 900 ˚C. The activation energy of biochar combustion is 461.10kJmol^{-1} and 108.45% kJmol^{-1} in the ranges of 290 ˚C to 314 ˚C and 314 ˚C to 518 ˚C respectively [14].

Tao et al., 2016; they studied *Lignocellulosic biomass pyrolysis: A review of product properties and effects of pyrolysis parameters.* The aim of their paper was to review the properties and applications of pyrolysis products, as well as the effects of pyrolysis parameters on biomass pyrolysis product yields and properties. Depending on the heating rate and residence time, biomass pyrolysis can be divided into three main categories slow (conversational), fast and flash pyrolysis mainly aiming at maximising either the bio-oil or Biochar yields. Biomass pyrolysis generally follows three step mechanism comprising of dehydration, primary and secondary reactions. They showed that a number of parameters affect the biomass pyrolysis process, yields and properties of products such as biomass type, retention time, reaction

atmosphere, temperature and heating rate. Also, provided are a review of the parameters that affect biomass pyrolysis and a summary of the state of industrial pyrolysis technologies [15].

Michael et al., 2016; they investigated the *impact of Biochar on the anaerobic digestion of citrus peel waste.* Batch type process has been used. They well established that the addition of black carbon, including Biochar, to contaminated soil and sediments can reduce the mobility and bioavailability of potential toxic chemicals. However, to the author's knowledge, the impact of Biochar on the performance of anaerobic digestion and methanogensis has not been reported. Citrus peel has an inhibitory effect on anaerobic digestion. They found that the presence of Biochar had two effects: a reduction in the length of the lag phase and greater production of the methane relative to citrus peel waste only incubations. The microbial lag phases decreased with increase in citrus peel to Biochar ratios, with 2:1 having the longest lag phase of 9.4 days and 1:3, the shortest, with the value of 7.5 days [16].

Ronsse, 2013; screw pyrolysis reactors for carbonization operate on a similar principle, except that the biomass is transported through the heated reactor zone by means of rotating, helical screw. Rotating screw reactors are characterized by transport of the solid material being near plug flow conditions which allows for proper control biomass residence time in the reactor. The flow of the biomass through the reactor can be adjusted by manipulating the rotational frequency of the screw. Ronsse decreased the screw speed from maximum rpm to *13.5 to 8.5* rpm but increased the material residence from 90s to 180s to study the effect of final temperature on the yield. The use of mechanical force to move the solid material is advantageous if the particle properties in terms of its dimensions and cohesiveness could case blockage in gravity fed processes. A well-known example of a screw based Biochar production system is the Pyreg 500 reactor from Pyreg (Germany) and capable of producing 1ton/day Biochar [17].

Dusan Klinar; He studied the *Universal model of slow pyrolysis technology producing Biochar and heat from standard biomass needed for the techno-economic assessment*. A universal model of mass and heat balance contribute to the understandings of influential technological and economic parameters related to the new technology implementation. His work aimed to provide a theoretical background of mass and heat balance of typical slow pyrolysis process as a basic for techno-economic assessment (TEA) performing and develop more users' friendly TEA model. The objective of his work is to develop;

1. Theoretical background of the general mass and heat balance model.
2. Calculate typical case of wood chips waste biomass use.

3. Compare results with published data and assess reliability, and
4. Develop a model of mass and heat balance adapted for full support of techno-economic assessment.

The materials used in the model were in the form of wood chips of standard size in range of 3.15-16mm. Slow pyrolysis model assumes pyrolysis process with only two products at the output: solid Biochar and heat in the form of hot media like water. The technology used was continuous systems that produce Biochar are of screw or moving bed type reactors. The model show rather exact internal distribution of the energy flow among the process streams. It also give perspective to improvements of the process streams. Results of the model calculation of typical case enable modification of the mass and heat balance that support views and needs of investors in the preparation of a techno-economic assessment of the technology [18].

Qiang et al., 2015; they studied *the densification of Biochar: Effect of pyrolysis temperature on the qualities of Pellets*. The densification of Biochar pyrolyzed at different temperature was investigated to elucidate the effect of temperature on the properties of Biochar pellets and determine the bonding mechanism of pellets. Their study focused on the palletisation of Biochar derived from different pyrolysis temperatures. Process optimization in relation to the compacting conditions of compressive pressure and water addition content was initially explored. Subsequently, densification of different Biochar mixtures were carried out and qualities pertaining to volume, density, compressive strength, energy consumption and moisture adsorption properties of the resulted pellets were investigated in an effort to explain the influence of the pyrolysis temperature on the pelletization. The main factors contributing to the cohesion of Biochar at the different temperatures were hydrophilic functional groups, particle size and binder. Biochar pellets formed at the compressive pressure of 128MPa, water content of 35% and pyrolysis temperature of 550 ˚C to 650˚C, exhibited superior properties to be handled [19].

Jin et al., 2016; *Production and utilization of Biochar: A review*

In this article the thermochemical conversion processes for production of biochar was studied. They indicated the pyrolysis takes place over a temperature range of 150^{o}C to 900^{o}C. In this review paper, researches on biochar production processes are discussed and method to modify its production was investigated. Different processes for Biochar production, such as pyrolysis, gasification, hydrothermal carbonization are compared. Physical and chemical activation methods used to improve the physicochemical properties of Biochar and their effects are also compared. Various environmental application fields of biochar including adsorption (for

syngas upgrading, for biodiesel production, and for air pollutant treatment), and soil conditioning are discussed. They able to produce biochar which are used in an increasing number of fields [20].

Liyi et al., 2016; they studied *Properties of Biochar obtained from pyrolysis of bamboo shoot shell.* Their work was conducted to search the influence of temperature on the output properties of produced biochar from bamboo shoot shell. Production of Biochar from bamboo shoot shell was performed on temperature ranging from 300 to 500˚C under N_2 flow. All of the Biochar obtained was low in density, but high in PH value, carbon content, nitrogen content, surface functional group content, iodine adsorption value and inorganic nutrients. They performed elemental analysis of bamboo shoot shell and biochar. They found that nitrogen content and PH value in bamboo shoot shell were first increased and then decreased with increasing of pyrolysis temperature [21].

2.4. Biomass conversion Processes

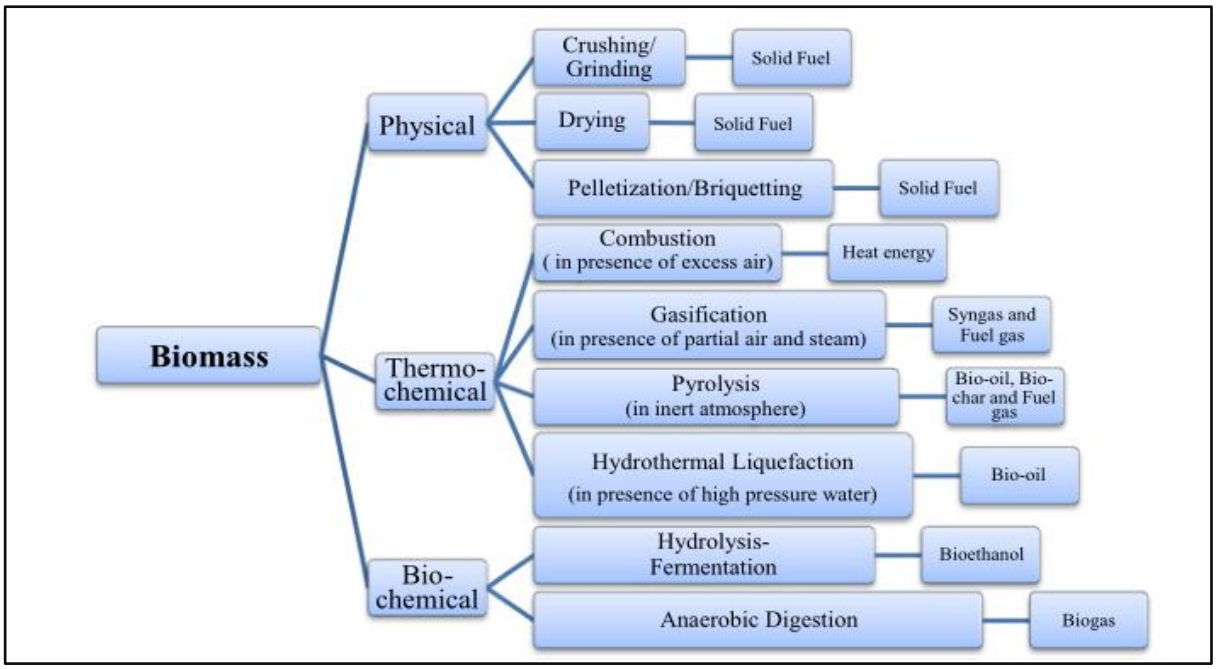

Figure 2.1. Processes flow diagram for Biochar production processes and the biomass to bioenergy conversion pathway *[22]*.

A number of different processes can be used to convert biomass into useful forms of energy. The bulky and inconvenient form of biomass is a major barrier to a rapid shift from fossil to biomass fuels. Unlike gas or liquid, biomass cannot be handled, stored, or transported easily, especially in its use for transportation. This provides a major conversion of solid biomass into

liquid, solid (Biochar) gaseous fuels, which can be achieved through one of two major paths [22].

a. Biochemical (fermentation)
b. Thermochemical (pyrolysis, gasification)

2.4.1. Biochemical conversion

It perhaps the most ancient means of biomass gasification. Biochemical conversion is based on the use of microorganisms or enzymes combined with chemical agents to convert biomass into gaseous or liquid products with high energy content [22]. This process is much slower than thermochemical conversion, but doesn't require much external energy. The three principal routes for biochemical conversion are:

1. Digestion (anaerobic and anaerobic)
2. Fermentation
3. Enzymatic or acidic hydrolysis

Anaerobic digestion is the conversion of organic material into biogas, which is a mainly a mixture of methane and carbon dioxide. Bacteria access oxygen from the biomass itself instead of from ambient. Aerobic digestion, or composting, is also a biochemical breakdown of biomass, except that it takes place in the presence of oxygen.

In fermentation, part of the biomass is converted into sugars using acid or enzymes. The sugar is then converted into ethanol or other chemicals with the help of yeasts. It is used on a large scale to produce ethanol from sugar and starch crops, and recently from lignocellulosic biomass. This path is not the scope of this research, so no farther details are given on this tittle.

2.4.2. Thermochemical

In thermochemical conversion, the entire biomass is converted into gases, which are then synthesized into the desired chemicals or used directly. Production of thermal energy and synthesis of syngas into liquid transport fuels are examples of thermochemical conversion processes. The conversion process has the following main path ways:

1. Combustion
2. Pyrolysis
3. Gasification and
4. Liquefaction.

2.4.2.1. Combustion

Combustion involves high-temperature conversion of biomass in excess air into carbon dioxide and steam.

Table 2.1. Comparison of Four Major Thermochemical Conversion Processes [22].

Process	Temperature $(^{\circ}C)$	Pressure (MPa)	Catalyst	Drying
Liquefaction	250-330	5-20	Essential	Not required
Pyrolysis	380-530	0.1-0.5	Not required	Necessary
Combustion	700-1400	>0.1	Not required	Not essential, but may help
Gasification	500-1300	>0.1	Not essential	Necessary

2.4.2.2. Pyrolysis

Pyrolysis is a method of splitting a substance to new compounds by using heat in a low oxygen environment. It comes from Greek words for fire and splitting. Pyrolysis is a thermal process mainly used for converting solid materials to gas, liquid and new solid formations. It is the first stage of the thermal break down processes before the gasification stage and the full combustion stage [23].

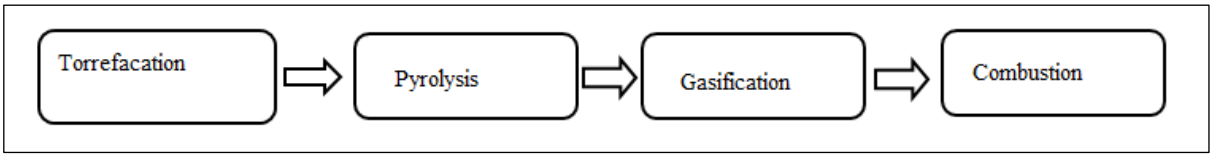

Figure 2.2. Thermal process depending on amount of reacting oxygen in the process

2.4.2.3. Gasification

Gasification involves a chemical reaction in an oxygen-deficient that converts biomass into a combustible gas mixture by partial oxidation at high temperature. Gasification can be conducted by various gasification agents such as air steam or oxygen. The product gases mainly consists of CO, H_2, CH_4 and CO_2, often referred to as producer gas. Syngas is the upgraded producer gas to a mixture of H_2 and CO. Syngas allows the production of methanol and hydrogen, which can be used as a potential fuel for transportation.

2.5. Literature on Types of Pyrolysis

Heat transfer rate during pyrolysis is one of the most important parameters for determining the yield and property of products. High heat rate yield larger percentage of bio oil than Biochar. High heating rates can only be achieved when using very small particles ($< 2mm$). Depending on the particle heat transfer rate achieved, it is possible to identify two types of pyrolysis reactors.

Table 2.2. Typical operating parameters and products for Pyrolysis [24].

Pyrolysis process	Solid residence time(s)	Heating Rate(K/s)	Particle size(mm)	Temperature(K)	Product yield (%)		
					Oil	Char	Gas
Slow	450-550	0.1-1	5-50	550-950	30	35	35
Fast	0.5-10	10-20	<1	85-1250	50	20	30

2.5.1. Fast pyrolysis

It is to describe a pyrolysis regime in which vapor production is enhanced and char minimized by rapid heating.

Fast pyrolysis is characterized by high heating rates and short vapor residence times. This generally requires a feedstock prepared as small particle sizes and a design that removes the vapors quickly from the presence of the hot solids. There are a number of different reactor configurations that can achieve this including ablative systems, fluidized beds, stirred or moving beds and vacuum pyrolysis systems. A moderate (in pyrolysis terms) temperature of around 500℃.

2.5.2. Slow pyrolysis

Slow pyrolysis can be divided into traditional charcoal making and more modern processes. It is characterized by slower heating rates, relatively long solid and vapors residence times and usually a lower temperature than fast pyrolysis, typically 400℃ . The target product is often the solid char, but this will always be accompanied by liquid and gas products although these are not always recovered. Among productions methods slow pyrolysis appears to be the optimal process for maximizing Biochar output. Any reactor that utilizes particles larger than 2mm in diameter is considered a slow pyrolysis reactor. Modified slow pyrolysis is shown as follows [25].

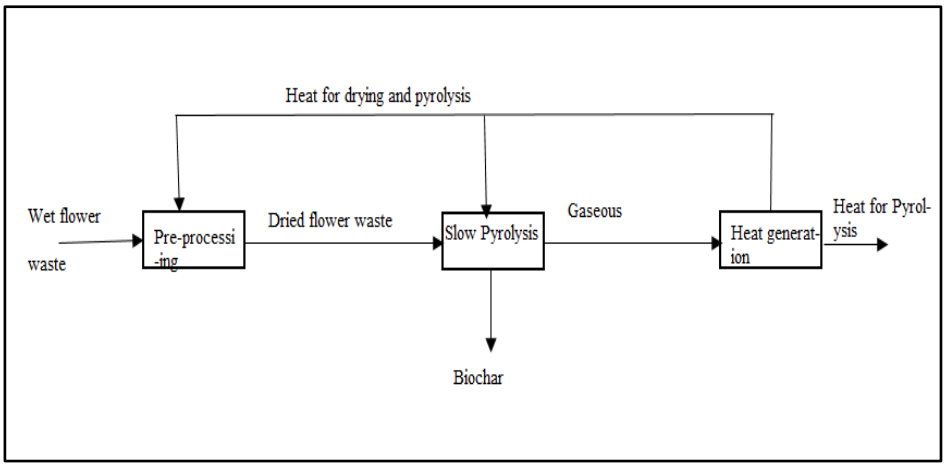

Figure 2.3. Process flow chart of slow pyrolysis

It is also known as, conventional pyrolysis or carbonization, has been around for thousands of years where it was mostly used for charcoal production. To optimize the yield and quality of char, the following parameters are required:

- A reaction temperature in the region of 400-500℃ for most biomasses
- A slow heating rate (1-50^{o}C/min) with large particle sizes typically <5cm and
- A long vapor residence time: 5-30 minutes biochar contact time to promote secondary reactions.

2.6. Traditional processes

Traditional processes, using pits, mounds or kilns, generally involve some direct combustion of biomass, usually wood, as heat source in the kiln. Liquid and gas products are often not collected but scape as smoke with consequent environmental issues.

2.7. Mode of operation

Based on the mode of operation, pyrolysis reactors can be classified as batch, semi-batch and continuous [26].

2.7.1. Batch operation

Batch-type kilns are the technology that was developed centuries ago to produce one of the first charcoal fuels. The production methods with different variations have mostly been used up until the present. The introduction of pyrolysis gas recirculation in the pyrolysis chamber, thus supplying the heat that is necessary for the pyrolysis process without using a part.

2.7.2. Semi-continuous Operation

The semi-batch operated system is portable and makes better use of hot ovens. Heat containing vapors are recycled between batch reactors. Some of these systems allow recovery of liquid products, but most are typically used to produce Biochar. These semi-portable steel kilns have two advantages;

1. They can be moved easily (which may be useful for small-scale production) Shorter cycles result when biomass is dispersed.
2. Kilns cool quickly.

2.7.3. Continuous Operation

Continuous operation reactors are designed to run nearly continuously with occasional down time for maintenance. Most continuous operation reactors are justified only if the flow rate is high. A typical continuous unit for the production of Biochar has a capacity over 2.75ton/hr. They are often more economical for large-scale production.

2.8. Method of heating

There are two general strategies or methods to heat pyrolysis reactors. 1. The first uses a hot carrier (typically a gas) produced by the combustion of wood, oil, gas, etc. in an external combustion chamber. 2. The second strategy allows a limited amount of combustion to occur inside the pyrolyzer by burning part of the wood and using this heat to dry and carbonize the remaining wood. Some authors further break out pyrolysis reactors into three categories depending on the heating method used.

1. Pyrolysis by partial combustion (auto-thermal systems)
2. Pyrolysis by injection of a hot gas in the load (direct heating with an inert hot gas)
3. Pyrolysis in an enclosed reactor or retort (indirect heating)

The following figures shows the three systems [27] .

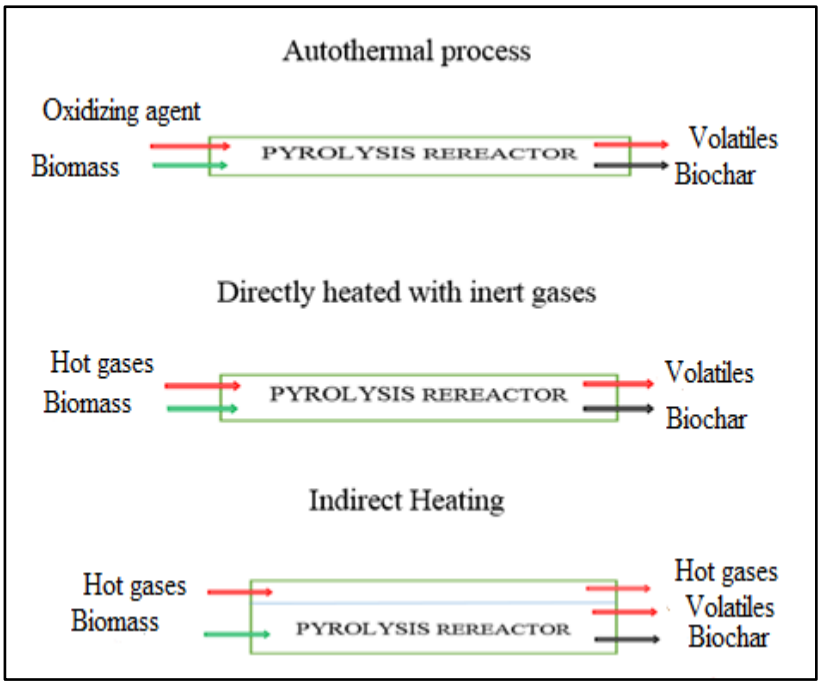

Figure 2.4. Types of Pyrolysis technologies according to heating methods used

3. Chapter 3: Materials and Methods

Working this thesis started with discussing on the title, soon decided it was followed with gathering a reference group where stakeholders and experts with great relevant experiences were chosen. Studies on pyrolysis technology and the pyrolysis end products was carefully reviewed on the topic of study. Important materials needed and the methods to be followed is discussed as follows.

3.1. Materials

Materials needed for investigation of continuous biochar production from flower waste include the following:

1. Pre-processing equipment, these include grinding and drying.
2. Material handling equipment's, these include feed hopper.
3. Feeding equipment (screw feeder).
4. Biochar reactor i.e. screw reactor.
5. Cyclone: to separate the gases and biochar.
6. After burner and a compressor.
7. A motor.
8. A blower.

3.2. Methods

The overall approach is: raw material collection, preparation of feedstock (drying and grinding to about 6mm diameter), characterization of flower waste, designing size of the components and manufacturing the prototype. An experiment was conducted on the manufactured prototype to see the temperature distribution on the length of screw reactor and produce biochar. In doing so biochar from the selected biomass was produced. Then 3D of the reactor with the screw conveyor is modelled using CATIA software and then it was imported in COMSOL 5.0. Finally, an isothermal flow has been simulated to study temperature distributions. Subsequently, heat transfer were added to investigate the temperature profile on the reactor.

3.3. Assumption's made

The key assumption in the conservation energy is the presence of a thermal equilibrium between the gas and solid phases [11]. This is a standard assumption common to all pyrolysis models. The outer surface of the reactor is adiabatic as it is well insulated by best insulating material. The general assumptions made are as follows

1. Time dependent
2. One-Dimensional heat transfer in the radial (cylindrical) direction
3. Constant properties for insulation material
4. Negligible radiation exchange between insulation outer surface and surroundings.

3.4. Software used

CATIA P3V5R19 is used to model the reactor and certain components of the machines. The modelled reactor were imported in to COMSOL 5.0. to study the heat transfer analysis and temperature distribution along the length of the reactor.

COMSOL 5.0. enforces the conservation laws over a discritized flow domain in order to compute the systematic changes in mass, momentum and energy as fluid or solid crosses the boundaries of each descrite region. A standard screw housing is taken to be dimension of the inner reactor and program was writen in Matlab software to size the raector.

3.5. Feed stock

The phrase agricultural waste describes all the organic materials which are produced as the by-products from agricultural activities such as wheat and barley straw, coffee husks, flower wastes and animal wastes etc. Ethiopia is the second largest flower exporter in Africa [28] . In this study, flower waste is the chosen raw material for biochar production using pyrolysis process. The flower waste was 6mm in diameter and 3mm in thickness. The proximate and ultimate analysis of the selected biomass will be discussed in the next title.

3.6. Pyrolysis

Simulation and experimental investigation of continuous biochar production from flower waste was conducted using continuous screw reactor. The reactor system consists of feedstock bin (hopper), screw feeder, screw conveyor, outer and inner reactors made of stainless steel, a motor, pulleys, gear box, V-belts, a cyclone and an afterburner. Biochar and ash were removed by cyclone connected to the inner reactor. An air added making use of compressor to pyrolysis gases and vapours in the afterburner to produce pyrolysis temperature. The basic type of solid movement during pyrolysis is caused by mechanical forces i.e. by rotating screw.

4. Chapter 4 : Design of components

4.1. Conical Hopper

The hopper is used to store and supply feed material to the screw feeder. It is converging part.

4.1.1. Flow theories

The gravity flow of bulk solids occurs under the pressure corresponding to the equivalent of static head of the material. The limits for conical hoppers and plane hoppers depend on the hopper half angle θ, the effective angle of internal friction δ and the wall friction angle ϕ.In the function form

$\theta = f(\delta, \varphi)$ i.e. The hopper angle = f (wall friction angle, effective angle of internal friction). For the case of conical hoppers, it is recommended that the half- angle be chosen to be 3° less than the limiting value [29].

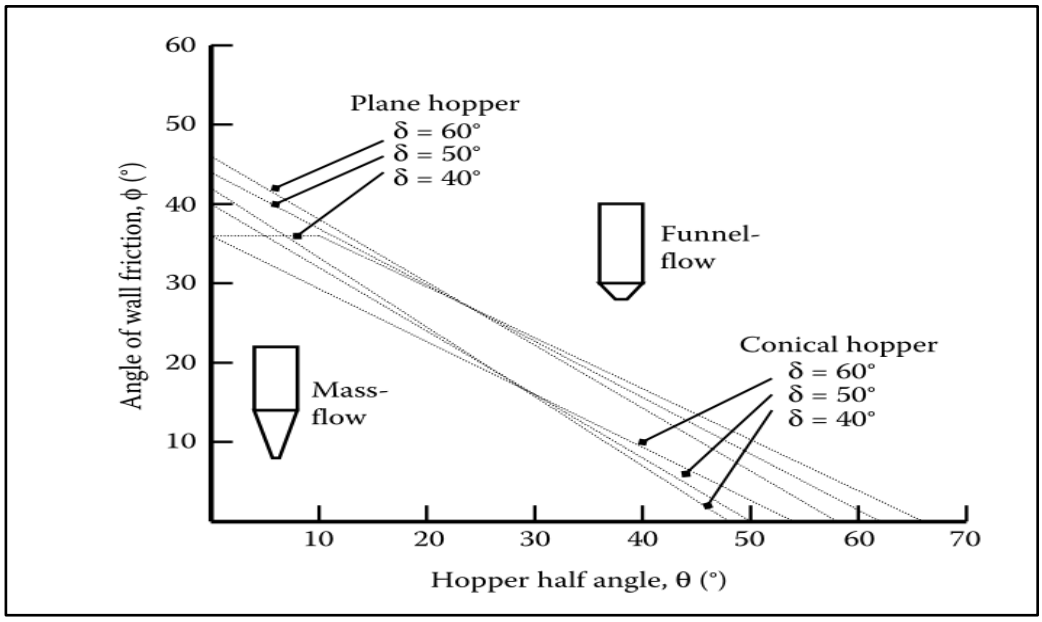

Figure 4.1. Limits for mass flow in conical and plane flow channels

4.1.2.Flow Types

Funnel flow: is a flow pattern in which solid flows in a channel formed within stagnant material [30].

Mass flow: flow pattern in which all solids in bin is in motion whenever any of it is withdrawn.

Expanded flow: flow pattern which is combination of mass flow and funnel flow.

4.1.3. Hopper Opening for Coarse Bulk Solids

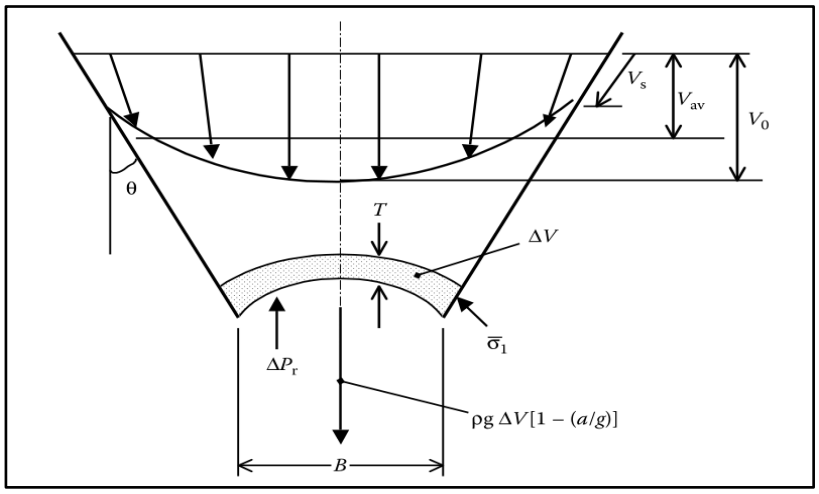

Figure 4.2. Flow channels and equilibrium forces on the arch formed on a hopper *[29]*.

According to the diagram shown in *Figure 4.2* the accelerated flow of bulk solids in the region of the out let of the hopper can be considered when air pressure gradient ΔP_r equals zero. Analysing the forces it may be sown that: [29].

$$\bar{\sigma}_1 = \frac{\rho_b g B}{H(\theta)}\left[1-\frac{a}{g}\right] \tag{4.1}$$

Where $\bar{\sigma}_1$ is the stress acting in arch at 45° ρ_b is the bulk density of solids, g is the acceleration due to gravity, B is the hopper opening, a is the acceleration of discharging bulk solids and $H(\theta)$is a factor to account for the variation in arch thickness, hopper half –angle, and hopper type whether conical or plane. It has an approximate value of 2.2 for plane –flow hoppers and 2.4 for conical hoppers.

The minimum hopper opening to just prevent a cohesive arch from forming occurs when static equilibrium prevails, that is, when the acceleration of the discharging bulk solids approaches zero, and thus substituting $a = 0$ into above equation and transposing

$$B_{\min} = \frac{\bar{\sigma}_1 H(\theta)}{\rho_b g} \tag{4.2}$$

Hopper half-angle is chosen from mass flow limits as shown in Figure 4.1, while the condition for $\bar{\sigma}_1 = \sigma_c$ is obtained the intersection point of the flow factor ff line and failure function FF as illustrated in Figure 4.3 .

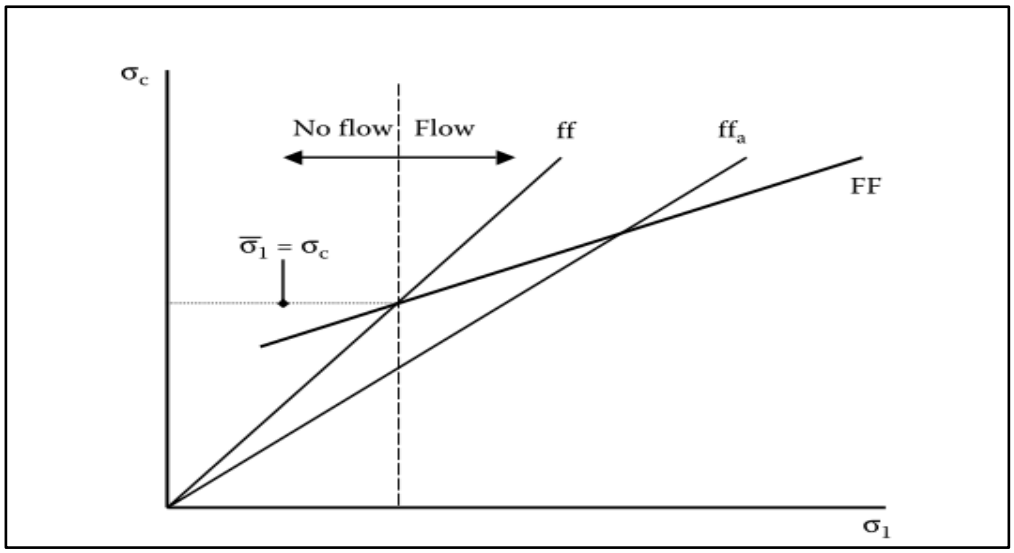

Figure 4.3. Design Graphic for Hopper Geometry

The flow factor *ff* can be defined by the relationship $ff = \frac{\overline{\sigma_1}}{\sigma_c}$ (4.3)

The flow factor *ff* and function H (θ) are given as design curves like the one given below in *Figure 4.4*. Following the work of Johansson, it may be shown that the acceleration may be expressed as

$$a = g\left[1 - \frac{ff}{ff_a}\right] \tag{4.4}$$

Where ff is the critical flow factor based on the minimum arching dimension and ff_a is the actual flow factor based on the actual opening dimension. This actual flow factor may be represented as the relationship between stresses, according to *Figure 4.3* by

$$ff_a = \frac{\sigma_1}{\sigma_c} \tag{4.5}$$

Where σ_1 is the major consolidation pressure at outlet corresponding to dimension B.

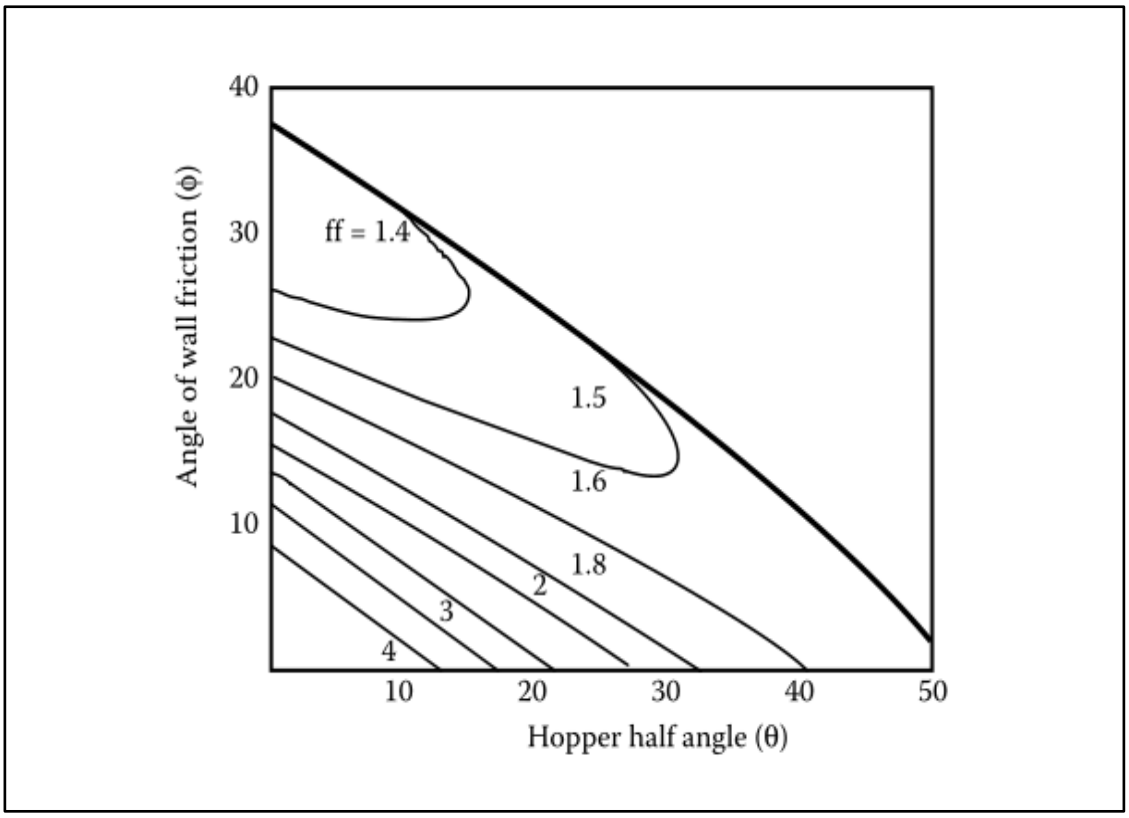

Figure 4.4. Flow factor graph for conical hopper and effective angle of internal friction.

$$\delta = 40^{\circ}$$

The acceleration has two components $a = a_c + a_v$

Where a_c is the convergence component due to flow channel and a_v is the component due to velocity increase as flow is initiated. This last component may be represented as a function by

$$a_v = g\left[1 - \frac{ff}{ff_a}\right] - \frac{2V^2(1+m_c)\tan(\theta)}{B} \tag{4.6}$$

Where V is discharge velocity and m_c is a constant which takes the value of zero for plane hopper and unity for axisymmetric or conical hoppers.

The above equation shows that as the discharge velocity V increases, the component due to velocity increase as flow is initiated a_v tends to zero. Thus, an average terminal discharge velocity V_a is reached when $a_v = 0$, that is,

$$V_a = \sqrt{\frac{Bg}{2(m_c+1)\tan(\theta)} * \left[1 - \frac{ff}{ff_a}\right]} \tag{4.7}$$

The flow rate m_0 may be calculated by the following equation:

$$m_o = \rho_b B^{(1+m_c)} L^{(1-m_c)} \left(\frac{\pi}{4}\right)^{m_c} V_a \tag{4.8}$$

$$H(\theta) = 2 + \frac{\theta}{60} \tag{4.9}$$

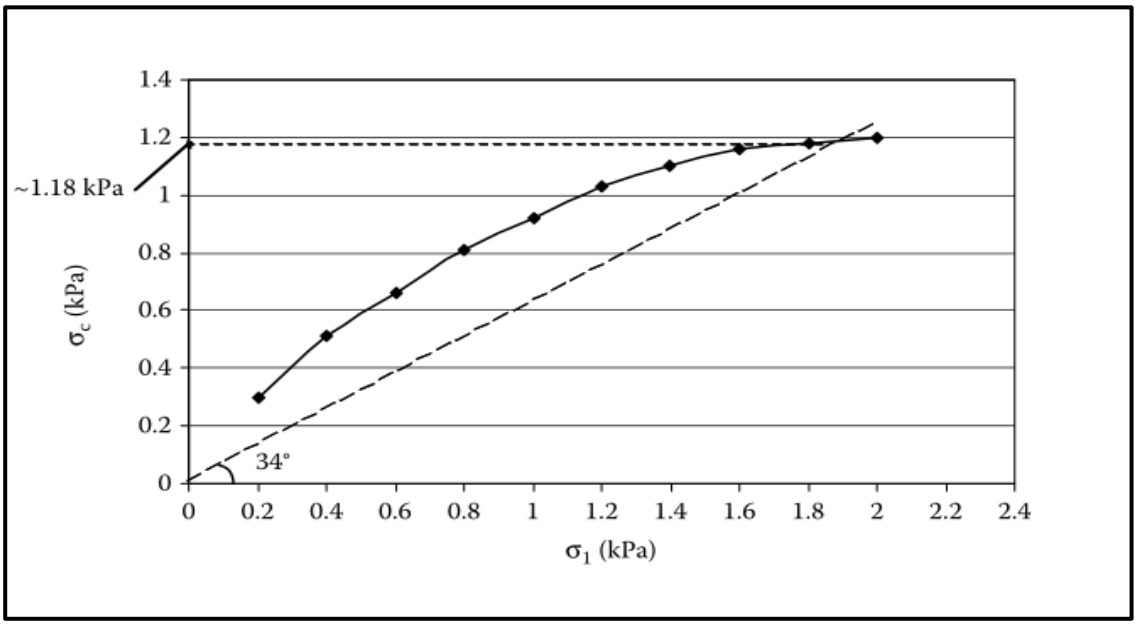

Figure 4.5.Critical stresses for bulk solids at effective angle of friction *[29]*.

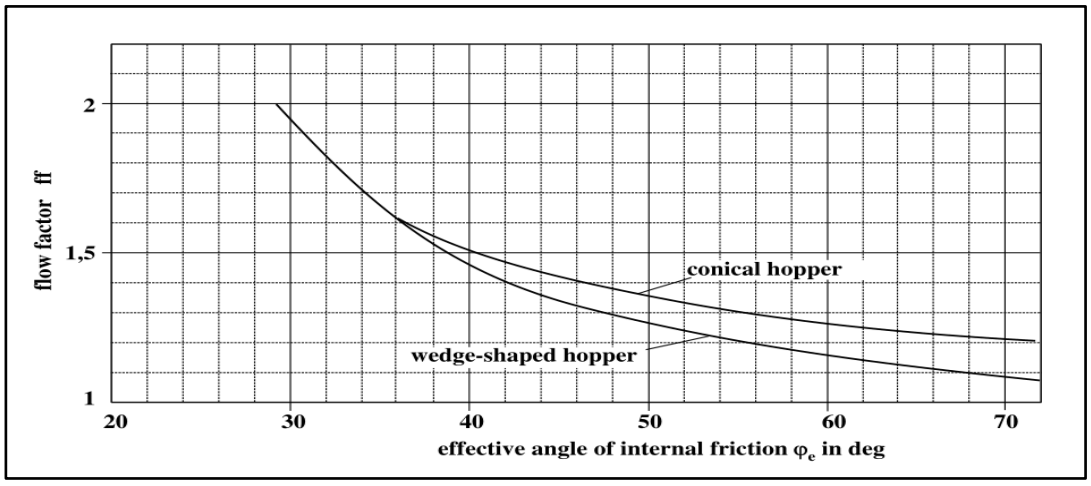

Figure 4.6 effective angle of internal friction

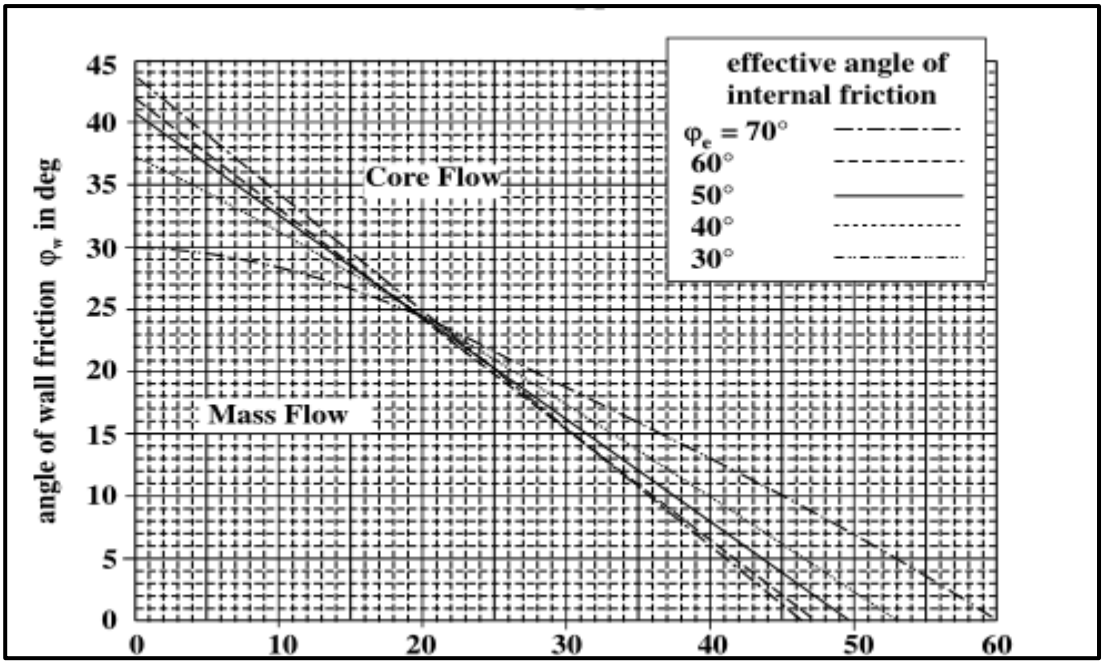

Figure 4.7. Hopper angle versus Vertical *[29]*.

The design of the hopper out let significantly affects the flow of solids. Mass flow hopper are smooth and steep. The flower waste flow behaviour in a hopper is governed by:

a. The shear properties of the flower waste – how easily the particles move relative to each other
b. Wall friction –how easily the flower waste flows over the inner surface of the container.
c. Compressibility –how application of a consolidating stress changes bulk density

These variables define how the flower waste will behave in the hopper when consolidated (steady flow) by the weight of the material in the hopper. Potentially a stable arch can form across the hopper outlet and if this is strong enough to support the rest of the flower waste in the hopper then discharge ceases. For any given combination of powder or crushed and size reduced material, hopper half angle and outlet size determined as follows [31].

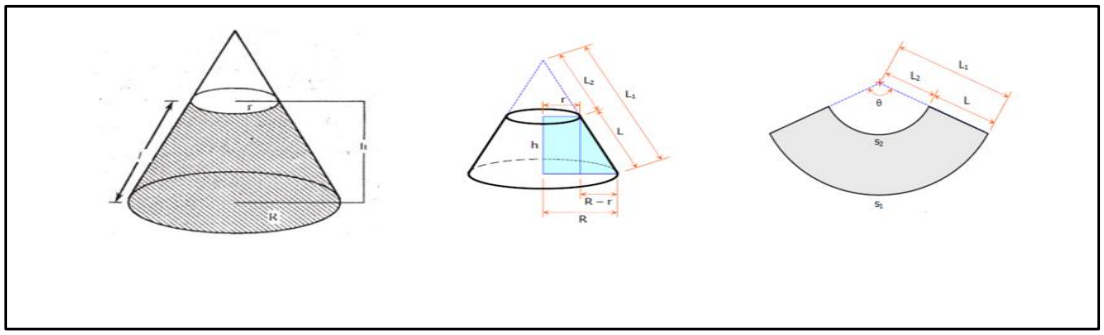

Figure 4.8. Feed hopper development

4.2. Gear box

This gear box is made from spur gear. Spur gears are used to transmit rotary motion between parallel shafts. They are cylindrical, and the teeth are straight and parallel to the axis of rotation. Thus they are not subjected to axial thrust due to tooth load. The pinion is the smaller of two meeting gears; the larger is called the gear. At the time of engagement of the two gears, the contact exceeds across the entire width on a line parallel to the axis of rotation. This results in sudden application of load, high impact stress and excessive noise at high speeds.

A conventional gear train is made up of two or more gears. There will be a change in the angular velocity and torque between an input and output shaft. The spur gear and its gear teeth is shown as follows.

The American Gear Manufacturers Association has recommended that the basic pressure angle α be either 20° or 25° with full depth addendums equal to $\frac{1}{P}$. Important parameters of the gears are:

a. Diameteral pitch is the number of teeth in the gear per inch of pitch diameter.

$$P_d = \frac{N}{d} \tag{4.10}$$

b. Module

$$m = \frac{d}{N} \tag{4.11}$$

Fundamentals for spur gears Pitch line velocity is given as follows

$$V_p = |r_1\omega_1| = |r_2\omega_2| \text{ Or } \left|\frac{\omega_1}{\omega_2}\right| = \frac{r_2}{r_1} = \frac{d_2}{d_1} \tag{4.12}$$

Kinematics

$$\left(N_g \big/ d_g\right) = \left(N_p \big/ d_p\right) \tag{4.13}$$

The velocity ratio $$VR = \left(\frac{\omega_p}{\omega_g}\right) = \left(\frac{d_g}{d_p}\right) = \left(\frac{N_g}{N_p}\right) \quad (4.14)$$

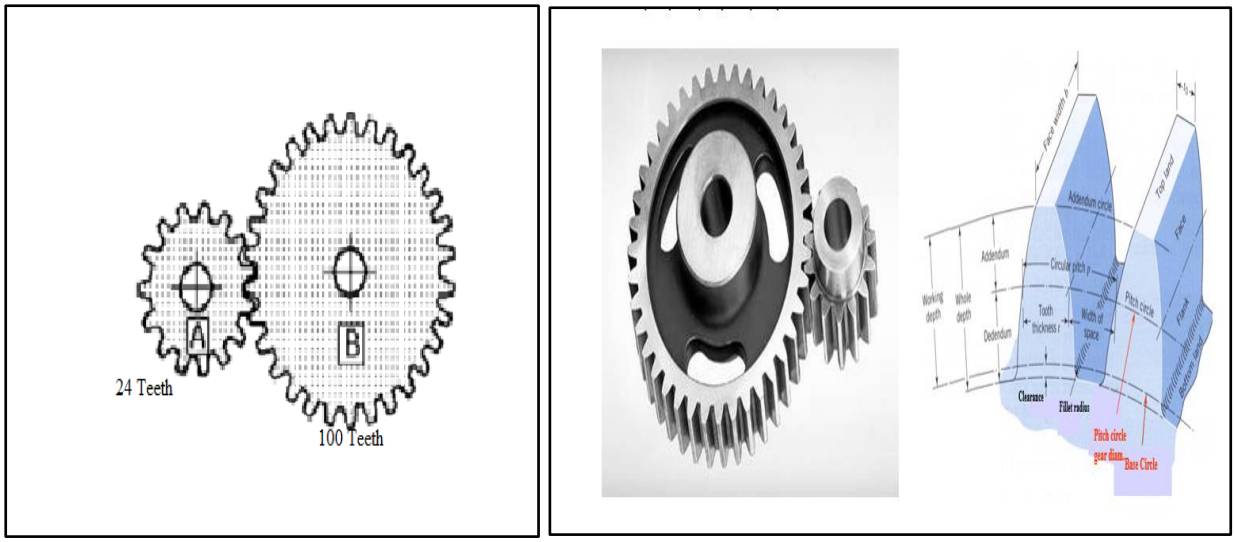

Figure 4.9. Spur Gears *[32]*.

4.3. Motor selection

A detailed understanding of type of motors, mounting, enclosures, duty helps in identifying appropriate type of motor for intended application'. The criteria for motor selection includes; operating conditions, driven equipment starting requirements (including the use of adjustable speed drives), electrical specifications, mounting requirements, enclosure and bearing parameters and accessory equipment needs.

4.3.1. Operating conditions

Basic motor specifications begin with determining the motor nameplate HP and RPM. These are determined by the process equipment supplier and are based upon a steady state equipment operation. For continuous biochar production from flower waste motor specification is 50/60 rpm, 220V and 3kW i.e. from industrial guide book of motor selection.

Since the required rpm for continuous feeding and discharging is very small the rpm can be reduced using speed reducer like pulleys and gearbox.

4.3.2. Power requirements

The power required to operate a horizontal screw conveyor is based on uniform and regular feed rate to the conveyor. The power requirement is the total power to overcome friction and the power to transport the material at the specified rate multiplied by the over load factor and divide by the total drive efficiency or

The power P required to drive a screw conveyor depends on the dimensions of the system and the characteristics of the material. A rough approximation for normal horizontal operation can be determined from the following relation.

$$P = \dot{W} = \frac{T_s \omega}{1000} = \frac{T_s n}{9549} \tag{4.15}$$

F is a factor based on the type of material [33].

Material Factors for Horizontal Screw Conveyors

Type a (F = 1.2) Light, Fine, Nonabrasive, Free-Flowing Materials ρ_b: 480 to 640 kg/m³	Type b (F = 1.4–1.8) Nonabrasive, Granular or Fines Mixed with Lumps ρ_b: up to 830 kg/m³	Type c (F = 2.0–2.5) Non and Mildly Abrasive, Granular or Fines Mixed with Lumps ρ_b: 640–1200 kg/m³	Type d (F = 3.0–4.0) Mildly Abrasive or Abrasive, Fine, Granular or Fines with Lumps ρ_b: 830–1600 kg/m³
Barley	Cacao seeds	Borax	Bauxite
Corn flour	Coffee seeds	Brown coal	Bone meal
Cotton seed flour	Corn	Charcoal	Cement
Crushed coal	Corn meal	Cocoa	Chalk

Figure 4.10. Materials factors F for horizontal screw conveyor

Therefore, for capacity of screw conveyor the required power

$$P = T\omega = FTn \tag{4.16}$$

4.4. Selection of belt drive

The following are the various important factors up on which the selection of a belt drive depends;

1. Speed of the driving and driven shafts
2. Speed reduction ratio
3. Power to be transmitted
4. Centre distance between the shafts
5. Space available and
6. Service conditions.

V-belt: the v-belt is mostly used where a great amount of power is to be transmitted, from one pulley to another, when the two pulleys are very near to each other.

Since the two pulleys are very near to each other V-belt type has been selected. The advantage of this belt is it can be easily installed and removed. The material used for belts and ropes must

be strong, flexible and durable. It must have high coefficient of friction. Rubber belt has been selected.

4.4.1. Design Specification for V-belt derive

The maximum centre distance of belt in use depends on the size of two pulleys and is given as:

$$X_{max} = 2(D + d) \tag{4.17}$$

Centre distance (adjustment for centre distance must be provided or use idler pulley) nominal range $D_2 \prec C \prec 3(D_2 + D_1)$

The speed ratio of the V-belt is calculated as follows:

$$\frac{N_1}{N_2} = \frac{D_2}{D_1} \tag{4.18}$$

The length of the belt can be calculated as follows

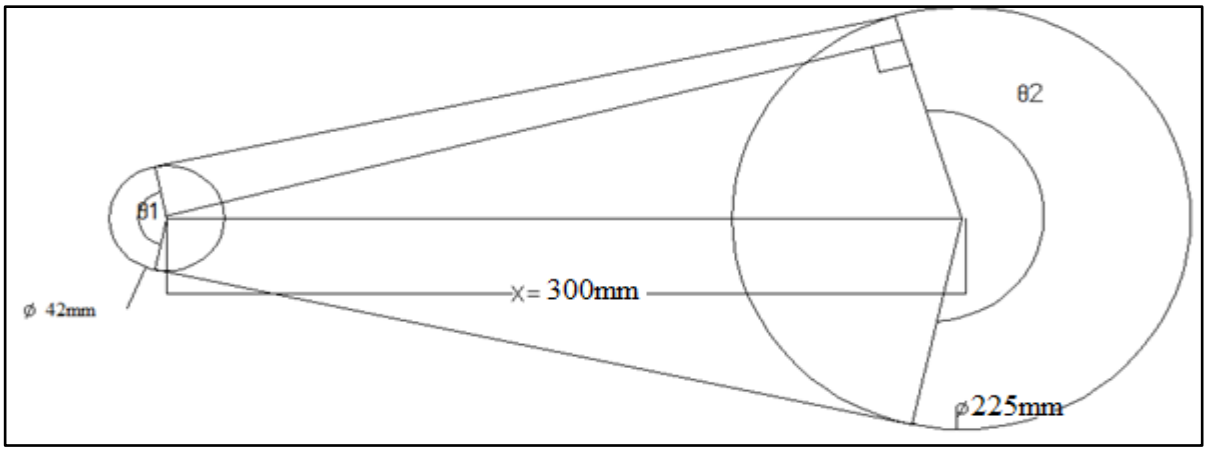

Figure 4.11. Geometry of pulley and Belt

Coefficient of friction from above figure $\sin\alpha = \frac{D_2 - D_1}{2X}$ (4.19)

Now the angle of contact on small pulley: $\theta_1 = 180^\circ - 2\alpha$ (4.20)

Angle of contact on larger pulley (θ_2): $\theta_2 = 180^\circ + 2\alpha$ (4.21)

When pulleys have different angles of contact (θ), then the design will refer to a pulley for which the value of $(\mu * \theta)$ is small. μ Coefficient of friction for belt material and balata material has 0.32 value.

$$(\mu * \theta) = \mu * \theta_1 \operatorname{cosec}\beta \tag{4.22}$$

Since $(\mu * \theta)$ is small for smaller pulley, therefore the design is based on smaller pulley.

Belt speed: $(V_b) = \frac{\pi * D * N_1}{60}$ (4.23)

Mass of the belt per meter length will be

$$\text{Mass}(m_b) = Area(A) * centerdistance(X) * density(\rho_{bm}) \quad (4.24)$$

4.4.2. Centrifugal Action

The belt is having some mass and as it passes over the pulley it moves over a circular path. Hence, it is subjected to centrifugal forces. Considering the small element of length $R\delta\theta$ and mass m per unit length, the centrifugal force on the element is:

$$F_c = (m_b R\delta\theta) * \frac{V^2{}_b}{2} = m_b V^2 * \delta\theta \quad (4.25)$$

If T_c is the tension in the belt due to centrifugal effect, then equilibrium equation gives:

$$2T_c \sin\frac{\delta\theta}{2} = F_c \text{ Or } T_c\delta\theta = m_b V^2{}_b * \delta\theta \Rightarrow T_c = m_b V^2{}_c \quad (4.26)$$

the maximum tension in belt; $T = \sigma * A$ (4.27)

Total tension in belt; $T = T_1 + T_c$ (4.28)

According to Hannah and Stephens (1970), the power transmitted by belt is given by

$$P = (T_1 - T_2)V_b \text{ But } V_b = \frac{(\pi DN)}{60} \text{ and also } 2.3\log\left(\frac{T_1}{T_2}\right) = \mu * \theta \cos ec\beta \quad (4.29)$$

4.5. Design of Shaft

A shaft is a rotating member, usually of circular cross section, used to transmit power or motion. It provides the axis of rotation of elements such as gears, pulleys and the like and controls the geometry of their motion. The shaft is the elements that supports rotating parts like gears and pulleys and intern themselves supported by bearings resulting in the rigid machine housings. The shafts perform the function of transmitting power from one rotating member to another supported by it or to it. Thus, they are subjected to torque due to power transmission and bending moment due to reactions on the members that are supported by them.

4.5.1. Shaft Materials

Shafts could be made in mild steel, carbon steels or alloy steels such as nickel, nickel-chromium or chrome-vanadium steels. Heavily loaded shafts are often made in alloy steels which because of their high strength would result in smaller diameters. Modulus of Elasticity for most steels is $200GPa$.

The following stresses are induced in the shafts;

1. Shear stresses due to the transmission of torque
2. Bending stresses (tensile or compressive) due to forces acting upon machine elements like gears, pulleys etc. as well as due to the weight of the shaft itself.
3. Stresses due to combined torsional and bending loads.

According to American Society of Mechanical Engineers (ASME) code for the design of transmission shafts, the maximum permissible working stresses in tension or compression may be taken as;

a. $112MPa$ for shafts without allowance for keyways
b. $84MPa$

And the maximum permissible shear stress may be taken as;

a. $56MPa$ For shafts without allowance for key ways.
b. $42MPa$ For shafts with allowance for key ways.

Shafts with keyways used for continuous Biochar production from flower waste.

4.5.2. Shaft design specification

1. Shaft material is alloy steel
2. Power is constant $3kW$ i.e. from motor selection
3. Allowable shear stress of shaft material $(\tau) = 42MPa$
4. Approximate mass of flight = $5kg$
5. Mass of larger pulley = $4kg$

The pulley is keyed to the shaft and receives 3kW at 11.6 rpm which is transmitted to a smaller pulley to rotate the screw conveyor at the same speed as screw feeder.

From V-belt design we have

$N_2 = 11.6rpm, T_1 = 2997.45N$, $T_2 = 963.81N$ and $R_2 = 0.1125m$

Torque transmitted by driven or the shaft from V-belt design $T_t = \frac{60 * p}{2\pi * N_2}$ (4.30)

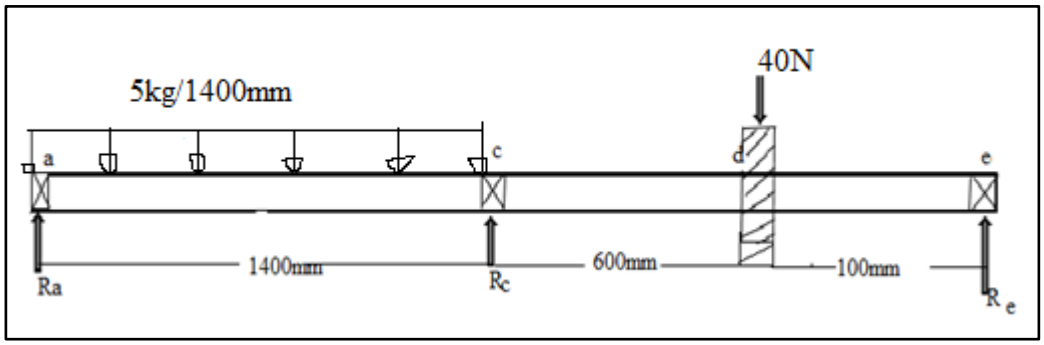

Figure 4.12. Free Body Diagram on Shafts

From equilibrium equation;

$$\sum F_y = 0 \quad (4.31)$$

$$R_a - W_b + R_c - W_p + R_d = 0$$

According to maximum shear stress theory, equivalent twisting moment is given as;

$$T_e = \sqrt{(M)^2 + (T)^2} \quad (4.32)$$

Now the equivalent twisting moment: $T_e = \frac{\pi}{16} * \tau * d_s^{\,3}$ (4.33)

4.6. Design of Pulley

The pulleys are used to transmit power from one shaft to another by means of flat belts-belts or ropes. Since the velocity ratio is the inverse ratio of the diameters of driving and driven pulleys, therefore the pulley diameters should be carefully selected in order to have desired velocity ratio. The pulleys may be made of cast iron, cast steel or pressed steel and aluminium. For the continuous Biochar production pulleys material is aluminium. The following procedures adopted for the design of aluminium pulleys;

a. Dimensions of pulleys

i. The diameter of the pulley D may be obtained either from velocity ratio consideration or centrifugal stress consideration. We know that the centrifugal stress induced in the rim of the pulley. $\sigma_t = \rho V^2{}_b$ (4.34)

ii. From width of the belt, the width of pulley or face width of the pulley (B) is :

The dimension of standard V-grooved pulley is selected from which we find that for D type belt.

$W = 20mm, d = 21mm, a = 8mm, c = 14mm, f = 18$ And $e = 30$

Now the face width of the pulley

$$B_p = (n-1)e + 2f \quad (4.35)$$

The following are the width of V-belt of aluminium pulleys in mm:
16,20,25,32,40,50,63,71,80,90,100,112,125,140,160,180,200,224,250,315,355,400,450,560 and 630.

4.7. Selection of Bearing

Rotating shafts are required to be supported at suitable places. The mechanical device which can take up the load and support the shaft called bearing. The bearing is so named because the surface of support is subjected to a bearing load. A bearing is machine elements which support another moving machine element (known as journal). It permits a relative motion between the contact surfaces of the members, while carrying the load. In the bearings, the relative motion between the two mating surfaces causes friction and generates heat. Any substance placed between the two surfaces which reduces friction, wear and takes away heat, known as lubricant. In order to reduce frictional resistance and wear in some cases to carry away the heat generated, a layer fluid (known as lubricant) may be provided. The lubricant used to separate the journal and bearing is usually a mineral oil refined from petroleum, but vegetable oils, silicon oils, greases etc. maybe used.
Based on the direction of load bearing may be broadly classified in to two categories.

a. Radial bearings; radial bearings carry external load perpendicular to the axis of rotation of the shaft. Journal bearings and some types of ball and roller and roller bearings belong to this category.
b. Thrust bearings; in these bearings, the load acts along the axis of rotation, e.g. hydrostatic bearings and antifriction thrust bearings.

Based on the nature of contact bearings are also classified according to the nature of relative motion between members.

a. Sliding contact bearings; Bearings with sliding friction between the members are called sliding bearings, e.g. journal bearings and hydrostatic bearings.

b. Rolling contact bearings; Bearings with rolling contact friction between the members are known as rolling contact bearings; e.g. ball, roller and taper roller bearings. These bearings have either point contact or line contact.

4.7.1. Selection of bearings

The selection of bearing for a particular application is based on several characteristics relating to mechanical, environmental and economic requirements.

i. Mechanical requirements

The following considerations are of paramount importance in the selection of bearings;

Load: the rolling element bearing are superior to slider bearings because they can carry high unidirectional and cyclic loads whereas the load carrying capacity of slider bearings depends on the speed of journal.

Speed: Both sliding and rolling element bearings have a practical limit to the peripheral velocity, fixed by different criteria. In sliding bearings, the speed limitation is on account of the rise in temperature of lubricating oil caused by high speed shearing action. In the rolling element bearings, the limit speed is a function of the product of shaft diameter (mm) and speed in rpm.

Misalignment: A slider bearing can tolerate misalignment better than what the rolling element bearing can because the later has rigid structure and close tolerances.

Frictional loss: Rolling element bearings have low starting friction but journal bearings attain lower coefficient of friction only when sufficient pressure is built up.

Space: Journal bearings occupy less space in radial direction whereas rolling element bearings require less space in axial direction.

4.7.2. Bearing material

A bearing however, carefully and properly designed, may fail either due to deflection, temperature distortion, and surface roughness or due to faulty selection of the bearing material. Therefore, a proper selection of bearing material is very important. Since the rolling elements and the races are subjected to high local stresses of varying magnitude with each revolution of the bearing, therefore material of the rolling element i.e. steel should be of high quality. The balls are generally made of *high carbon chromium steel.* The material of both the balls and races are heat treated to give extra hardness and toughness.

4.7.3. Life of Bearing

The life of an individual ball (or roller) bearing may be defined as the number of revolutions (hours at the some given constant speed) which the bearing runs before the first evidence of fatigue develops in the material of one of the rings or any of the rolling elements. The rating life of a group of apparently identical ball or roller bearings is defined as the number of revolutions (or hours at some given constant speed) that 90 percent of a group of bearings will complete or exceed before the first evidence of fatigue develops (i.e. only 10 percent of a group bearings fail due to fatigue). The term minimum life is also used to denote the rating life. We may say that the average life of a bearing is 5 times the rating life (or minimum life). It may be noted that the longest life of a single bearing is seldom longer than the 4 times the average life and the maximum life of a single bearing is about 30 to 50 times the minimum life.

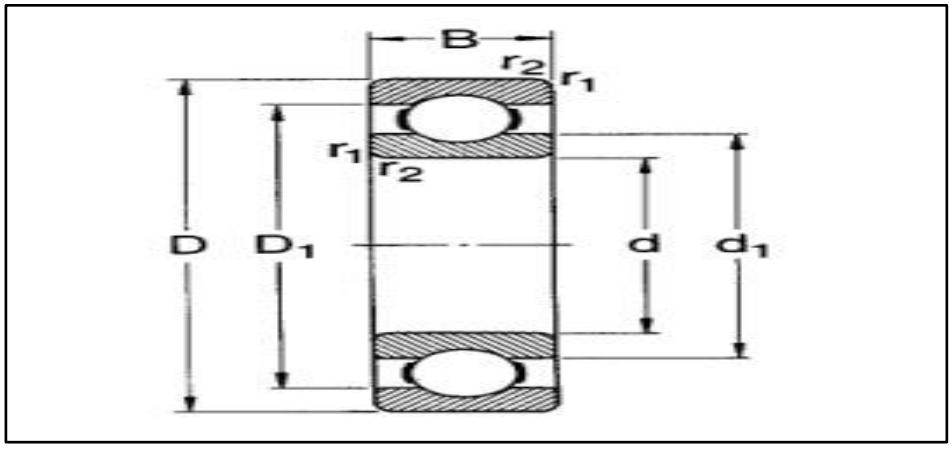

Figure 4.13. Single Row Deep Groove Ball Bearing with Full Outer Ring Shoulders

Table 4.1.Selection of Bearings *[32]*.

Bore d (mm)	Outside diameter D (mm)	Width B (mm)
10	30	9
12	32	10
15	35	11
17	40	12
20	47	14
25	*52*	*15*
30	*62*	*16*
35	72	17
40	80	18
45	85	19
50	90	20
55	100	21
60	110	22
65	120	23

Table 4.2. Basic Capacities of Bearings [32].

Bearing Bore No. in mm	Basic Capacities in KN			
	Single row deep groove ball bearing		Single row angular contact ball bearings	
	Static (C_o)	Dynamic(C)	Static (C_o)	Dynamic(C)
10	2.24	5.07	2.12	4.94
12	3.10	6.89	3.05	7.02
20	6.20	12.7	6.55	13.3
25	*6.95*	*14*	*7.65*	*14.8*
30	*10*	*19.5*	*11*	*20.3*

The static equivalent radial load (W) for radial bearings under combined radial and axial or thrust loads is given by the greater magnitude of those obtained by the following equations;

a. $W = Y_o W_R + X_o W_A$ (4.35)

b. And $W = W_R$ (4.36)

W_R Is the radial load, W_A is axial load, Y_o radial load factor, X_o axial load factor.

The approximate rating (or service) life of ball bearings is based on the fundamental equation:

$L = \left(\frac{C}{W}\right)^K * 10^6$ Revolution where L is rating life, C is basic dynamic load bearing, W equivalent dynamic load and $K = 3$, for ball bearing, $K = 10/3$ for roller bearing

The relationship between the life in revolutions (L) and the life working hours (L_H) is given by

$L = 60N * L_H$ (4.37)

For continuous Biochar production machine single row deep groove ball bearing from known shaft diameter (d=30mm and d=25mm) which is equal to bore diameter (30mm and 25mm) of bearing.

Using bore diameter from a text book of machine design by Khurmi and Gupta the following data is selected.

1. Bearing type single row deep groove ball bearing
2. Outside diameter for bore diameter of d=25mm and d=30mm is 52mm and 62mm consecutively.
3. Bearing width for bore diameter of d=25mm and d=30mm is 15mm and 16mm consecutively.

Basic static (C_o) and dynamic (C) capacities of various types of radial ball bearings single row deep groove ball bearing using diameter of shaft (bore diameter of 25mm and 30mm) that have basic capacities of static $(C_o) = 10kN$ and dynamic $(C) = 19.5kN$ for bore diameter 30mm and $(C_o) = 6.95kN$, $(C) = 14kN$ for bore diameter of 25mm.

1. From shaft design we have a radial load $(W_R) = 40N$
2. From belt design the speed $(N) = 11.6rpm$
3. $K = 3$, for ball bearing.

4.8. Screw feeder

A screw feeder is mounted directly under the opening of a hopper. The flower waste therefore rests on the part of the screw and the screw flight is filled completely. It is used to introduce material in the screw reactor. Material from the hopper enters the feed screw and the mass flow is determined by the rotational frequency of the feed screw. In this way, the feed screw determines the mass flow through the screw reactor. However, if the frequency of the feed screw is too large compared to screw conveyor, the reactor will be overloaded and consequently block.

Similar to screw conveyor, screw feeder is either right hand or left hand depending on the form of helix. The hand of screw is easily determined by looking at the end of the screw [33].

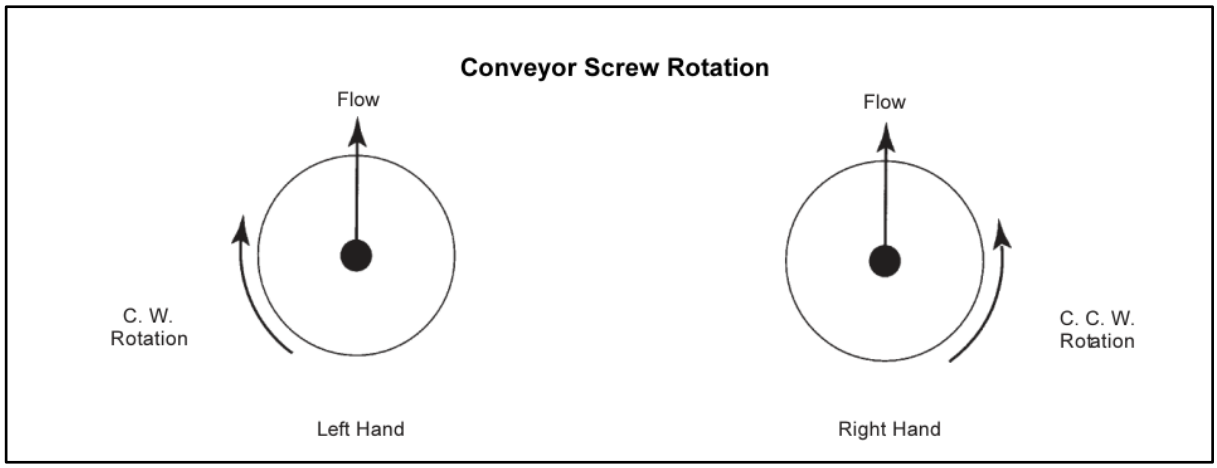

Figure 4.14. Simple means of determining screw rotation

Right hand screw feeder has been selected for screw reactor case. *Roberts* developed the theory to predict the performance of screw conveyors of any specified geometry and also proposed a model to predict volumetric performance of screw feeding and studied effect of vortex motion [34]. The theoretical maximum throughput (material) Q_t, of screw feeder is obtained if the feeder were running full with the particulate material moving purely in the axial direction. The selected screw feeder is with a hollow shaft.

Maximum throughput

$$Q_t = A\omega D^3 \tag{4. 38}$$

$$A = \frac{1}{8}\left[\left(1+2\frac{C}{D}\right)^2 - \left(\frac{D_c}{C}\right)^2\right]\left[\left(\frac{P_s}{D} - \frac{t_s}{D}\right)\right] \tag{4. 39}$$

Important Design parameters of screw feeder bought on local market for reverse design are:

C = radial clearance between screw and tubing= 3mm

D = screw diameter = 160mm

D_c = shaft diameter = 50mm

P_s = the screw pitch = 100

t_s = thickness of the screw flight = 3mm

ω = 11.6rad/min rotation of screw feeder

The overall length of the screw feeder is 65cm.

The actual volumetric throughput (material) of the screw conveyor Q_{act} is less than the theoretical and is quantified by volumetric efficiency and is given by: $\eta_v = \frac{Q_{act}}{Q_t}$ the intention is to attain volumetric efficiency 0.90 of the screw feeder so its actual throughput

The major factor in determining volumetric efficiency is the rotational motion of the bulk material. As rotational speed increases, rotational motion decreases and volumetric efficiency increases. Other factor is friction between the bulk material and the flow channel.

4.9. Design of Reactors

The main part of a pyrolysis plant is the reactor. The most common pyrolysis systems employ the following types of reactor: rotary kiln, moving-bed with cocurrent or countercurrent flow (in convensional pyrolysis).

4.9.1. Types of reactors

All over the world researchers have been studying the pyrolysis of agricultural residues(straw, husks, corncobs, tea residues, sesame stalks, hazelnuts, sugarcane, sorghum, almond shells, rapeseeds, tobacco stalks and leaves, algea, cotton straw, sunflower bagasse, switch grass , woods and forestry residues, and many others) by utilizing a variety of different fluidized beds [35]. The different types of reactor design are the following:

1. Fluidized bed reactor (this include Bubbling Fluidized Bed and Circulating Fluidized Bed).
2. Ablative Reactor
3. Rotating cone Reactor
4. Vacuum Reactor
5. Screw Reactor

Only Screw reactor is to be discussed indepth. The majority of pyrolysis reactor technologies are grouped in the following groups based on how heat transfer occurs to biomass.

a. Directly heated
b. Indirectly heated

Directly heated reactors: In directly heated reactors, biomass is heated by direct contact with the heating media that must be either completely free of oxygen or with limited amount of oxygen. The heating media could be hot gas, hot solids, superheated steam or electromagnetic radiation.

Indirectly heated reactors: In indirectly heated reactors biomass is heated across the wall of the reactor. Here the heat carrying medium does not contact the biomass.

Screw or stationery shaft: here the pyrolysis reactor (circular or rectangular cross section) is stationery, and it could be vertical , horizontal or inclined. A rotating screw mates and moves the biomass though the reactor to enhance heat transfer between wall and the bulk of the biomass and at the same time to move the biomass along its length. Similar to indirectly heated drum, hot outer wall heats the biomass indirectly and hence avoids direct contact with oxygen laden heating medium.

4.9.2. Screw reactor

In screw reactor biomass is not directly mixed with a dense heat carrier in the screw reactor. By using high thermal conductivity heat carriers, the energy required for slow pyrolysis is rapidly transferred to the biomass. Biochar produced is separated from the heat carrier independent of the pyrolysis reactions.The advatages of screw reactor are low pyrolsis temperature, compact, flexible design, no carrier gas and quility biochar produced and its disadvantages are plugging risk, lower bio-oil yield, moving parts in the hot zone and heat transfer limitations at large scale. The reactors were designed as concentric tube heat exchangers, with an inner reactor pipe containing the biomass during the process and an outer pipe surrounding the reactor pipe carrying hot gas. Hot conbustion gases from the after burner/combustiom chamber were introduced to the area between the two reactors as flue gas, while the biomass and pyrolysis gases were treated as an inner stream.

4.9.3. Material selection for construction of auger reactors

Table 4.3. Physical properties of stainless steel AISI [32].

Grade	Density (Kg/m^3)	Elastic modulus (GPa)	Mean coefficient of thermal expansion			Thermal conductivity		Specific heat	Electrical Resistivity n. $\Omega.m$
			0-100℃ μm/m/℃	0-315℃ μm/m/℃	0-538℃ μm/m/℃	At 100℃ (W/m.K)	At 500℃ (W/m.K)	0-100℃ (J/kg.K)	
All	7900	193	17	17.2	18.2	16.3	21.5	500	720

For the screw reactor construction, a corrosion resistant material is required due to tarry compounds. Stainless steel is commonly used in the chemical industry and there are wide ranges available.

4.9.4. The dimension of reactor

The volume of the cylinder

$$V = \pi * L * r^2 \tag{4.40}$$

For the simplification of fabrication a cylindrical reactor has been considered for the system using stainless steel.

i. Dimension of reactor

The system has double reactor i.e. the outer reactor in which the syngas is used for pyrolysis is occupied and the inner reactor in which the pyrolysis will take place and flower waste occupies. The convenient assumptions made to size the reactors is taking the inner reactor as standard screw conveyor housing and capacity of outer reactor as three times that of inner reactor.

- The capacity of outer reactor is $= 0.08 m^3$
- The capacity of inner reactor is$= 0.0281 m^3$

The outer volume of the cylindrical reactor would be as follows

$$V_o = \pi L_o r_o^{\,2} \Rightarrow \pi L_o r_o^{\,2} = 0.080 m^3$$

$L_o r_o^{\,2} = 0.0255$ And solving for one variable

$$r_o^{\,2} = 0.0255\left(\frac{1}{L_o}\right)$$

The inner volume of a cylindrical reactor would be as follows

$$V_i = \pi L_i r_i^{\,2} \Rightarrow \pi L_i r_i^{\,2} = 0.0281344 m^3$$

$$r_i^{\,2} = 0.008963\left(\frac{1}{L_i}\right)$$

Therefore, from the Mat lab result the maximum outer length of the reactor selected is 1.1m and the inner reactor length is 1.4m.

The maximum volume of area for the gas is determined by the difference between the outer reactor volume and the inner reactor volume as follows.

$$V_{\max,gas} = \pi R^2{}_o L_o - \pi R_i^{\,2} L_i$$

The maximum mass of flower waste occupied in the inner reactor is

$$M_{flower.Wast} = V_i * \rho_{dry}$$

4.10. Screw conveyor

The function of screw conveyor is to provide sufficient mixing and to convey the flower waste through the reactor as it is decomposed, so it can be operated in a continuous process. Some important points about screw conveyor is discussed as follows.

4.10.1. Hollow shaft horizontal Screw conveyor

This screw conveyor consists of a hollow shaft and helical blade which enclose the shaft. The shaft is coupled to driving unit and it is supported by bearings at both ends. Important dimensions of the screw conveyor bought in local market are:

C = radial clearance between screw and tubing= 3mm

D = screw diameter = 160mm

D_c = shaft diameter = 50mm

P_s = the screw pitch = 100

t_s = thickness of the screw flight = 3mm

ω = 11.6 rad/min reduced speed of motor

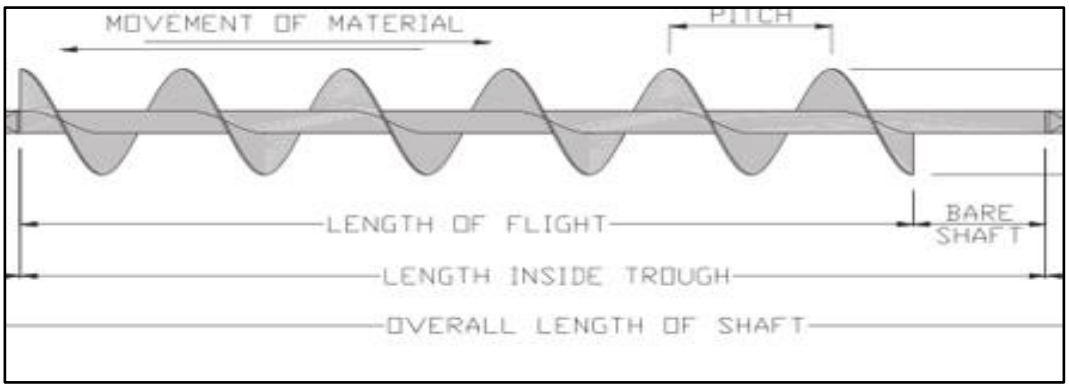

Figure 4.15. Hollow shaft screw Conveyor *[36]*.

Solid shaft is generally used only on short conveyors operating under extreme loads requiring extreme torque capacity.

Screw conveyors are widely used for transporting and/or elevating particulates at controlled and steady rates [36]. This horizontal screw conveyor is used to convey flower waste from screw feeder to discharging section. The characteristic dimensions of screw conveyor bought in local market:

1. Shaft diameter
2. Pitch length
3. Flight length
4. Screw diameter

The design of the screw is very important for mixing and characterization of the granular flow. The degree of mixing is an important factor in the heat transfer as the particle contact with the heated wall (inner reactor).

4.10.2. Material selection for screw conveyor design

Tempered Stainless steel screw conveyors are flights can be welded continuously to ideal for used where extreme temperatures are a problem. Stainless steel conveyor screws and parts are manufactured to the same specifications as are standard mild steel. The flights can be welded continuously to both sides of the hollow shaft and the weld may then my specifications.

4.10.3. Conveyor speed

For screw conveyors with screws having standard pitch helical flights the conveyor speed may be calculated by the formula.

$$V_{cs} = \frac{P_s n}{60} \qquad (4.\ 41)$$

n Revolutions per minute of screw (screw rotating speed)

P_s Is screw pitch

The effect of conveyor diameter to corresponding speeds is given by non-dimensional specific speed number by Revolutions per minute of screw shown in appendix B.

4.10.4. Conveyor throughput

The throughput of an enclosed screw conveyor is influenced by the rotational or vortex motion of the bulk material during transportation and the degree of fill or fullness of the screw. As the

rotational speed of the conveyor increases, the rotational or vortex motion decreases up to a limiting value, making for a more efficient conveying action. The net result for the throughput of the screw conveyor to reach a limiting value as illustrated in *Figure 4.16*.

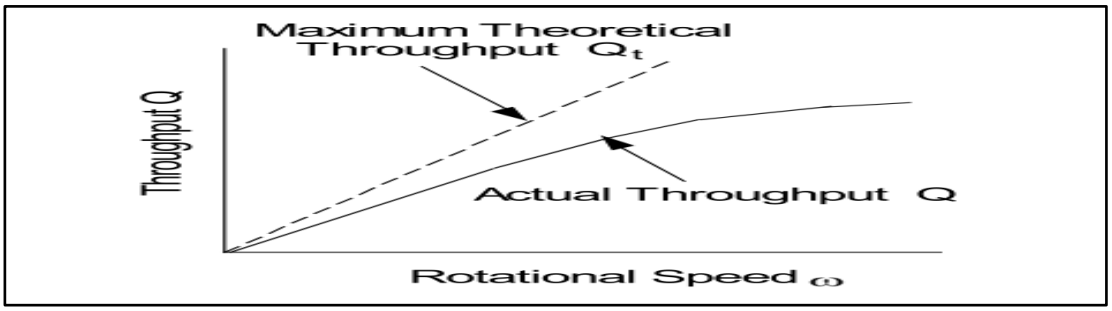

Figure 4.16. Conveyor Throughput

The volumetric through put of screw conveyor is given by equation (4.42) similar to screw feeder.

$$Q = Q_t * \eta_v \qquad (4.42)$$

Where $Q_t = A\omega D^3$

$$A = \frac{1}{8}\left[\left(1+2\frac{C}{D}\right)^2 - \left(\frac{D_c}{C}\right)^2\right]\left[\left(\frac{P_s}{D} - \frac{t_s}{D}\right)\right]$$

Q_t= maximum theoretical volumetric throughput with conveyor running 100% full and the bulk material moving axially without rotation.

The mass throughput- the influence of bulk density (ρ): the mass throughput of screw conveyor in kg/s is given by :

$$Q_m = \rho Q = Q_t \rho \eta_v$$

4.11. Cyclone

Cyclone separators are used as a collection device in continuous biochar production systems to separate the solid biochar and gasses. It employs a centrifugal force to separate biochar from a gas stream. The separation techniques: the biochar enters the cyclone with the flowing gas. The gas stream enters tangentially at the top of barrel and travels downward into the cone forming an outer vortex as shown in Figure 4.17 b.

Cyclone collection efficiency increases with increasing particle size, particle density, inlet gas velocity, cyclone body length, number of gas revolutions and smoothness of the cycle wall.

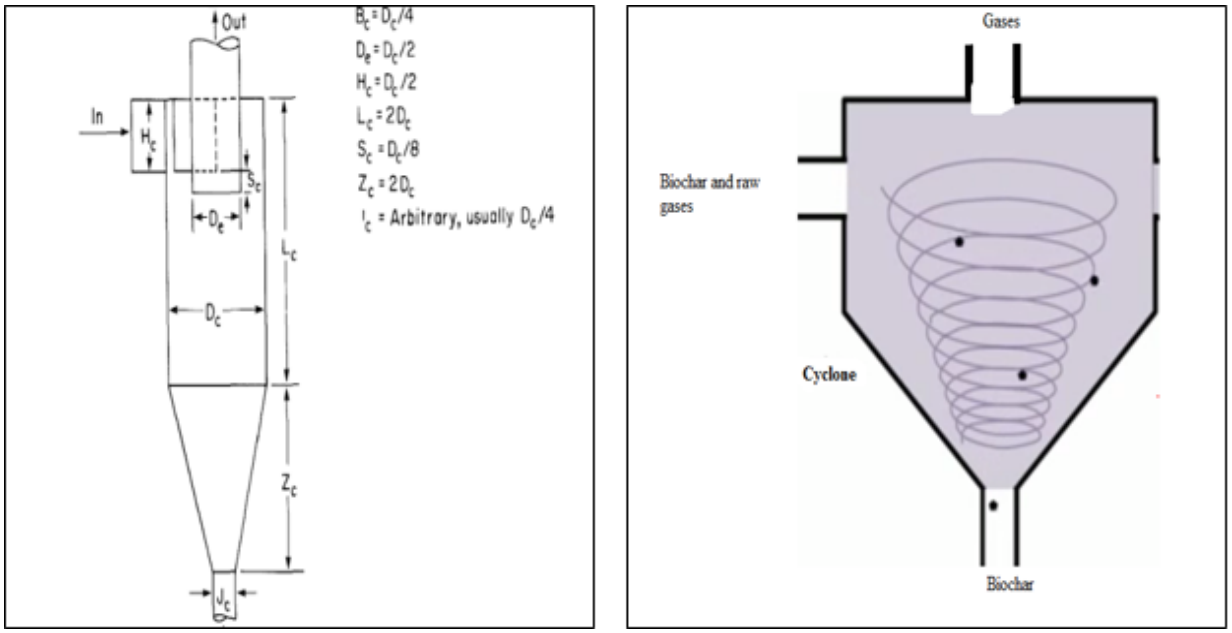

Figure 4.17. A. Modified geometric specification of a Cyclone [37]. B. Vortex flow

The inlet (H_c) of the cyclone is equal to the diameter of the internal reactor and is $H_c = 170mm$

Therefore the rest dimension of the cyclone will be determined as follows

$$H_c = \frac{D_c}{2} \qquad (4.\ 43)$$

4.12. Afterburner/combustion chamber

The afterburner unit supplies the reactor with warm combustion gases for external heating. The fuel used for starting the pyrolysis process is wood. Then this wood is combusted to initiate the pyrolysis. An air ratio was added to the system to assure a complete combustion and to be able to control the temperature of the combustion using compressor. This air ratio AR is at 100% theoretical air required for the combustion. The mass flow of the fuel controls the flow of the combustion gases into the system, while the air ratio controls the temperature of the incoming gases.

4.13. Manufactured Prototype and its manufacturing cost

The manufacturing process was done using the designed dimension. Based on the availability of the material in the market and machines in the workshop.

The parts of the machine that were manufactured are:

- Feed hopper
- Outer and inner Reactors
- Cyclone
- Afterburner/combustion chamber
- Frame
- Pulleys

Other components like a motor, belts, a compressor, gear box and screw conveyor were purchased based on the design analysis from local market.

Table 4.4.Total cost of the machine

No	Items	Description	Quantity	Unit price	Total cost in birr
1	- Motor	Medium duty	1	5000	5000
	- belt		2	200	400
	- Pulleys	Ø=170mm	2	600	1200
2	Inner reactor	Ø=170mmL=1400mm	1	1200	1200
3. Outer reactor		Ø=305mm L=1100mm	1	1200	1200
		90˚ elbow	4	50	200
		Cap	1	120	120
		Sheet metal	3	1100	3300
4.	Biomass preparation &characterization(lab)		1	2000	2000
5.	Total				14,620

5. Chapter 5: Heat Transfer, model and simulation

5.1. Heat transfer Analysis on the reactor

In screw reactor heat transfer involves the following:

1. Conduction
2. Convection in moving gas and
3. Radiation between wall and particles.

The flower waste enters screw reactor at an ambient temperature and the flue gas from afterburner/combustion chamber enters the outer reactor at $773^{\circ}C$. This shows that there was a temperature gradient inside a screw reactor during the slow pyrolysis processs due to heat transfer. For the first few minutes after the experiment started, the temperature inside the reactor gradually increases and reaches pyrolysis temperature.

The energy balance of the reactor contains several different parts that interact through different heat transfers. To simplify the calculations and attain temperature profile of the reactor, a discretization is made.

The heat transfers in the systems for conduction and convection.

$$\dot{Q} = \frac{\Delta T}{\sum R} \qquad (5.1)$$

$\dot{Q}$ The heat transfer rate

R Total thermal resistance for heat transfer.

For heat transfers based on mass transfer the following formula is used. The formula based on the mass transfer between control volumes ṁ, the specific heat capacity of the mass and the temperature difference in the control volumes.

$$\dot{Q} = m_o * C_p * \Delta T \quad \Rightarrow \quad \dot{Q} = m_o * C_p * (T_2 - T_1) \qquad (5.2)$$

From design of reactors inner reactors with $r_i = 0.085m$ and outer reactor $r_o = 0.125m$ and its length (outer reactor $L_o = 1.1m$ and inner $L_i = 1.4m$) has been determined. The $\dot{Q} = 3.58^{kg}/_{s} * 500^{J}/_{kg.K} * (773-298)K = 850250^{J}/_{s} = 850.25kW$ thermal conductivity of the material of which the reactor is made is $k = 21.5^{w}/_{m.k}$ and its specific heat capacity is $C_p = 500^{J}/_{kg.K}$. Heat rate calculated as follows.

5.2. Heating method

The hot combustion gases enter the reactor through a pipe in the side of reactor and exits the reactor in one end. This design was chosen to give heat convection covering the entire reactor. The entry point of the combustion gases was assumed to be the point where the gases changes from parallel flow to counter flow. The counter heat transfer or exchange is used to give an even temperature increase in the biomass, producing a linear increase in temperature.

The parallel flow is then used to keep an even high temperature in the biomass until the reactor exit. These two flows take place between the inner and outer reactor similar in the annular heat exchanger.

5.3. Governing equation for the system

Cylindrical and spherical systems often experience temperature gradients in the radial direction only and may therefore be treated as one dimensional. The cylindrical system is analysed by means of standard method implementing appropriate Fourier's law [38].

5.4. Conduction heat transfer through circular cylinders

For one dimensional steady-state conditions heat conduction with no heat generation, the appropriate form of equation. Conduction heat transfer can be expressed by Fourier's law of heat conduction as [39]:

$$\frac{1}{r^2}\frac{d}{dr}\left(kr^2\frac{dT}{dr}\right)=0 \tag{5.3}$$

$$T(r)=T_{s,1}-\{T_{s,1}-T_{s,2}\}\left[\frac{1-r_1/r}{1-r_1/r_2}\right] \tag{5.4}$$

For a cylinder with length very large compared to diameter, it may assumed the heat flows only in the radial direction, so that the only space coordinate needed to specify the system is radius(r). The area for heat flow in cylindrical system is

$$A_r=2\pi rL \tag{5.5}$$

So that Fourier's law is written as

$$q_r=-kA_r\frac{dT}{dr}=-2\pi Lk\frac{dT}{dr} \tag{5.6}$$

$$q_r = -kA\frac{dT}{dr} = \frac{4\pi k(T_{s,1} - T_{s,2})}{\left(1/r_1 - 1/r_2\right)}$$

The heat loss per unit length is the insulation glass wool having the following properties

$$T = 645K : k = 0.089 W/m.k$$

$$\dot{q}_r = \frac{q_r}{q_L} = \frac{2\pi K(T_{s,1} - T_{s,2})}{\ln\left(D_2/D_1\right)} = \frac{2\pi(0.089 W/m.K)(773-298)K}{\ln(0.25/0.17)} = 689.58 W/m$$

Heat transferred to the outer surface is dissipated to the surroundings by convection and radiation. To account for this an insulation was provided.

The thermal resistance has been calculated based on the method of heat transfer and the surface area of the transfer surface. The thermal resistance for conduction and convection is calculated as follows.

$$R_{cond} = \frac{L}{k * A_s} = \frac{L_i}{k * A_i} \qquad (5.7)$$

The thermal resistance associated with conduction of heat is the ratio of driving potential to transfer rate for conduction in radial system

$$R_{t,cond} = \frac{\frac{1}{r_1} - \frac{1}{r_2}}{4\pi k} = \frac{\frac{1}{0.085} - \frac{1}{0.1525}}{4 * 3.14 * 21.5} = 0.01928 km^2/W$$

Thermal resistance may be associated with heat transfer by convection at a surface. The resistance for convection is then;

$$R_{conv} \frac{1}{h * A_s} \qquad (5.8)$$

The property of material and parts used for reactor is selected from heat transfer book.

Heat transfer analysis on this reactor can be modelled as counter flow heat exchanger just by considering the general case of axial variation of temperature in a reactor with the wall at uniform temperature T_o (pyrolysis temperature) and biomass flowing inside the inner reactor *Figure 2.1*.

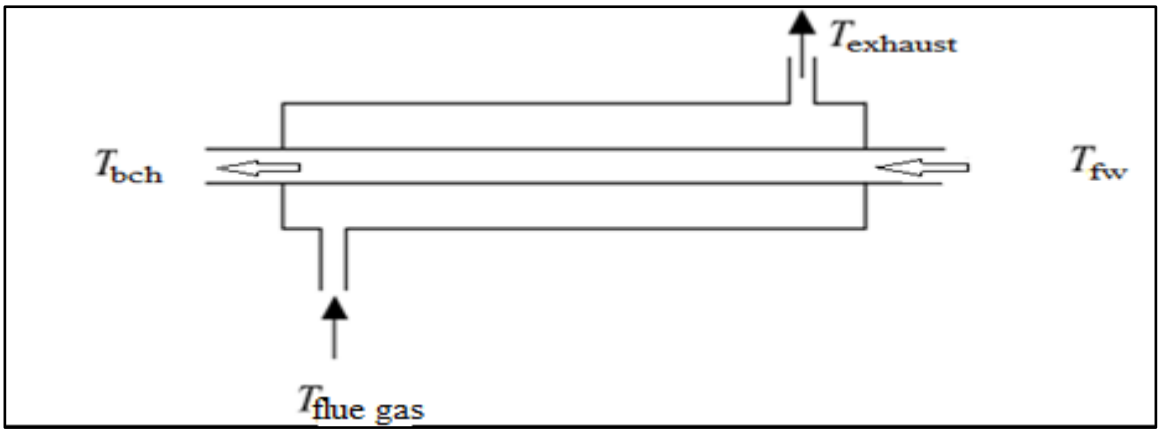

Figure 5.1 Heat transfer on reactors (similar to counter flow heat exchanger)

5.5. Insulation

The addition of insulation material on a surface reduces the amount of heat flow to the ambient.

Requirement of the insulation

1. To maintain temperature condition in the slow pyrolysis process
2. To reduce heat loss or gain
3. To maintain the effective operation of chemical reaction
4. To assist in maintaining a product at constant temperature
5. Assisting in the reduction of environmental pollution
6. To conserve energy

Heat transfers through insulation material occur by means of conduction, while heat loss to or gain from atmosphere occurs by means of convection and radiation.

Table 5.1. Insulation types and applications

Type	Temperature Range , $^{\circ}C$	Thermal conductivity $W/m^{\circ}C$	Density kg/m^3	Application
Fiberglass board	20-450	33-52	25-100	Boilers, tanks, heat exchangers
Calcium silicate blocks, boards	230-1000	32-85	100-160	Hot piping, boilers, chimney linings
Mineral wool blocks	450-1000	52-130	175-290	Hot piping
Glass wool	645	0.089		

Boundary conditions

$T = T_i$ And $r = r_i$

$T = T_o$ And $r = r_o$

Therefore the solution for Fourier equation is

$$q_r = \frac{2\pi kL(T_i - T_o)}{\ln\left(r_o / r_i\right)} \tag{5.9}$$

And the thermal resistance in this case is

$$R_{th} = \frac{\ln\left(r_o / r_i\right)}{2\pi kL} \tag{5.10}$$

A thick-walled tube of stainless steel with k=21.5 with 305 outer diameter with 170 inner diameter is covered a 0.5cm layer of insulation glass wool $k = 0.089 W/m.K$ if the inside wall of the reactor is maintained at $500^{o}C$ so we need to calculate the heat loss or gain at length of 1.1m and inner reactor to insulation interface temperature. From design of reactors inner reactors with $r_i = 0.085m$ and outer reactor $r_o = 0.125m$ and its length (outer reactor $L_o = 1.1m$ and inner $L_i = 1.4m$) has been determined. The thermal conductivity of the material of which the reactor is made is $k = 21.5 w/m.k$ and its specific heat capacity is $C_p = 500 J/kg.K$

The heat rate per length

$$q_r = \frac{2\pi(T_1 - T_2)}{\frac{\ln(r_2/r_1)}{k_{steel} L_i} + \frac{\ln(r_3/r_2)}{k_{glasswool} L_o}} = \frac{2*3.14*(873-373)K}{\frac{\ln(85/80)}{(21.5 w/m.k)*1.4m} + \frac{\ln(152.5/85)}{(0.245 w/m.k)*1.1m}} = 1446.4 w/m$$

To find the interface temperature between the wall of outer reactor and the insulation this heat loss is used.

$$q_r = \frac{T_a - T_2}{\frac{\ln(r_3/r_2)}{2\pi k_{glasswool} L_o}} = 1446.4 w/m$$ Solving for unknown variable and inserting the values to obtain the interface temperature

$$T_a = 872.5k$$

Critical thickness of insulation

The inner temperature of the insulation is fixed at T_i, and the outer surface is exposed to a convection environment at T_∞. From the thermal network the heat transfer is

$$q = \frac{2\pi L(T_i - T_\infty)}{\frac{\ln(r_o/r_i)}{k} + \frac{1}{r_o h}} \qquad (5.11)$$

To determine the outer radius of insulation r_o maximize the heat transfer so the condition will be

$$\frac{dq}{dr_o} = 0 = \frac{-2\pi L(T_i - T_\infty)\left(\frac{1}{kr_o} - \frac{1}{hr_o^2}\right)}{\left[\frac{\ln\left(r_o/r_i\right)}{k} + \frac{1}{r_o h}\right]^2}$$ Which give the result $r_o = \frac{k}{h}$

$r_o = \frac{k}{h}$ Expresses the concept of critical radius of insulation. If the outer radius is less than the value given by $r_o = \frac{k}{h}$, then the heat transfer will be increased by adding more insulation. For outer radii greater than the critical value an increase in insulation thickness will cause a decrease in heat transfer. The central concept is that for sufficiently small values of h the convection heat loss may actually increase with addition of insulation because of increased surface area. At the motion of screw conveyor, the heat transfer is strengthened past regular conduction of materials. In this mode the motion of screw conveyor causes the heat transfer to reach state of convection.

The heat transfer coefficient is in this case based on the radius and length of the reactor segment covered by biomass in the radial direction, along with the biomass properties conductivity, density and specific heat capacity will be given as follows

$$h = \sqrt{\frac{2\pi r}{L_i}\left(k * \rho * C_p\right)} \qquad (5.12)$$

5.6. Convection heat transfer

The flower waste flows opposite to the direction of flue gas along the inner reactor. The flower waste flows inside the inner reactor and the flue gas (steam) flows though the annulus (the outer reactor). The heat transfer take place through the inner reactor surface, from the steam part to the solid part i.e. across the surface of the inner reactor by convection.

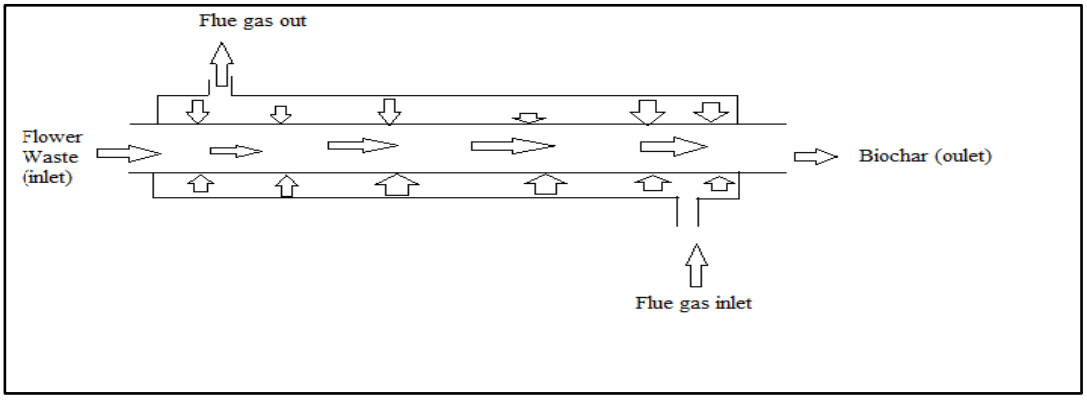

Figure 5.2. Convection Heat transfer

Since in my assumption the outer surface of the reactor is adiabatic, the rate at which energy is generated within the reactor wall must equal the rate at which it is converted to biochar.

$$E_{gen} = q_{conv} \tag{5.13}$$

$$E_{gen} = q * \frac{\pi}{4}\left(D_o{}^2 - D_i{}^2\right) * L_o \text{ But } E_{gen} = C_p * m\left(T_{m,o} - T_{m,i}\right) \text{ then} \tag{5.14}$$

$$C_p * m\left(T_{m,o} - T_{m,i}\right) = q * \frac{\pi}{4}\left(D_o{}^2 - D_i{}^2\right) * L_o$$

$$L_o = \left[\frac{4C_p * m\left(T_{m,o} - T_{m,i}\right)}{q * \pi * \left(D_o{}^2 - D_i{}^2\right)}\right] \tag{5.15}$$

So if the mass of biomass varies what would be the length of the reactor will be studied using Mat lab software.

5.7. Energy input and Feed rate

5.7.1. Enthalpy Analysis for selected biomass (flower waste)

The design of the system may vary with respect to heat transfer issues or sizing of the reactor on the basis of the energy required to carry out the pyrolysis. Enthalpy for pyrolysis, h_p, is defined as the energy required to raise biomass from room temperature to the reaction temperature and convert the solid biomass into the reaction products of gas, Biochar and probably liquids. Or it is the total energy consumed by the biomass during pyrolysis. We have two types of enthalpy in this case these are: sensible enthalpy and reaction of enthalpy. The Sensible enthalpy refers to energy absorbed by the biomass to raise its temperature only. The enthalpy of reaction is the energy required to drive the pyrolysis reactions [40].

5.7.2. Energy balance on the pyrolysis reactor

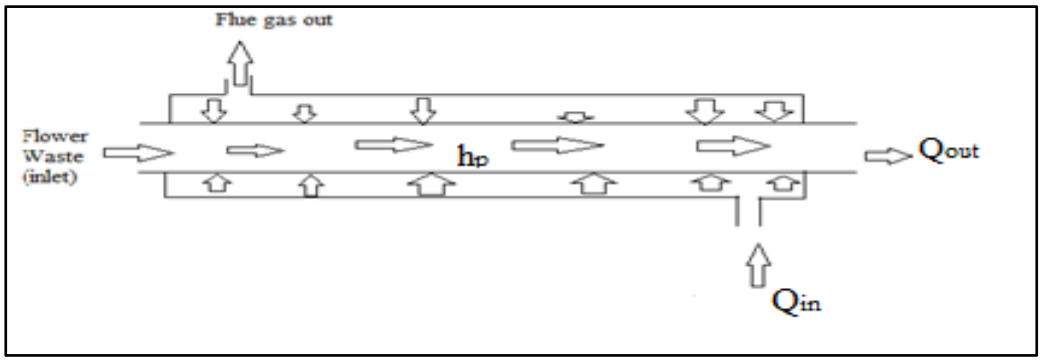

Figure 5.3. Energy Balance on the Pyrolysis Reactors

The energy flows for pyrolytic reactor are illustrated in *Figure 5.3*. There are two primary heat flows and as well as two flow of enthalpy. The first inflow, represented by $H_{bio,in}$ is enthalpy introduced to the reactor from the feedstock flowing into the system. The second inflow energy,Q_{in} is associated with the heat transfer into the system that results from the combustion of vapours and gases in the afterburner/combustion chamber. The energy out flows is the enthalpy, H_{out} is associated the exiting flue gas. In addition, a heat loss Q_{loss} also is considered in the analysis. Last, the enthalpy flow H_p is consumed by the biomass in the pyrolysis process. The resulting energy balance used to describe the system is

$$H_p = Q_{in} + H_{bio,in} - Q_{loss} - H_{out} \tag{5.16}$$

During this pyrolysis process the system was assumed and brought to steady state with respect to the bed temperature. All parameters remained constant at their initial values except for the mass flow rate of the biomass until constant bed temperature was achieved in specified residence time. The inlet and exit temperatures of the biomass were monitored with IR thermometer. The biomass heat flows were calculated with the following equation.

$$H_{bio,in} = \dot{m}_b * C_{p,in} * (T_{in} - T_{amb}) \tag{5.17}$$

Simpson and TenWolde (1999) report that the heat capacity of dry biomass is approximated related to temperature by the following equation. The temperature range for the correlation is not mentioned.

$$C_{p,biom} = 0.1031 + 0.003867T \tag{5.18}$$

The biomass specifically flower waste enter into the reactors at reference temperature i.e. $25^{\circ}C$

$$C_{p,in,fw} = 0.1031 + 0.003867(298K)\,{}^{kJ}\!/_{kg.K} = 1.255\,{}^{kJ}\!/_{kg}.K$$

$$H_{bio,in} = 3.58\,{}^{kg}\!/_{s} * 1.255\,{}^{kJ}\!/_{kg.K} * (373 - 298)K = 336.97kW$$

The output enthalpy can be evaluated as follows

$$H_{out} = \dot{m}_b * C_{p,out} * (T_{out} - T_{amb}) \tag{5.19}$$

$$C_{p,biom} = 0.1031 + 0.003867(1173K)\,{}^{kJ}\!/_{kg.K} = 4.63909\,{}^{kJ}\!/_{kg}$$

$$H_{out} = 3.58^{kg}/_{s} * 4.63909^{kJ}/_{kg.K} * (1173 - 298)K = 14531.949kW$$

$$Q_{in} = H_{RP} + \sum_{R}(\Delta H_i) - \sum_{P}(\Delta \mathrm{H}_i)$$

H_{RP} = enthalpy of combustion of syngas (vapours and gases in air)

$\sum_{R}(\Delta H_i)$ = sensible enthalpy of the entering reactant (biomass), is equal to zero because reactants enter at essentially at the reference temperature.

$$Q_{in} = H_{RP} - \sum_{P}(\Delta \mathrm{H}_i) \qquad (5.20)$$

$\sum_{P}(\Delta \mathrm{H}_i)$ The sensible enthalpy of the exiting producer gas from combustion process in the afterburner. This enthalpy was calculated from the knowledge of the gas and air flow rates at steady state in the afterburner. The heat of combustion of the gas was calculated assuming complete combustion of the fuel (Thermodynamics book). The enthalpy associated with the exiting hot gas is defined as follows

$$\sum_{P}(\Delta \mathrm{H}_i) = \sum_{i}\left(\dot{m_g} *\right)\left(C_{p,i}\left(T_{hot,gas} - T_{amb}\right)\right) \qquad (5.21)$$

$$\sum_{p}(\Delta \mathrm{H}_i) = 0.2747^{kg}/_{s} * 10^{J}/_{kg.K} * (920 - 298)K = 1.709kW$$

Lastly rearranging $H_p = Q_{in} + H_{bio,in} - Q_{loss} - H_{out}$

$$Q_{loss} = Q_{in} + H_{bio,in} - H_p - H_{out}$$

Enthalpy for pyrolysis on a mass basis can be calculated as follows for any biomass

$$h_p = \frac{H_p}{\dot{m}} \qquad (5.22)$$

5.8. Heat Losses from the Reactor Surface

5.8.1. Radiation

Radiation can be a major form of heat loss. In this system, radiation losses occur from the outer reactor surfaces i.e. on the whole sides of the reactor. Calculation of the radiation heat transfer

coefficient assuming the surface of the reactor is $500^{\circ}C$. In order to reduce the insulation thickness and overall reactor size, a surface $500^{\circ}C$ was selected. The radiation heat transfer coefficient for the surface temperature of $500^{\circ}C$.

$$h_{rad} = \varepsilon\sigma\left(T_{surf}{}^{2} - T_{surr}{}^{2}\right)\left(T_{surf} + T_{surr}\right) \tag{5.23}$$

$$\sigma = 5.67*10^{-10}\ \frac{W}{m^2 k}$$

$$h_{rad} = 0.63*5.67*10^{-10}\left(773^2 + 298^2\right)(773+298)$$

$$h_{rad} = 0.2626\frac{W}{m^2}k^2$$

Radiation heat loss from the reactor surfaces

$$Q_{rad} = h_{rad}A_{surf}\left(T_{surf} + T_{surr}\right) \tag{5.24}$$

$$Q_{rad} = 0.2626*2\pi*0.1525*1.1(773+298) = 296.28W$$

The heat losses due to radiation become more significant as the surface temperature of the reactor increases.

5.8.2. Convection Heat Losses

Convection heat losses can occur from the top of the reactor, the sides of the reactor, on the surface of the reactor and the wall of the reactor. Losses due to convection can be determined by variety of methods. Calculating the convective heat transfer coefficient using standardized method (Welty, 1978) is one where the heat transfer coefficient, h_c is a function of the Nusselt number N_u. K is the thermal conductivity of material from the reactor is made and L_{reac} is the length of the reactor.

$$h_c = \frac{N_u * k}{L_{reac}} \tag{5.25}$$

5.9. Modelling biomass pyrolysis

The first step in modelling the pyrolysis process of a biomass is creating a model for the chemical processes taking place.

The three major processes that influence the pyrolysis rates are chemical kinetics, the heat transfer and the mass transfer.

Kinetic model

The slow pyrolysis of biomass is typically carried out in a relatively low temperature range and the initial products are non-condensable gases (like CO, CO_2, H_2 and CH_4) and solid biochar. This decomposition occurs partly through gas-phase homogeneous reactions and partly through gas-solid phase heterogeneous thermal reactions. Condensable and non-condensable vapour are separated from the biomass, leaving the pyrolysis zone [41].

Types of kinetic model of biomass pyrolysis

a. One stage global single reaction

The pyrolysis is modelled by a one-step reaction using experimentally measured mass loss rates. The commonly used equation for a single step reaction, combined with an n^{th} order reaction model, was used to describe the kinetics of biomass pyrolysis;

$$\frac{d\alpha}{dt} = k(1-\alpha)^n$$

b. One stage, multiple reactions

Several parallel reactions are used to describe the degradation of biomass into char and several gases. A one-stage simplified kinetic model is used for these parallel reactions. It is used for determination of product distribution.

c. Multi step kinetic model

This model includes both primary and secondary reactions, occurring in series.

The first step in the modelling of the biomass pyrolysis is creating a model for the chemical processes taking place. This model should describe the used fuel, the reactions taking place and the products created in the process.

The multi-step kinetic model of biomass pyrolysis is based on convectional multistep de-volatilization models of three main biomass components (cellulose, hemi-celluloses and lignin) and gives detailed information on the composition of the yields of gas, tar and solid residue [41].

One-stage Global Single-Reaction Model

This reaction model is based on a single oveall reaction;

$$Biomass \rightarrow Volatile + Char$$

The rate of pyrolysis depends on the un-pyrolyzed mass of the biomass. Thus, the decomposition rate of mass, m_b, in the primary prolysis process may be writen as [22].

$$\frac{dm_b}{dt} = -k(m_b - m_c) \tag{5.26}$$

m_c is mass of the char remaining after complete conversion (kg), k is the first order reaction rate constant (s^{-1}) and t is the time (s).

The fractional change, X, in the mass of the biomass may be writen in nondimensional form as

$$X = \frac{(m_o - m_b)}{(m_o - m_c)} \tag{5.27}$$

Where m_0 is the initial mass of the biomass (kg). Substituting fractional conversion for the mass of biomass in 5.27. equation

$$\frac{dX}{dt} = -k(1 - X)$$

Solving this equation to get

$$X = 1 - A\exp(-kt) \tag{5.28}$$

The temperature dependency of the rate constant can be expressed in Arrhenius form as

$$k = A.e^{\frac{-E}{RT}}$$

Where A is pre-exponential factor coefficient, E is the activation energy $\left(J/_{mol}\right)$, is the gas constant $\left(J/_{mol.K}\right)$ and T is the temperature (K). Activation energy is the minimum amount of energy required to initiate chemical reaction i.e. pyrolysis process.

Owing to the difficulties in extracting data from dynamic thermogravimetric analysis, reliable data on pre-exponential factor and activation energy are not easily available for fast pyrolysis.

However, for slow heating we can obtain some reasonable values. If the effect of second cracking and heat transfer limitation can be restricted, the weight loss rate of pure cellulose during pyrolysis can be represented by an irrevarsible, one-stage global first order equation.

Solving Arrhenius equation for only two data points by taking ln both sides

$$\ln k = \ln\left(Ae^{-E_a/RT} \right)$$

$$\ln k = \ln A - E_a/RT \Rightarrow \ln k = \ln A - \frac{E_a}{R} * \frac{1}{T}$$

For two data points i.e. @ T_1, k_1 and T_2, k_2

$$\ln k_1 = \ln A - \frac{E_a}{R} * \frac{1}{T_1} \qquad *$$

$$\ln k_2 = \ln A - \frac{E_a}{R} * \frac{1}{T_2} \qquad **$$

$\ln A$ doesnot change with temperature and so subtract equation ** from equation * to get the following expression

$$\ln k_1 - \ln k_2 = -\frac{E_a}{R}\left(\frac{1}{T_1} - \frac{1}{T_2} \right) \text{ but } \ln k_1 - \ln k_2 = \ln\left(k_1/k_2 \right)$$

$$\ln\left(k_1/k_2 \right) = \frac{E_a}{R}\left(\frac{1}{T_2} - \frac{1}{T_1} \right)$$

$\left(\frac{1}{T_1} - \frac{1}{T_2} \right)$ can be writen as $\left(\frac{1}{T_1} - \frac{1}{T_2} \right) = \frac{T_1}{T_1 * T_2} - \frac{T_2}{T_2 * T_1} = \frac{T_1 - T_2}{T_1 * T_2}$

$$\ln\left(k_1/k_2 \right) = \frac{E_a}{R}\left(\frac{T_1 - T_2}{T_1 * T_2} \right) \qquad (5.29)$$

Table 5.2. The chemical process

Temp($^\circ C$)	Time(s)	Temp(K)	$\frac{1}{T(K-1)}$	$\frac{1}{t(s-1)}$	$\ln\left(\frac{1}{t}\right)$
50	30	323	3.10E-03	3.33E-02	-3.40
200	45	473	2.11E-03	2.22E-02	-3.81
350	60	623	1.61E-03	1.67E-02	-4.09
500	75	773	1.29E-03	1.33E-02	-4.32
650	90	923	1.08E-03	1.11E-02	-4.50
800	105	1073	9.32E-04	9.52E-03	-4.65

The chemistry of pyrolysis is strongly influenced by the chemical composition of the fuel. The elemental composition of the fuel is obtained from ultimate analysis. The percentage of the major products of pyrolysis (volatiles and char) is obtained from proximate analysis.

5.10. Simulation

5.10.1 Adding Physics

COMSOL Multiphysics uses the finite element method (FEM) to solve the model. The problem studied was 3D, transient and time dependent heat transfer problem.

5.10.2. Defining Geometry

The geometry i.e. inner screw reactor and outer reactor was first designed using ACATIA V5R19 software based on the dimensions obtained under design of components which later assembled and then was saved in an igs. Model. The model was later simulated using COMSOL 5.0 Multiphysics. Heat is transferred by conduction through the outer reactor to the inner screw reactor, where there is gases and released by convection to the wall of inner reactor, conducted through the wall. The flow is assumed to be time dependent.

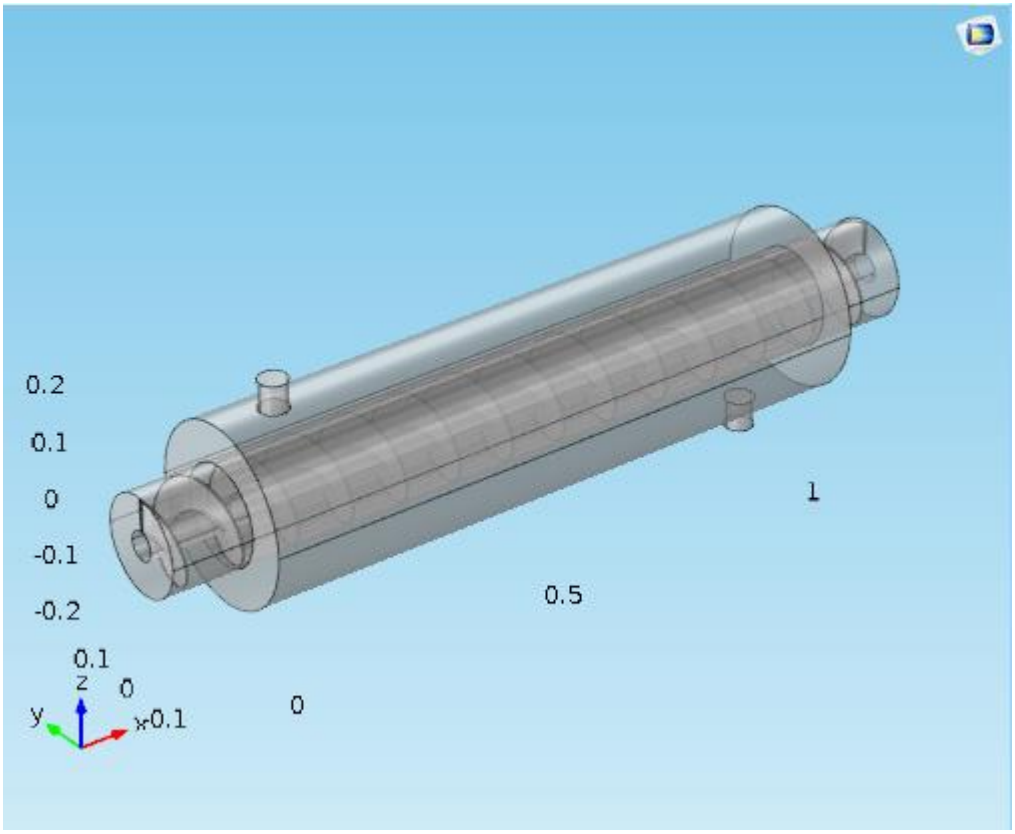

Figure 5.4. Internal detail of screw reactor

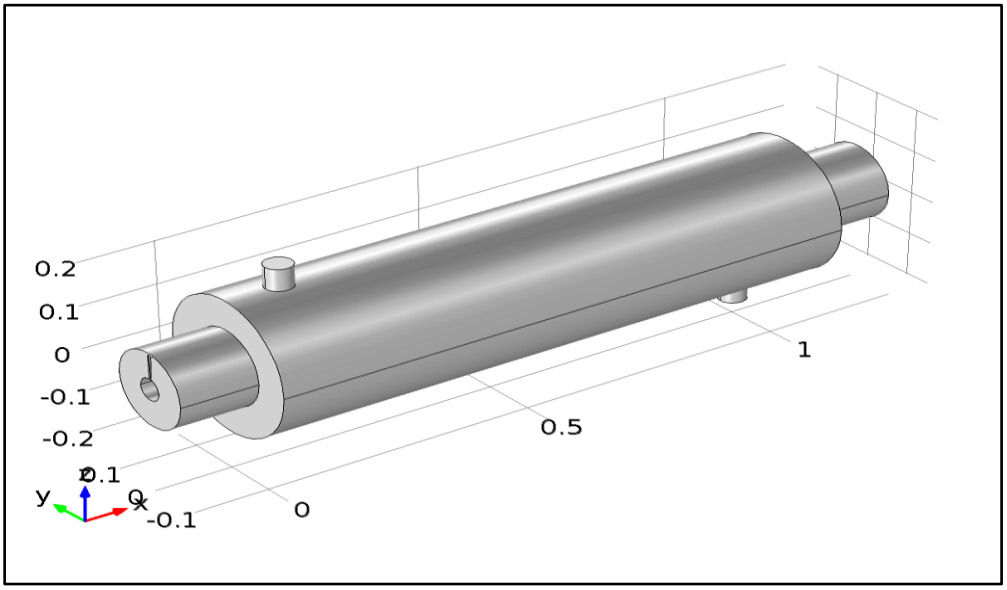

Figure 5.5. 3D geometry

5.10.3. Material Selection

Steel AISI 4340 were selected on the material browser and values of the selected parameters were supplied on the material. The material content of all used material were tabulated as follows:

Table 5.3. Material contents of Flower waste

Property	Name	Value	Unit	Property group
Heat capacity at constant pressure	C_p	1200	$J/Kg.k$	Basic
Density	ρ	540	Kg/m^3	Basic
Thermal conductivity	K	0.023	$W/m.k$	Basic

Table 5.4. Material contents of flue gas

Property	Name	Value	Unit	Property group
Heat capacity at constant pressure	C_p	1500	$J/Kg.k$	Basic
Density	ρ	2310	Kg/m^3	Basic
Thermal conductivity	K	0.173	$W/m.k$	Basic

Table 5.5. Material content of Steel AISI

Property	Name	Value	Unit	Property group
Heat capacity at constant pressure	C_p	500	$J/Kg.k$	Basic
Density	ρ	7900	Kg/m^3	Basic
Thermal conductivity	K	21.5	$W/m.k$	Basic

Heat transfer in solids

For an incompressible flower waste material heated under constant pressure, the thermal energy equation is given by equation 4.30.

$$\rho C_p \frac{\partial T}{\partial t} + \rho C_p U.\nabla T = \nabla.(K\nabla T) + Q \quad (5.30)$$

Convective heating

$$-n.(-K\nabla T) = h.(T_{ext} - T) \quad (5.31)$$

5.10.4. Meshing

The mesh chosen was free tetrahedral. The completed mesh consists of 534353 elements and the maximum element size of 0.14mm and minimum element size of 0.0252mm.

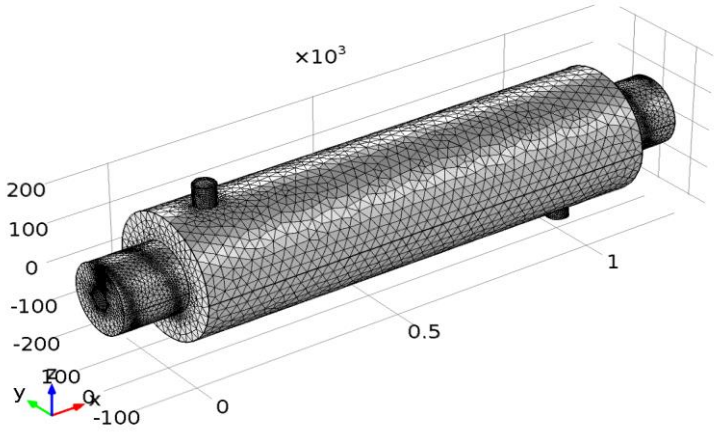

Figure 5.6. Meshing

4.10.5 Study

A time dependent study was chosen at a range of 0, 0.1,30 in the edit field, before all temperature (ht) plot was updated at a time discrete solver.

Table 5.6.Boundary conditions values used

Description	Symbol	Value	Unit
In let inner reactor temperature	T_fw	25	^{o}C
Inlet outer reactor temperature	T_s	500	^{o}C
Flue gas inlet velocity	V_s	5	m/s
Outlet gas pressure	P_out	0	Pa

Table 5.7.Parameters used

Description	Symbol	Value	Unit
Length of the outer reactor	L_o	1.1	m
Length of the inner reactor	L_i	1.4	m
Diameter of the inner reactor	D_i	170	mm
Diameter of the outer reactor	D_o	305	mm

4.10.6 Model post-processing

The obtained simulated results from the COMSOL Multiphysics are presented as follows:

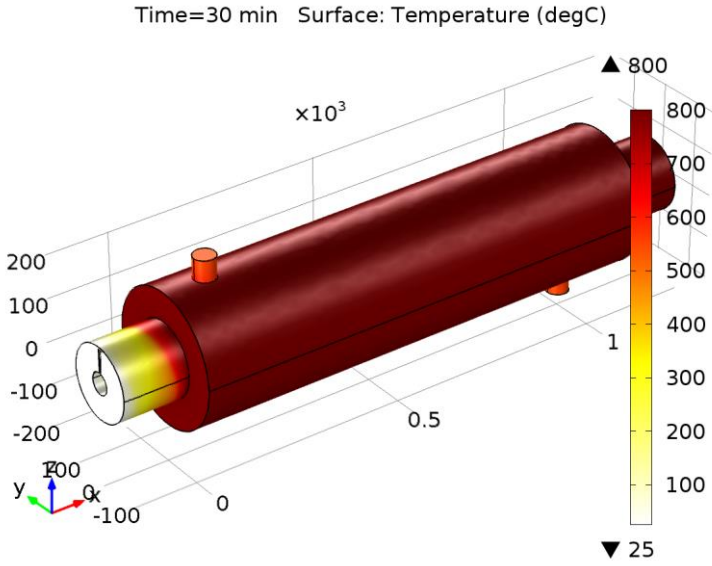

Figure 5.7. Simulation of heating flower waste with temperature 25 to 800 ^{o}C at 30min.

Temperature along xy plane

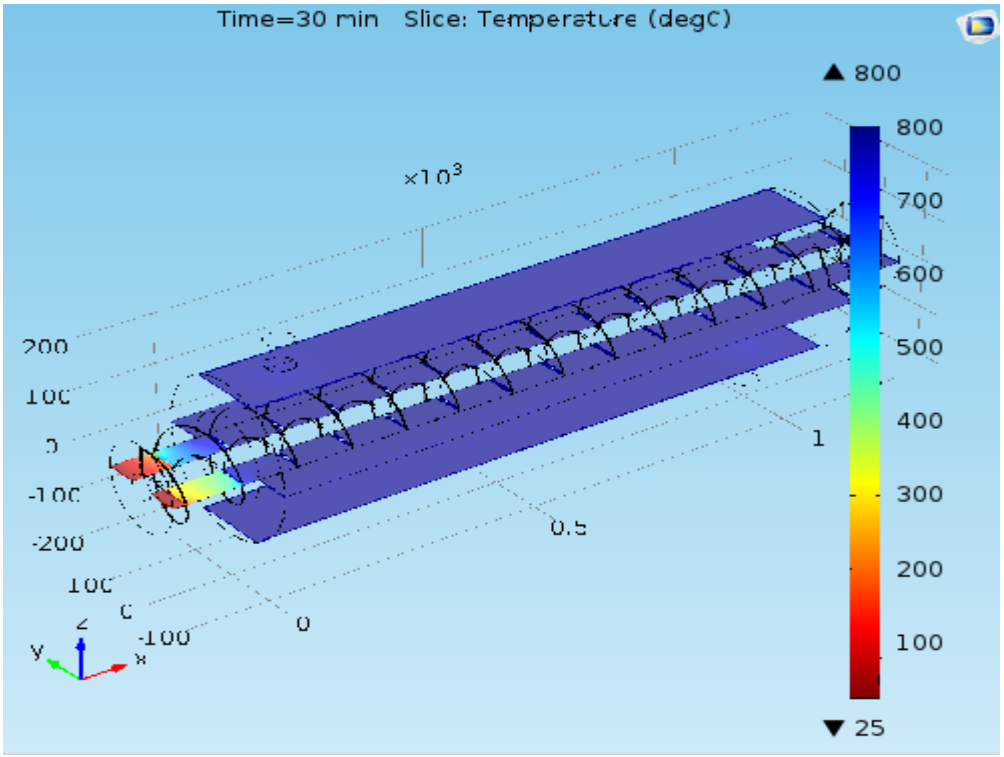

Figure 5.8. Simulation of Temperature profile 3 planes along xy[a]

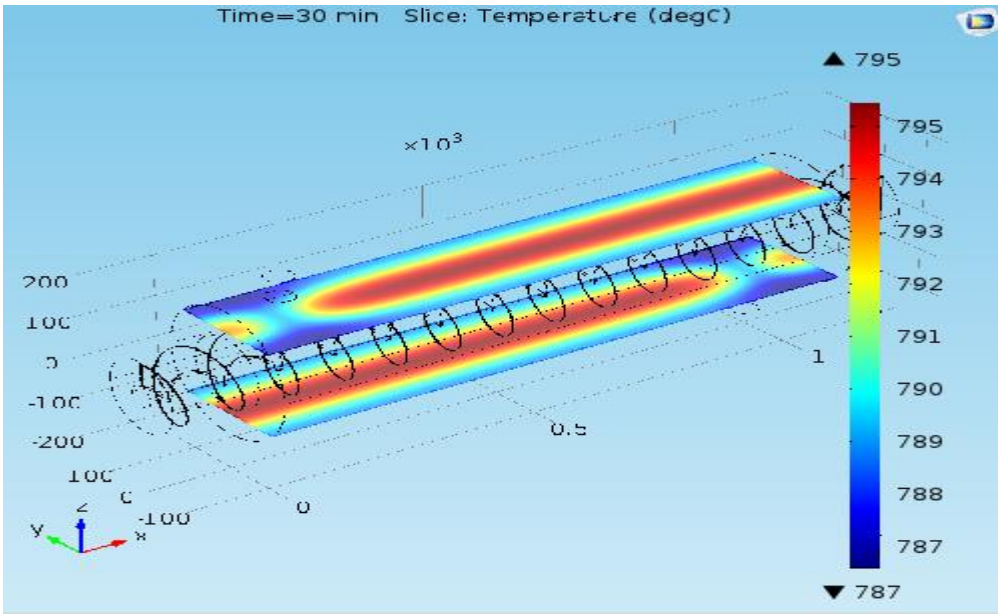

Figure 5.9.Temperature profile 2 planes along xy[b]

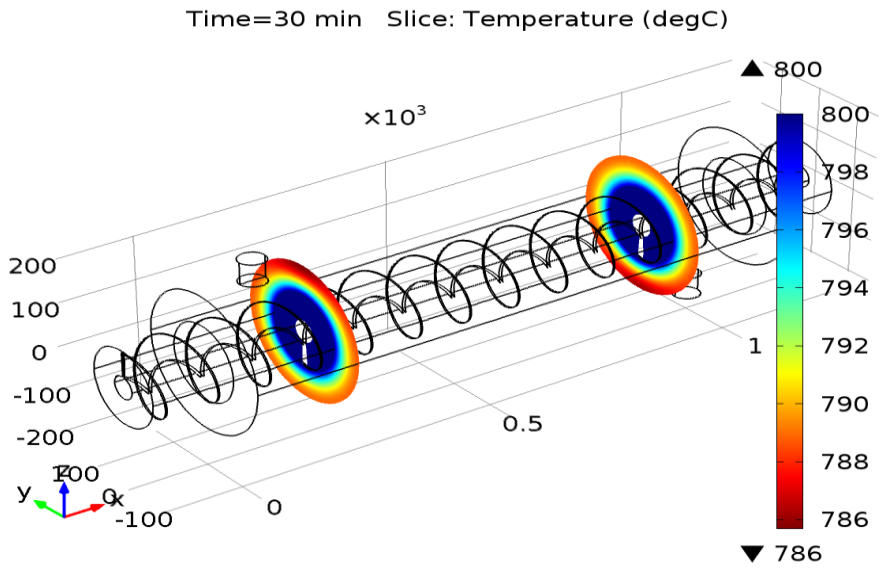

Figure 5.10.Temperature profile planes along yz.

The desired value of temperature 800 ^{o}C was achieved in 30min the pyrolysis process and entire flower waste had converted into biochar *Figure 5.10*.

6. Chapter 6: Experimental investigation

6.1. Introduction

The general objective of this experiment is investigation of continuous biochar production from flower waste. During the experiment, the mass of sample or feed rate inside the feed hopper was 3.58kg with a particle diameter of 6mm and length 14mm. The sample in screw reactor is heated up to $800^{\circ}C$ and the biochar part generated during flower waste pyrolysis were measured.

Objectives of the experiment

a. Biochar production in continuous screw reactor : in doing so the following points was emphasized :
    - To record the temperature along the length of the reactor
    - To test the setup with and without insulation
    - To measure produced biochar

6.2. Experimental set up

In this experiment continuous slow pyrolysis of flower waste was conducted in screw reactor shown in *Figure 6.9* made of stainless steel with an inner diameter 170mm and length 1.4m, an outer reactor of diameter 305mm and 1.1m and screw conveyor of 160mm diameter and 1.5m length. This reactor made of continuous feeding, discharging and heating system. Here are all components of the setup:

a. A feed hopper

The conical feed hopper is used to store and supply feed material (flower waste) to the screw feeder. Its flow theory, opening, flow types and dimensions was discussed under design of components.

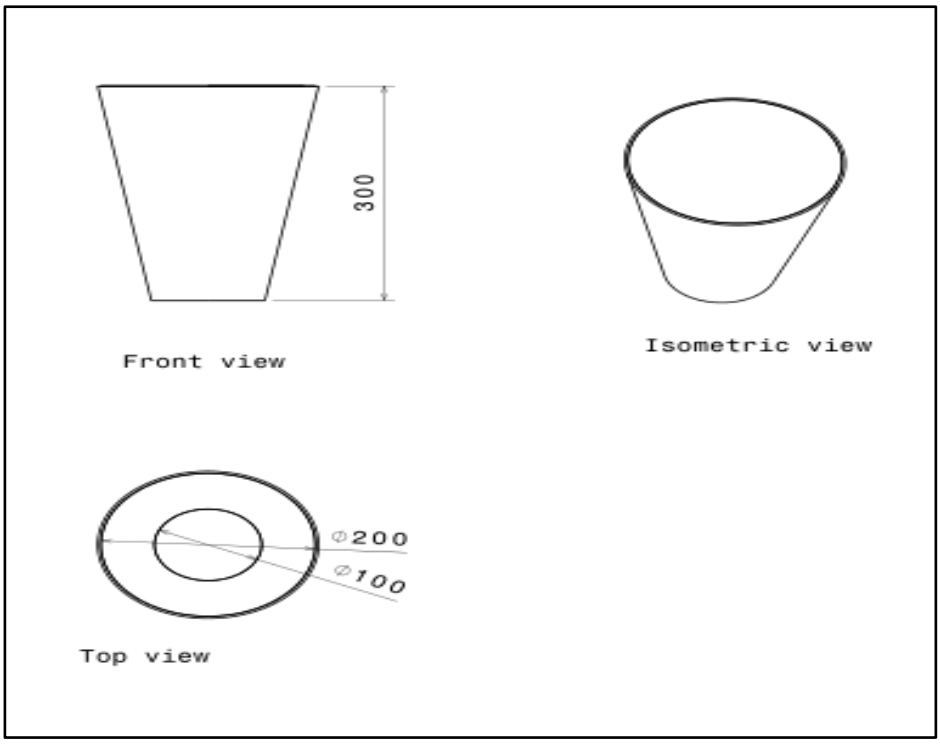

Figure 6.1. Feed hopper

b. Screw feeder

A screw feeder is mounted directly under the opening of a hopper. It is used to introduce material in the screw reactor.

c. Screw reactor

The screw reactors has inner and outer drum with an inner reactor containing the biomass(flower waste) during the process and an outer drum surrounding the inner reactor carrying flue gas. Hot conbustion gases from the afterburner/combustion chamber were introduced to the area between the two reactors as flue gas, while the biomass and pyrolysis gases were treated as an inner stream. The screw reactor was feed continuously at a feed rate of 3.58kg/s.

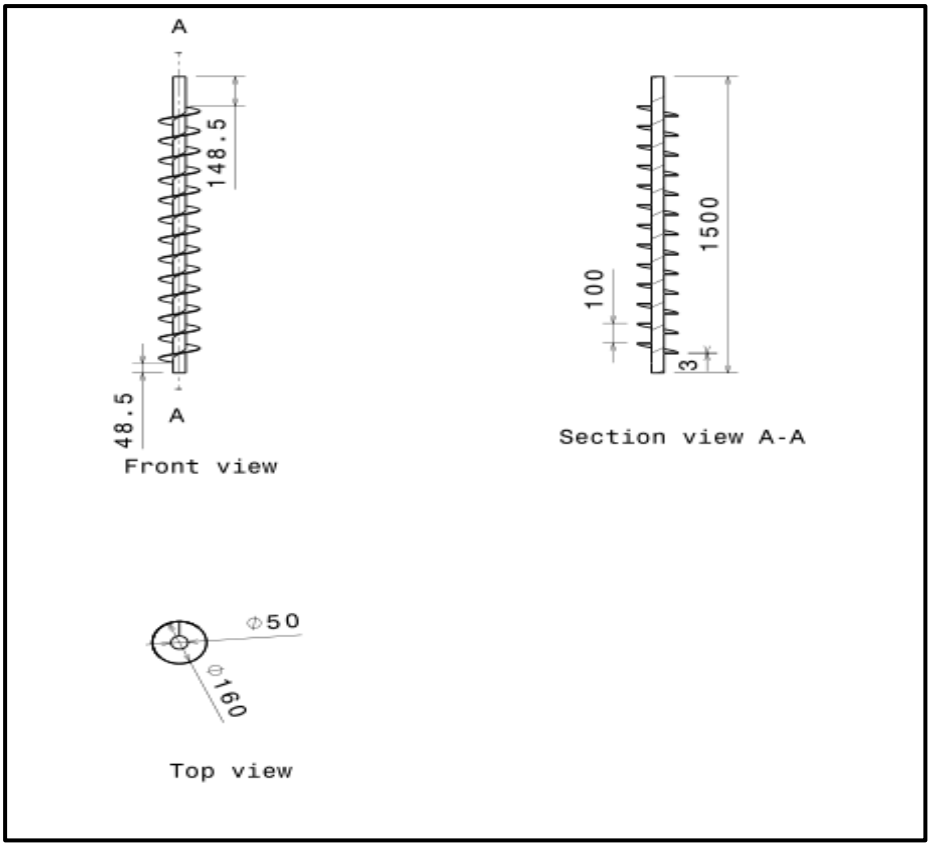

Figure 6.2. Screw conveyor

d. Cyclone

Cyclone separators are used as a collection device in continuous biochar production systems to separate the solid biochar and gasses. It used to remove a biochar.

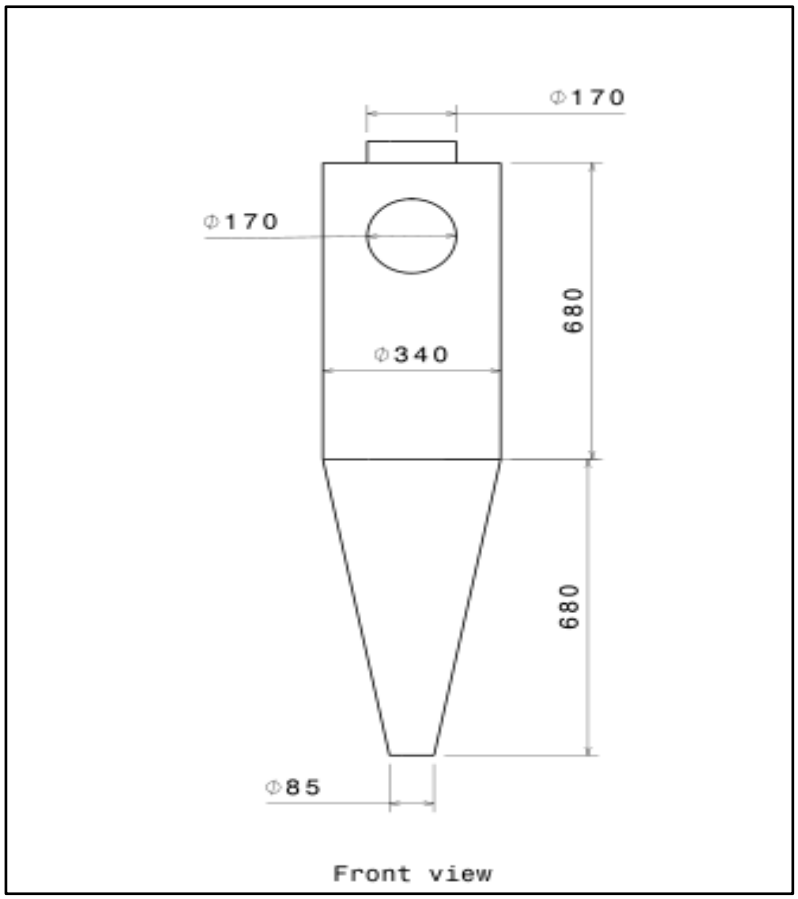

Figure 6.3. Geometry of cyclone

e. After burner

The afterburner unit supplies the outer reactor with warm combustion gases (flue gases) for external heating.

f. Combustion chamber

This unit also supplies the outer reactor with flue gas obtained from burning of wood.

g. Pulleys

Pulleys are used for speed reduction.

h. Belts

The v-belt is mostly used where a great amount of power is to be transmitted, from one pulley to another, when the two pulleys are very near to each other. Since the two pulleys are very near to each other V-belt type has been selected. The advantage of this belt is it can be easily installed and removed, its operation and pulley is quit.

i. Gear box

This gear box is made of spur gear. Spur gears are used to transmit rotary motion between parallel shafts.

j. A motor

For continuous biochar production from flower waste a motor specification is 50/60 RPM, 220V and 4HP i.e. from industrial guide book of motor selection. This selection was done after power requirement has been calculated.

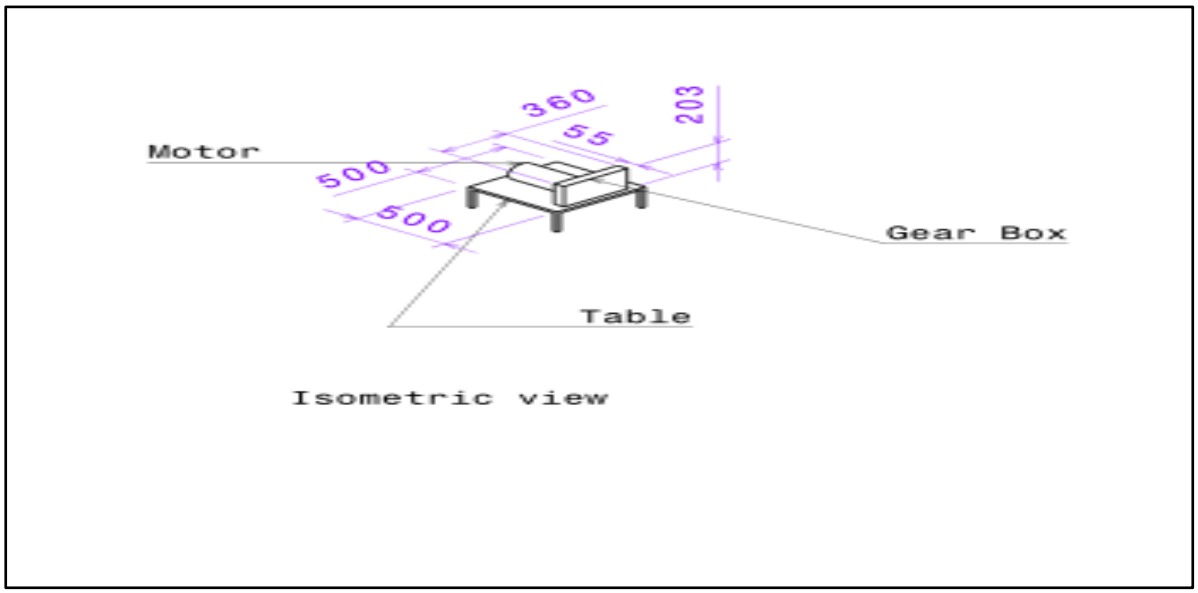

Figure 6.4. Gear box stand table

k. A compressor: Used to transport gases combusted in after burner.

Figure 6.5. Compressor and blower

l. A blower

6.3. Experimental procedures

The inputs was flower waste. Procedures to be followed to produce biochar is as follows:

a. Flower waste collection

One sample is used in this thesis i.e. flower waste. It was collected from flower farming.

Figure 6.6. Wet flower waste

b. Preparation of feed stock

This involves drying the feed and size reduction. First the waste kept under light for six days. Second its leaf part is removed. Later its size is minimized using knife as to make it suitable to crush in jaw crusher machine. The jaw crusher has sieve which has different diameters. A sieve of 6mm was used.

Figure 6.7. Flower waste preparation

c. Flower waste characterization

The characterization of flower waste is followed by series of steps. The first step begins with collecting the flower waste. It is followed by crushing it into pieces using knife to make them at appropriate size. Then these particles were crushed using jaw crusher.

In the second step, the flower waste sample is tested in model EA 1112 Flash CHNS/O analyser which carries gas flow rate of $120^{ml}/_{\min}$, reference flow rate $100^{ml}/_{\min}$, oxygen flow rate $250^{ml}/_{\min}$; furnace temperature of $900^{\circ}C$ and the oven temperature of $75^{\circ}C$ is used to perform the elemental analysis of selected biomass.

The results presented in Table 6.1 and it shows an average elemental analysis value.

In the third step proximate analysis of the flower waste is performed. The analysis is performed using Adiabatic Calorie Meter. The main purpose of using this analysis is to calculate the percentage of moisture, volatiles, fixed carbon and ash present in the sample. The instrument is calibrated using Adiabatic Calorie Meter. After calibration flower waste is tested. The weight of the sample is $500mg$. Elements to be determined i.e. Moisture content, volatile matter, fixed carbon, Ash content, Calorific value and bulk density obtained from hydrocarbon laboratory analysis is presented in *Table 6.2* and it shows the average value.

Finally, the sample is tested in model EA 1112 Flash CHNS/O analyser to find out the ultimate composition of the sample. The ultimate analysis provides the overall percentage of C, H, N, O and S present in the sample. The percentage of on oxygen was evaluated by difference.

Table 6.1. Proximate analysis and calorific value of flower waste

Field No. (code)	Lab No.	Moisture %	Volatile matter %	Fixed Carbon %	Ash %	Calorific Value cal/gm	Bulk density gm/cm^3
GN-001	2187/17	12.47	65.83	16.49	5.21	3712.11	0.52
GN-001	2187/17dup	12.40	65.83%	16.73	5.04	3761.50	0.55
Average		**12.44**	**65.83**	**16.61**	**5.13**	**3736.81**	**0.54**

The proximate analysis on flower waste contains 12.44% moisture, 65.83% volatile matter, 16.61% fixed carbon, and 5.13% ash on dry basis. Volatile matter content is the highest in all

the samples than other components and fixed carbon is the second highest component after volatile matter. Content of the ash is small in all the tests

Table 6.2. Ultimate Analysis

Element	%(sample code GN1)	%(sample code GN1a)	%(sample code GN1b)	**Average**
Carbon	45.21639	41.13663	42.20439	42.85247
Hydrogen	6.013647	5.369477	5.676344	**5.68649**
Nitrogen	0.694307	1.346226	0.972349	**1.0043**
Sulphur	0	0	0	**0**
Oxygen				**50.4567**
Molecular formula	$CH_{1.514}N_{0.0202}O_{0.883}$			

The selected biomass (flower waste) contains 42.85% carbon, 5.69% hydrogen, 1.004% nitrogen, 0% Sulphur and 50.46% oxygen on dry basis. Oxygen content is the highest in all the samples than other components and carbon is the second highest component after oxygen. Content of the Sulphur is negligible in all the samples. The molar composition can be determined by diving each of the mass percentages by atomic of the constituent. For convenient in stoichiometric calculations, the composition is then normalized with respect to carbon.

Element	Weight %	Mole/100g	Mol/mol. C
C	42.85/12	3.57	3.57/3.57=1
H	5.69/1	5.69	5.69/3.57=1.514
N	1.004/14	0.072	0.072/3.57=0.0202
S	0/32	0	0
O	50.46/16	3.154	3.154/3.57= 0.883

The chemical formula that describes the selected biomass is therefore,

$$CH_{1.514}N_{0.0202}O_{0.883}$$

d. Biochar preparation using slow pyrolysis in continuous screw reactor

The continuous biochar production using slow pyrolysis experiments of flower waste with and without insulation are investigated. Parameters that influence the products of the pyrolysis process include pyrolysis temperature, heating rate and residence time [20]. The pyrolysis temperature of this experiments comes from after burner for first test and from combustion chamber for second test. For the first test pyrolysis temperature of the experiments are $200\,^{o}C$ to $540\,^{o}C$ at feeding rate of 3.58kg/min and $350\,^{o}C$ to $700\,^{o}C$ for second test at the same feeding rate in continuous mode. The residence time of the experiments are performed in 1 min to 3min at pyrolysis temperature of $700\,^{o}C$. The biochar produced at 50ºC/min heat rate.

Biochar production procedures

1. Material needed like IR thermometer, moisture analyser, watch

a. Infrared thermometer b. Moisture analyser

c. Watch

2. Feed wood to the afterburner/combustion chamber where pyrolysis temperature is intended to be achieved.
3. Start-up heating wood in combustion chamber and connect compressor/ blower to it.
4. Wait for 20 min until the inner reactor reaches desired or pyrolysis temperature.

5. Feed flower waste of 3.5kg in the feed hopper at time.
6. Screw feeder receives this waste and it introduce to the Screw reactor which have screw conveyor.
7. Since the screw reactor reaches desired temperature value the biochar starts to be produced. Slow pyrolysis process assumes only two products at output: solid biochar and heat.
8. Record the temperature on the length of reactor noted as A, B, C, D and E for all tests.
9. Finally the produced biochar are weighted after the experiment was completed.

Test 1: With flue gas from afterburner/ combustion chamber

Feed the wood in after burner. A compressor is connected to it. Let the fire to start up. When the temperature of reactor reaches pyrolysis temperature the flower waste are fed into pyrolysis reactor continuously.

Combustion chamber is rectangular made of stainless steel having length of 1060mm and width 700mm. When the temperature of reactor reaches pyrolysis temperature the flower waste are fed into screw reactor continuously. The pyrolysis temperature was externally heated by heat generated from combustion at a heating rate of 50^{o}C/min to the desired temperature.

Figure 6.8. Combustion chamber

The temperature distribution from the experiment was recorded as follows:

Table 6.3. Temperature distribution on reactor with flue gas from afterburner/ combustion chamber

Stating time 4:30 Finishing time 6:20	Position	With flue gas from After burner (Temperature in ℃)	With flue gas from combustion chamber (Temperature in ^{o}C)
	A	150	302
	B	205	425
	C	395	530
	D	409	680
	E	520	790
Result: Pyrolysis temperature from combustion chamber was found to be good.			

Biochar which is a product of slow pyrolysis process shown below was obtained.

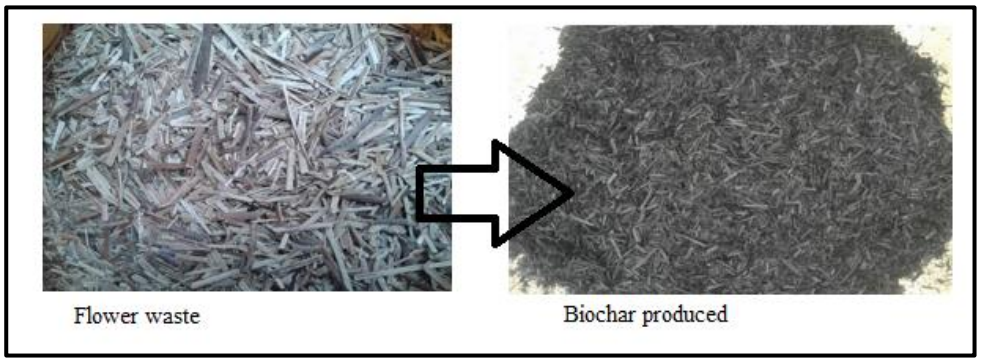

Test 2. With/without insulation

Figure 6.9. With/without insulation

Table 6.4. Temperature distribution on reactor with/without insulation

	Position	Temperature distribution on reactor with insulation (in ℃)	Temperature distribution on reactor without insulation (in ℃)
Stating time 9:30 Finishing time 11:30	A	293	300
	B	400	420
	C	516	525
	D	623	630
	E	773	800
Result: With out insulation much heat goes out.			

7. Chapter 7: Result And Discussion

7.1. Product Yield

The production efficiency of biochar reactor has been calculated based on the amount of flower waste used for biochar production and by weighing the amount of biochar produced after pyrolysis:

$$\text{Yield}(\%) = \frac{\text{Output}}{\text{Input}} * 100\% = \frac{\text{Produced biochar}}{\text{Flower waste}} * 100\% \quad (7.1)$$

Based on the experimental result, 66.7 % of biochar yield has been found by using 30kg flower waste to produce 20kg biochar. The continuous biochar production machine works for eight hours per day. The measured lower heating value of produced biochar is 26.56MJ/kg. The sample for study has been collected from flower farm in Ethiopia which is producing 700kg flower waste on daily basis.

Therefore, depending on the experimental result 470kg of biochar can be produced daily.

7.2. Income generated

A continuous biochar production machine can generate great amount of income by selling the produced biochar. In Ethiopia, the current cost of 50kg of wood charcoal is about 230 Ethiopian birr. The income generated can be evaluated as follows:

$$\text{Income generated} = \frac{\text{Dially Produced biochar}}{\text{50Kg}} * \text{Current cost of wood charcoal} \quad (7.2)$$

Therefore, by selling 470kg of produced biochar 2162 Ethiopian Birr can be generated per day.

7.3. Temperature Profile (Experimentral vs Simulation)

The simulation aims to study the temperature distribution along the length of reactor during flower waste pyrolysis process to produce biochar. This simulation was conducted using an inner screw reactor which has 0.17m diameter and 1.4m length and outer screw reactor 0.305m in diameter and 1.1m in length.

Table 7.1 Temperature Profile

Points on reactor	Experimental result in ^{o}C	Similation result in ^{o}C	Deviation
A	293	786	493
B	400	790	390
C	516	794	278
D	623	798	175
E	773	800	27

The temperature profile of the reactor during pyrolysis was measured with infrared thermometer. The temperature readings were taken at five notes on the reactor: A,B,C,D and E. The temperature at piont A is taken at the inlet of inner reactor, point B is 15cm from outer reactor left side, point C is 15cm from outer reactor right side. Temperature at point D is taken at flue gas exit and point E is taken at biochar exit i.e. inner reactor exit. The experimental temperature was recorded at 5 minute interval.

Taking experimental temperature as accepted value, the percentage error of the experiment and simulation can be calculated as foollows:

$$\text{Percentage error } \% = \frac{Experimantal\ Value - Simulation\ temperature}{Experimantal\ Value} * 100 \qquad (7.3)$$

$$\text{Percentage error} = \frac{773 - 800}{773} * 100 = 3.5\%$$

This percentage result shows how much inacurrete the simulation result is relative to experimental invetigation.

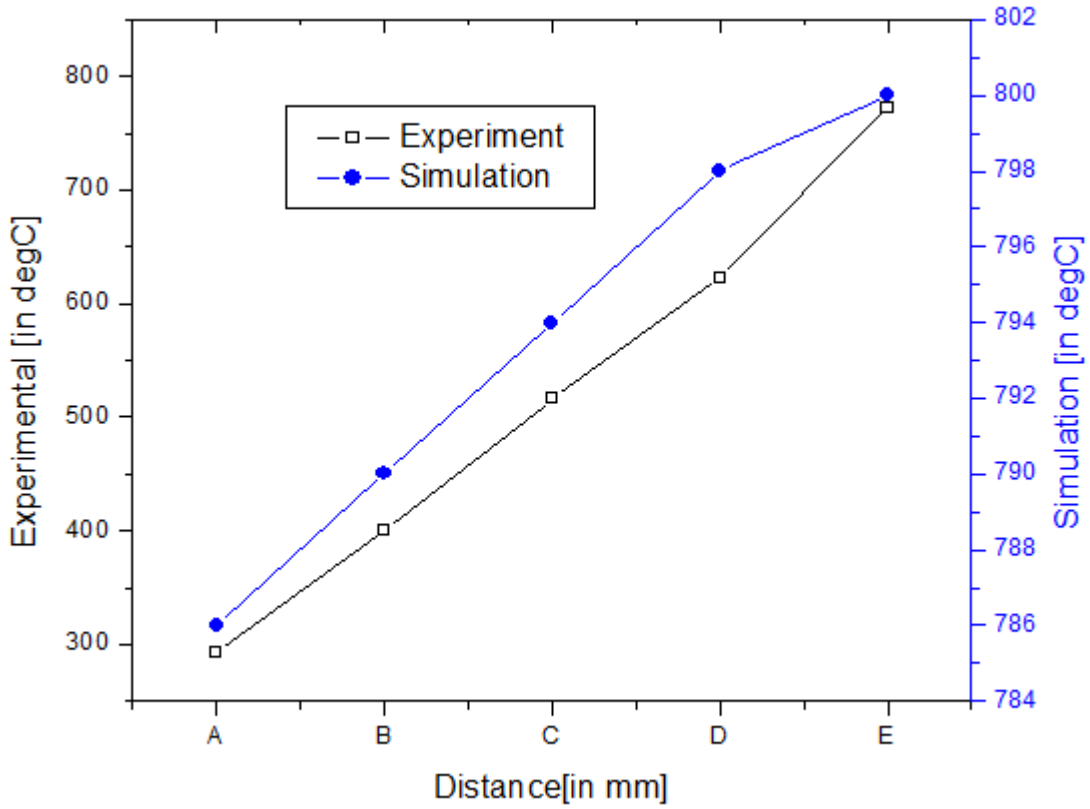

Figure 7.1. Comparison of Experimental and Simulation results

The experimental temperature at A,B,C,D and E were 293, 400,516,623 and 773$^{\circ}C$ respectively and its corresponding simulation temperature were 786,790, 794,798 and 800^{o}C. In the analyzed data the temperature deviation at point E is 27 and maximum at point A having 493 and 278 deviation respectively. Therefore, the obtained temperature promise/camparable with the result indicated in literarture riview of [24] ranging from 277^{o}C to 797^{o}C.

7.4. CO Emission (Traditional Biochar Vs. Biochar Produced)

Biochar (CO)	Charcoal (CO)
1.5 PPM	5 PPM

As indicated in the literature traditional biochar production includes direct combustion of biomass as heat source in the earth mound kiln. Consequently, great amounts of gases and other unburned hydrocarbon products escape as smoke which can cause environmental pollution. This traditional charcoal production is inefficient and leads to deforestation as the most people use woody biomass to produce charcoal in Ethiopia [28]. The emission of carbon monoxide

from traditional biochar production was found to be 5PPM [42]. *CO* emission from traditional charcoal production is maximum because it is produced by open burning of biomass.

Continuous biochar production is a new alternative that can be applied to convert biomass into valuable products. Slow pyrolysis (without oxygen) process is accepted to produce biochar that is efficient and environmentally friendly. The flower waste was indirectly heated by flue gas but burning the wood in an external combustion chamber was used to start the pyrolysis process. The hot carrier gas, (flue gas) which is non-condensable gas, has been produced as one of a byproduct of pyrolysis process were not directly escape to the environment. Implementing indirect heating were method of reducing the emission of CO to the environment. From test result produced biochar has 1.5PPM carbon monoxide. From this experiment since the CO emission produced biochar were less than traditional biochar it insures that the technology is environmentally friendly.

7.5. Time of Biochar production (Continuous vs. Batch)

Figure 7.2. A. Continuous Biochar Production B. Batch type Biochar production [28]

Even though, most mode of biochar production is slow pyrolysis process batch type biochar production takes longer time compared to continuous biochar production. Because feeding the raw materials and discharging the product was performed by using screw conveyor which is driven by a motor, where as in batch type production process, feed and product is discharged manually.

Thus, one of the most benefits of continuous biochar production over batch is that it has no delay time for charging flower waste and discharging the product. Batch production process is one in which a limited amount of product is made that may take a few hours or days.

7.6. Economical Comparison (Continuous Vs. Batch)

Table 7.2. Economic Comparison

Paramters	Continuous	Batch
Daily Proudction	470kg	310.8 kg
Cost	$\frac{470kg}{50kg} * 230 = 2162$ Ethiopian birr	$\frac{310.8kg}{50kg} * 230 = 1429.68$ Ethiopian birr

From the experimental result, the production capacity of continuous biochar production is about 470 kg/day while the batch type biochar production about is 310.8kg/day *Bogale, 2017.* So, the income generated was calculated in aboveTable 7.2 by keeping their selling price and amount to be sold the same. Continuous biochar production generates 2162 Ethiopian birr per day while batch biochar production generates 1429.68 Ethiopian birr per day. The payback period is the time required for the annual invested in an asset to be repaid by the net cash flow generated by asset. The payback period is expressed in years and fractions of years. For continuous biochar production 14,620 birr was invested and the production plant produces positive cash flow of 43,240 birr per month while for batch biochar production 9500 birr was invested and the production plant produces a positive cash flow of 28,593.6 per month keeping working day same per week. For continuous biochar production the payback period is 0.05 month and for batch production plant 0.332 month. From this result investment on continuous biochar production recovers its initial outlay sooner than batch biochar production plant. Therefore it has been found that continuous biochar production is more economical than batch type.

7.7. Senstivity analaysis

7.7.1. Effects of Moisture on Biochar Yield

Numerous process conditions or parameters can be controlled to optimize the biochar production. In this experiment the variation of moisture in flower waste were investigated to evaluate the effect of moisture content on biochar results using moisture content analyser.

Table 7.3. Moisture Contents

Test No.	Moisture content in (%)		Test No.	Moisture content in (%)
1.	13		3.	8
2.	12		4.	10

In screw reactor, the moisture content of the flower waste intensely affects the biochar yield. The pre-processing consists of drying flower waste from 8% to 13% moisture content and grinding it to a final particle size of 6mm. The moisture content of flower waste varies within 8% to 13%. At high moisture content problems such as low bulk density and feeding problems dominates. Mathieu et al., 2013 marks moisture content of 10% to 20% are satisfactory for wood chips. Therefore, this result promise with the work of [10].

7.7.2. Effects of Insulation

Thermal insulation is a broad term which is used to express products that has the ability to reduce heat gain or heat loss by providing a barrier between areas that are significantly in different temperature. The temperature on manufactured prototype has been detected with and without insulation while the experiment was conducted making use of 568 Infrared thermometer. Therefore, as it can be observed from *Table 6.4* providing insulation was used to maintain temperature condition in the slow pyrolysis process, to reduce heat loss or gain, to maintain the effective operation of chemical reaction, to assist in maintaining a product at constant temperature and conserve energy.

7.7.3. Effects of rotational speed

The amount of flower waste to be conveyed influenced by the rotational speed of motors. A motor having 1450 revolution per minute and 3kW has been selected. If the system is directly

connected to this maximum rotational speed the product intended to be obtained become less or no product. Slow pyrolysis process operates at low rotational speed. In order to reduce the rotational speed, speed reduction driving unit like gear box and pulleys were used. In the gear box spur gear were used to transmit rotary motion between parallel shafts. A pinion has 20 teeth per inch while the gear (spur) has 100 teeth per inch so it can reduce the speed of motor by factor of $\frac{1}{5}$ on the first train and $\frac{1}{5}$ on the second train. The output speed of gear box was about $58rpm$. Since smaller revolution per minute needed further reduction of speed was made using pulley of $225mm$ in diameter for larger and $42mm$ for smaller. These pulleys again have capacity to reduce the speed by $\frac{1}{5}$. Therefore, through this the final rotational speed on the shaft or screw conveyor was found to be $11.6rpm$. The obtained result is comparable with the work of [17] , in which rpm decreased the screw speed from maximum rpm to *13.5* and *8.5* rpm, to study the effect of final temperature on the yield. The speed of screw feeder and screw conveyor has to be the same because if the speed of screw feeder is greater than the speed of screw conveyor the material to be conveyed will fill the screw conveyor completely and block the operation so it is fundamental factor for delay time.

The variation of rotation speed has direct influence on the product. To indicate this following test was conducted.

Table 7.4. Effects of rotational speed on the output

Rotation speed in rpm	Flower waste input in kg	Output product(biochar) in kg
1450	30	0
290	30	1.5
58	30	10
11.6	30	20

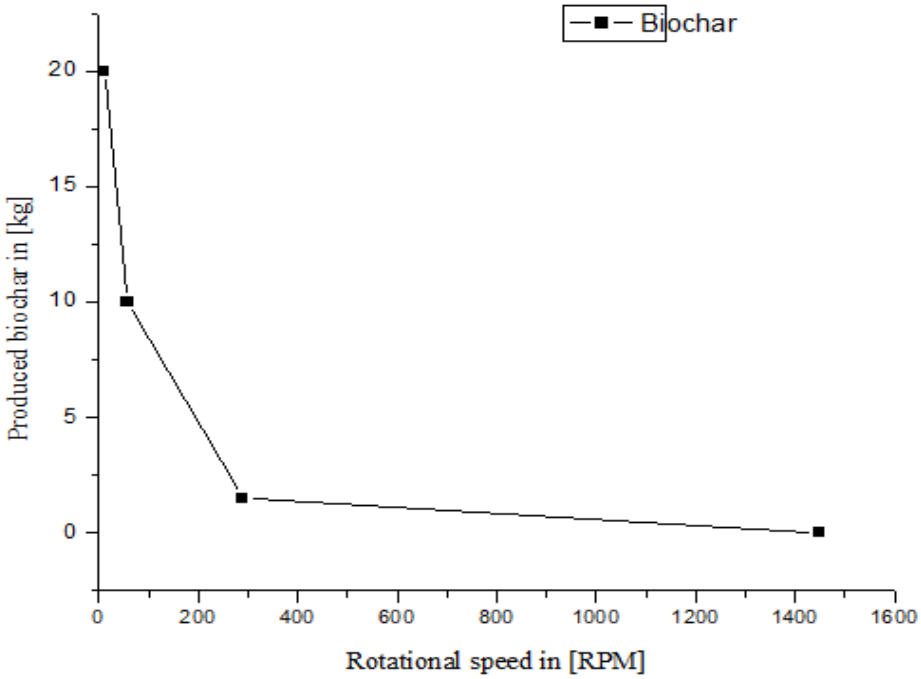

Figure 7.3.Effect of rotational speed

Based on this result as rotational speed increases the produced biochar become less.

8. Chapter 8: Conclusion and recommendation

8.1. Conclusion

In this study Simulation and Experimental investigation of Continuous Biochar production from flower waste was investigated. Flower waste pyrolysis was investigated both by experimental and simulation in continuous mode using screw reactors. The screw reactor was designed for slow pyrolysis in indirect heating mode. This work contributes a new approach for biochar production from flower waste. It is very important in producing biochar that is an attractive technology and excellent for even production of yields. Dealing with this study allows to know the temperature profile on reactors both by experimental and simulation investigation. The produced biochar have potentials in clean source of energy. The temperature profile of the reactor during pyrolysis was measured with infrared thermometer. The temperature readings were taken at five notes on the reactor: A,B,C,D and E. The temperature at piont A is taken at the inlet of inner reactor, point B is 15cm from outer reactor left side, point C is 15cm from outer reactor right side. Temperature at point D is taken at flue gas exit and point E is taken at biochar exit i.e. inner reactor exit. From the experiment, the temperature distribution has been studied in the reactor for the flower waste pyrolysis process. The temperatures at points A, B, C, D and E are: $293^{\circ}C$, $400^{\circ}C$,$516^{\circ}C$,$623^{\circ}C$ and $773^{\circ}C$. This value has 3.5% error with that of the COMSOL simulation. Therefore the model can be used to calculate the temperature inside the screw reactor. Its corresponding simulation temperature were $786^{\circ}C$,$790^{\circ}C$,$794^{\circ}C$,$798^{\circ}C$ and $800^{\circ}C$. In the analyzed data the temperature at point E is minimum and maximum at point A having 27^{o}C and 493^{o}C deviation respectively.Insulation was used to maintain temperature condition in the slow pyrolysis process, to reduce heat loss, to maintain the effective operation of chemical reaction, to assist in maintaining a product at constant temperature and conserve energy. The speed of screw feeder and screw conveyor has to be the same.Continuous biochar production which has a capacity of 470kg per day generates 2147.74 Ethiopian birr per day while batch biochar production generates 1429.68 Ethiopian birr per day. The cooling mechanisms was not included in this thesis work. It has been found that continuous biochar production is more economical than batch. In general an original screw reactor to produce biochar in continuous operating mode was designed, manufactured and tested. This findings support the potential to prepare biochar from flower waste by pyrolysis processes.

8.2. Recommendation

The study presented in this document obviously indicates that biochar can be produced from flower waste. These produced biochar should be bind with good binder material through an extruder machine. To improve the simulation result, multiphase flow heat transfer will be needed. The problem identified were pluging risk and gas leakage.

8.3. Future work

- Characteristics of produced biochar
- Manufacturing a compacting machine to increase density of biochar.
- Cooling mechanisms for produced biochar.
- Addition of reaction kinetics to improve biochar ptoduction composion.

References

[1] Abebe Nigussie, Thomas W. Kuyper and Andreas de Neergaard, "Agricultural waste utilization strategies and demand for urban waste compost: Evidence from smallholder farmers in Ethiopia," *Waste Management,* vol. 44, no. ScienceDirect, pp. 82-93, 31 July 2015.

[2] David G. et al.,2009, "Use of Biochar from the Pyrolysis of Waste Organic Material as a Soil Amendment," Washington State University, Pullman, July 2009.

[3] Xu Zhao, Xiaoyuan Yan, Shenqiang Wang, Guangxi Xing and Yang Zhou, "Effects of the addition of rice-straw-based biochar on leaching and retention of fertilizer N in highly fertilized cropland soils.," *Taylor and Francis,* vol. 59, pp. 771-782, 2013.

[4] M. Gustaffson, "Biochar-the primary by product," Swedish University, Sweden, 2013.

[5] S. Aramideh, "Numerical simulation of biomass fast pyrolysis in fluidized bed and screw reactors," in *Graduate Theses and Dissertations 14093.*, Ames, Iowa, 2014.

[6] Abhishek Sharma, Vishnu Pareek and Dongke Zhang, "Biomass Pyrolysis - A review of Modelling, Process parameters and catalytic studies," *Science Direct,* vol. 50, no. Renewable and Sustainable Energy Reviews, pp. 1090-1091, 2015.

[7] B. Intiative, "Biochar Intiative Group," Biochar Intiative Group, 20 June 2015. [Online]. Available: tinyurl.com/c7ktq. [Accessed 12 10 2017].

[8] Hussein Kisiki Nsamba, Sarah E. Hale, Gerard Cornelissen and Robert Thomas Bachmann, "Sustainable Technologies for Small-Scale Biochar Production," *Sustainable Bioenergy Systems,* vol. 5, pp. 10-31, March 2015 .

[9] NERC, "Biochar slashes bioenergy soil emissions," in *Canadian Biomass Magazine*, USA, 2013.

[10] Mathieu Milhe, Laurent Vande Steene, Michael Haube, Jean-Michael Commandre, Wanignon-Ferdinand Fassinou and Gilles Flamant, "Autothermals and allothermal pyrolysis in a continuous fixed bed reactor," *Journal of Analytical and Applied pyrolysis,* vol. 103, pp. 102-111, 1 April 2013.

[11] Thiago de Paula Protásio, Paulo Fernando Trugilho, Alfredo Napoli,Marcela Gomes da Silva and Allan Motta Couto, "Mass and energy balance of the carbonization of babassu nutshell as affected by temperature," *International Journal of Forestry Research,* vol. 49, pp. 189-196, February 17, 2014.

[12] Muhammad Irfan, Qun Chen, Yan Yue, Renzhong Pang, Qumei Lin, Xiaorong Zhao and Hao Chen, "platform for coproducing bio-oil and biochar. Biofuels Bioprod. Biorefin.," *Review of the pyrolysis,* vol. 211, pp. 457-463, 2009.

[13] Muhammad Irfan, Qun Chen, Yan Yue, Renzhong Pang, Qumei Lin, Xiaorong Zhao and Hao Chen, "Co-production of biochar, bio-oil and syngas from halophyte grass (Achnatherum splendens L.) under three different pyrolysis temperatures," *Bioresource Technology,* vol. 211, p. 457–463, 18 March 2016.

[14] Gao Ningbo, Liu Baoling, Li Aimin and Li Juanjuan, "Continuous pyrolysis of pine sawdust at different pyrolysis temperatures and solid residence time," *Journal of Analytical and Applied Pyrolysis,* vol. 114, no. Science Direct, p. 155–162, 27 May 2015.

[15] Tao Kann, Vladimir Strezov and Tim J. Evans, "Lignocellulosic biomass pyrolysis: A review of product properties and effects of pyrolysis parameters," *Renewable and Sustainable Energy Reviews,* vol. 57(2015), no. Science Direct, pp. 1126-1140, 8 January 2016.

[16] Michael O. Fagbohungbe, Ben M.J. Herbert, Lois Hurst, Hong Li, Shams Q. Usmani and Kirk T. Semple, "Impact of biochar on the anaerobic digestion of citrus peel waste," *Bioresource Technology,* vol. 216, no. Impact of biochar on the anaerobic digestion of citrus peel wast, pp. 142-149, 10 May 2016.

[17] Frederik Ronsse,Ghent University, "Report on biochar production techniques," Ghent University, Groningen, 2013.

[18] D. Klinar, "Universal model of slow pyrolysis technology producing biochar and heat from standard biomass needed for the techno-economic assessment," *Bioresource Technology,* vol. 206, no. Bioresource Technology 206 (2016) 112–120, pp. 112-120, 29 Jan 2016.

[19] Qiang Hu, Haiping Yang, Dingding Yao, Danchen Zhu, Xianhua Wang, Jingai Shao and Hanping Chen, "The densification of biochar: Effect of pyrolysis temperature on the qualities of pellets," *Bioresource Technology,* vol. 200, no. Science Direct, pp. 521-527, 27 October 2015.

[20] Jin Sun Chaa, Sung Hoon Park, Sang-Chul Jung, Changkook Ryu, Jong-Ki Jeon,Min-Chul Shin and Young-Kwon Park, "Production and utilization of biochar: a review," *Journal of Industrial and Engineering Chemistry,* p. 50, 13 6 June 2016.

[21] Liyi Ye, Jingmiao Zhang, Jie Zhao, Zhiming Luo, Song Tu and Yingwu Yin, "Properties of biochar obtained from pyrolysis of bamboo shoot shell," *Journal of Analytical and Applied Pyrolysis,* vol. 114, no. ScienceDirect, pp. 172-178, 28 May 2015.

[22] P. Basu, "Biomass Gasification and Pyrolysis," in *Biomass Gasification and Pyrolysis : Practical and Design and Theory*, Burlington,USA, Elsevier Inc., 2010, p. 22.

[23] J. Erik, Slow pyrolysis in Brista, an evaluation of heat and biochar in Sweden, Sweden: Brista, 2016.

[24] Mohammad I Jahirul , Mohammad G. Rasul , Ashfaque Ahmed Chowdhury and Nanjappa Ashwath, "Biofuels Production through Biomass Pyrolysis- A Technology Review," *Energies*, vol. 5, pp. 4952-5001, 23 November 2012.

[25] Pieters and Ronsse, "Heat and mass transfer modelling of auger reactors," Xiaogang Shi, Ghent, 2015-2016.

[26] Report, "Methods of producing Biochar and Advanced Biofuels in Washington State," Washington State Departement of Ecology, Washington, April 2011.

[27] S. RAYMOND, "Slow Pyrolysis of Maize Stover for Biochar," July, 2013.

[28] W. Bogale, "Preparation of Charcoal Using Flower Waste," *Journal of Power and Energy Engineering*, pp. 1-10, 2017.

[29] Group Taylor and Francis, "Unit Operations of Particulate Solids," in *Theory and Practice*, United State of Americal , New York, CRC Press, 2012, pp. 113-120.

[30] E. Ortega-Rivas, "Flow Theory," in *Unit Operations of Solid Particulate*, London New York, Taylor & Francis Group, 2012, pp. 113-120.

[31] T. Freeman, "Modern Tools for Hopper design," freeman Technology, April 2009.

[32] Shigley's, Design of Mechanical Elements, Spur and Helical Gears, Eighth Edition, North Carolina State University: The McGraw−Hill Companies, 2008.

[33] W. Group, "Screw Conveyor Catalog," WAM Group, Greek, 2006.

[34] Robert, A.W., "The influence of granular vortex motion on the volumetric performance of enclosed screw conveyors," *Powder Technology*, vol. 104, pp. 56-67, 1999.

[35] P. A.J.(Sandy) Marshall, "Commercial Application of Pyrolysis Technology in Agriculture," pp. 14-16, September 30,2013.

[36] Jigar Patel, Sumant Patel and Snehal Patel, "A Review On Numerical and Experimental Study Of Screw Conveyor," *International Journal of Advanced Engineering Research Studies*, vol. E, p. 2249–8974, 2006.

[37] C. Perry, Cyclone separator Design, USA: Moiraw-Hill Puplishing company, 1973.

[38] F. P. Incropera, Heat and Mass transfer, Jefferson City: Macmillan Company, 2011.

[39] Incropera/DeWitt, "One-Dimensional Steady-State Conduction; Radial Systems:Cylinder," in *Fundamentals of Heat and Mass Transfer*, Bergman, Lavine, six edition, pp. 125-128.

[40] Daren E. Daugaard and Robert C. Brown, "Enthalpy for Pyrolysis for Several Types of Biomass," *Energy & Fuels,* vol. 17, no. Received November 5, 2002. Revised Manuscript Received April 23, 2003, pp. 934-939, 2003.

[41] Nadezhda Kazakova, Venko Petkov and Emil Mihailov, "Modelling Of Biomass Pyrolysis," *Journal of Chemical Technology and Metallurgy,* vol. 50, no. 3, pp. 278-281, 25 March 2015.

[42] P. Raman, N.K. Ram and J. Murali, "Improved test method for evaluation of bio-mass cook-stoves," *Energy*, vol. 71, pp. 479 - 495, 23 May 2014.

[43] Rui Shu, Yongjie Wang and Huan Zhong, "Biochar amendment reduced methylmercury accumulation in rice plants," *Journal of Hazardous Materials*, vol. 313, no. ScienceDirect, pp. 1-8, 29 March 2016.

Appendixes

A: mat labcode

```
% Matlab program used to determine the outer radius of the reactor and
%length of outer reactor
% Define the values of Lo
 Lo=0.5:0.015:1.85;
% Evaluate ro
 ro=sqrt(0.0255./Lo);
plot(Lo,ro)
grid minor
xlabel('outer length of reactor in m')
ylabel('outer radius in m')
```

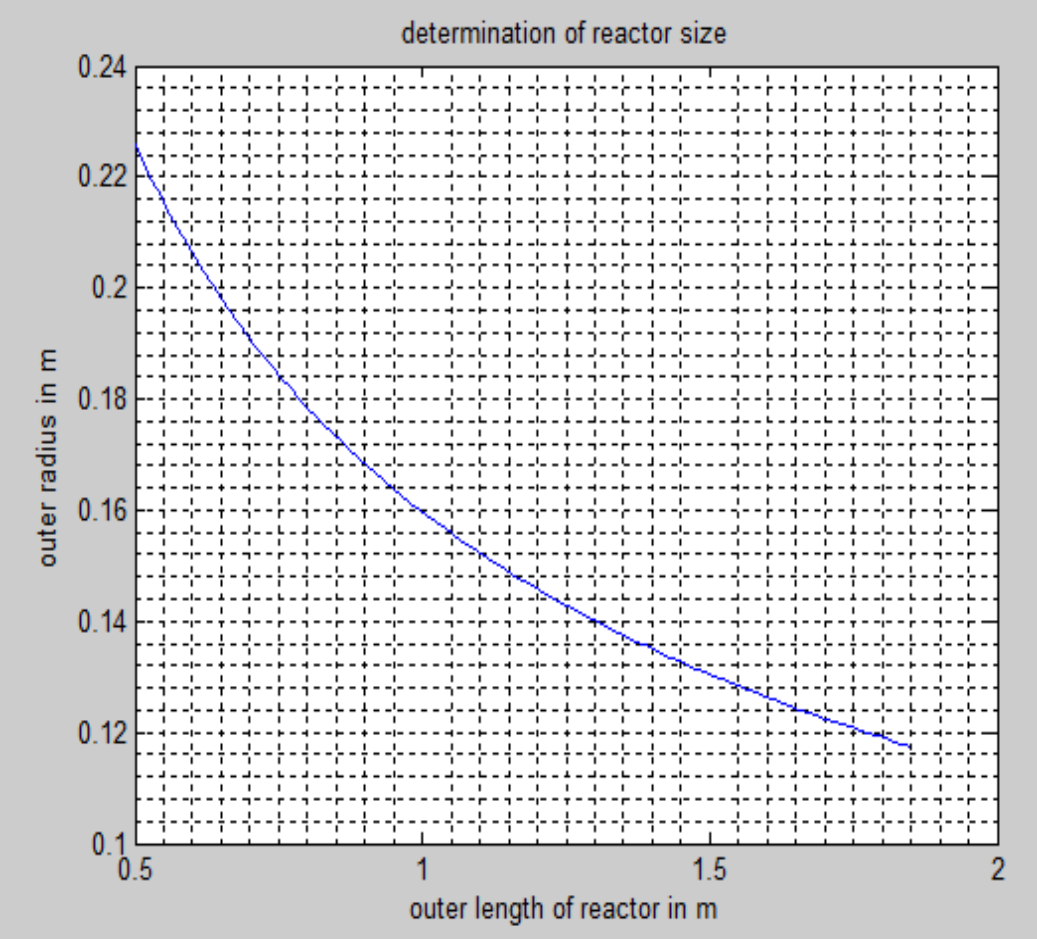

```
% Matlab program used to determine the inner radius of the reactor and
% Define the values of Li
 Li=0.65:0.015:1.85;
% Evaluate ri
 ri=sqrt(0.008963./Li);
plot(Li,ri)
grid minor
xlabel('inner length of reactor in m')
ylabel('inner radius in m')
title('determination of reactor size')
```

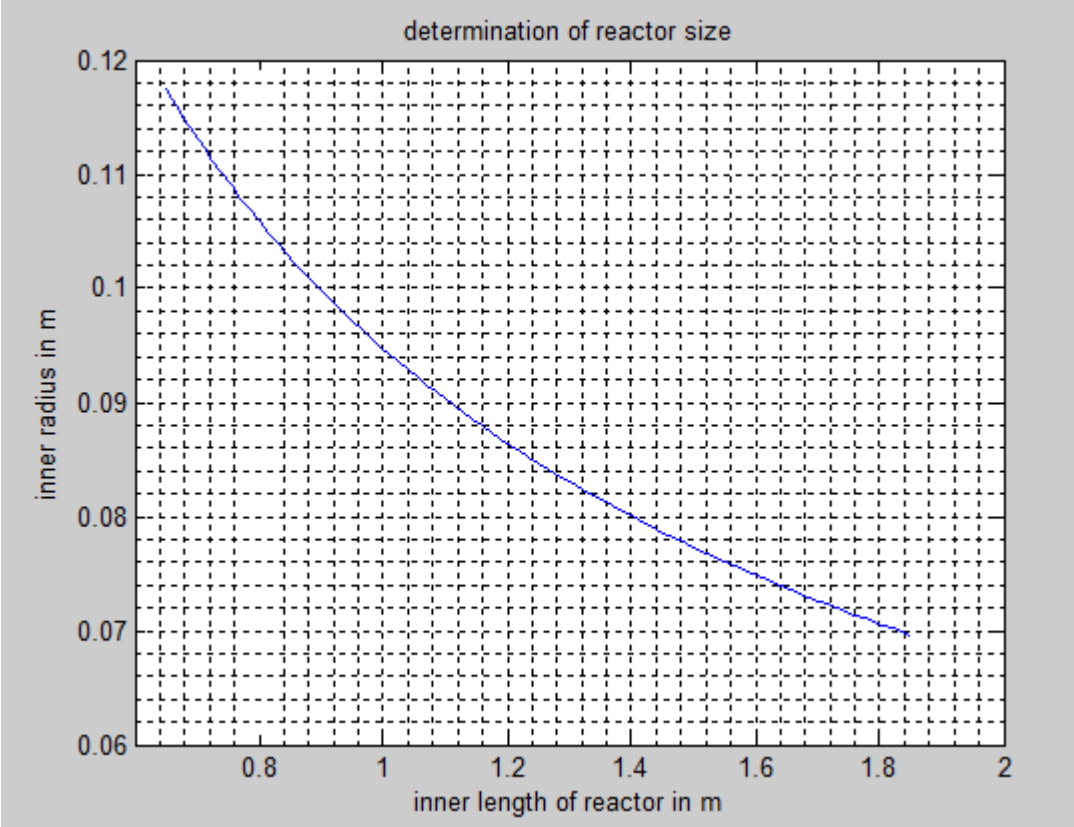

B. Calculation for design of components

B.1. Conical hopper

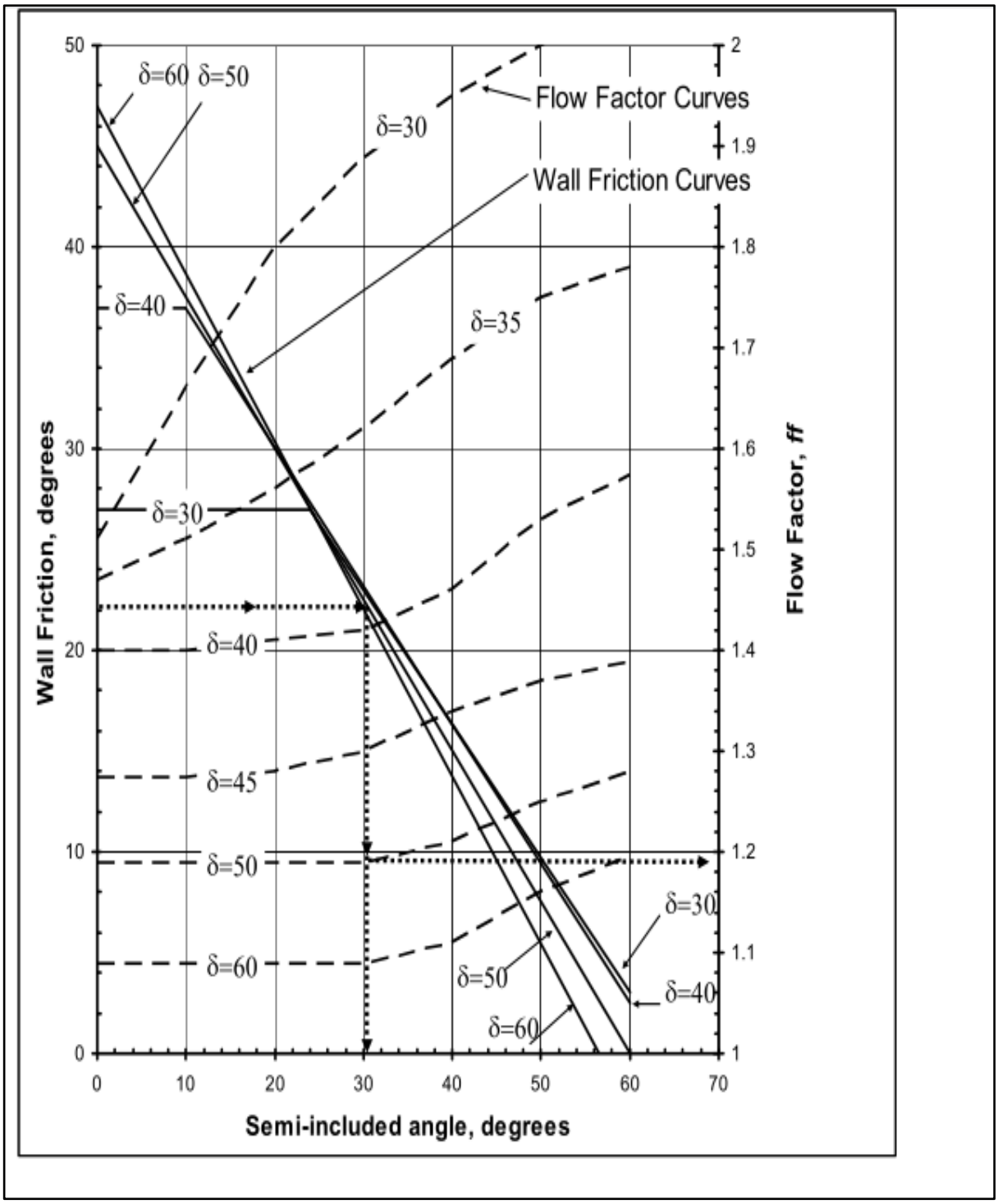

Parameters for hopper design

$$H(\theta) = 2 + \frac{\theta}{60} = 2 + \frac{22}{60} = 2.366 \cong 2.4$$

$$B_{\min} = \frac{H(\theta)\bar{\sigma}_1}{\rho_b g} = \frac{300^{N}/_{m^2} * 2.4}{540^{kg}/_{m^3} * 9.81^{m}/_{s^2}} = 100mm$$

The average tangential velocity is

$$V_a = \sqrt{\frac{Bg}{2(m_c+1)\tan(\theta)} * \left[1 - \frac{ff}{ff_a}\right]}$$ For conical hoppers $m_c = 1$ and $\frac{ff}{ff_a}$ approaches to zero

$$V_a = \sqrt{\frac{Bg}{2(m_c+1)\tan(\theta)}} = \frac{0.1m * 9.81 m/s^2}{2(1+1)\tan(19^\circ)} = 0.844 m/s$$

The mass flow rate m_o may be calculated as

$$m_o = \rho_b B^{(1+m_c)} L^{(1-m_c)} \left(\frac{\pi}{4}\right)^{m_c} V_a = 540 kg/m^3 * 0.1^{(1+1)} m * 0.5^{(1-1)} m * \left(\frac{\pi}{4}\right)^1 * 0.844 m/s = 3.58 kg/s$$

Also it can be calculated using Johnson Equation as follows

$$m_o = \rho_b A \sqrt{\frac{Bg}{2(1+m)\tan(\theta)}} = 540 kg/m^3 * \left(\frac{\pi}{4}\right)(0.1m)^2 \sqrt{\frac{0.1m * 9.81 m/s^2}{2(1+1)\tan(19^\circ)}} = 3.58 kg/s$$

The discharge mass flow rate of the hopper

Semi-included angle is 19°

$$\tan(\theta) = \left(\frac{B}{2}\right) L_2 \Rightarrow L_2 = \left(\frac{2\tan(19^\circ)}{10cm}\right) = 0.688mm$$

$$h_{new} = L_2 + H(\theta) \Rightarrow h = 0.688mm + 23.66mm = 24.35mm$$

$$\tan(\theta) = \left(\frac{r}{h}\right) = \left(\frac{r}{2.434}\right) \Rightarrow r = 2.434\tan(19^\circ) = 0.839mm$$

$$D = 2r = 2 * 100mm = 200mm$$

$$h \succ 1.5D \Rightarrow h = 1.5 * D = 1.5 * 200mm = 300mm$$

The slant height L can be evaluated from Pythagoras theorem as follows:

$$L^2 = h^2 + (R-r)^2 \Rightarrow L = \sqrt{h^2 + (R-r)^2} = \sqrt{(300mm)^2 + (100-50)^2 mm^2} = 304.14mm$$

$$L_1 = \frac{RL}{R-r} = \frac{100mm * 304.14mm}{50mm} = 608.28mm$$

$$L_2 = L_1 - L = 608.28mm - 304.14mm = 304.14mm$$

The length of arc circumference of the bases:

$S_1 = 2\pi R = 2*3.14*100mm = 628mm$ And $S_2 = 2\pi r = 2*3.14*50mm = 314mm$

B.2. Gear box

A. 100 is teeth number of gear and 180mm is diameter of the gear. Diameteral pitch is calculated as follows

$$P = {}^{N}\!/_{d} = {}^{100}\!/_{180} = 0.56/mm$$

B. Module

$$m = {}^{d}\!/_{N} = {}^{180}\!/_{100} mm = 1.8mm$$

C. The velocity ratio $$VR = \left(\frac{\omega_p}{\omega_g}\right) = \left(\frac{d_g}{d_p}\right) = \left(\frac{N_g}{N_p}\right) = \frac{100}{24} = 5$$

B. 3. Power requirements

From shaft design $T_s = 2470.898Nm$ and $n = 11.6rpm$

$$power = \dot{W} = \frac{T_s\omega}{1000} = \frac{T_s n}{9549} = \frac{2470.89Nm*11.6rpm}{9549} = 3kW$$

B. 4. V-belt design calculations

1. Power to be transmitted = $3kW$ is the power of a motor.
2. Input speed $(N_1) = 1450rpm$ from motor selection
3. Output speed $(N_2) = 11.6rpm$(reduced by 0.8% of input speed)
4. Outer diameter of larger pulley $(D_2) = 225mm$
5. The angle (2β) for V-belt is usually from 30° to 40°. For my design its value set to be 36°.
6. Balata belt material is used.
7. Density of belt material (Balata) = $(\rho_{bm}) = 1100 {}^{Kg}\!/_{m^3}$
8. Allowable stress for belt material $(\sigma_{all,belt}) = 4MPa$
9. Coefficient of friction between belt and pulley $(\mu) = 0.32$
10. Cross sectional area of the belt $(A) = 750mm^2$

Therefore the maximum centre distance

$$X_{\max} = 2(D + d) = 2(225 + 42) = 534mm$$

From speed ratio $= \frac{N_1}{N_2} = \frac{D_2}{D_1} \Rightarrow D_1 = \frac{N_2 D_2}{N_1} = \frac{11.6 * 225}{1450} = 18 \cong 20mm$

Coefficient of friction from Figure 4.11 $\sin\alpha = \frac{D_2 - D_1}{2X}$

$\sin\alpha = \frac{D_2 - D_1}{2X} = \frac{225 - 42}{2 * 300} = 0.305 \Rightarrow \alpha = 17.76^\circ$

Now the angle of contact on small pulley: $\theta_1 = 180^\circ - 2\alpha$

$\theta_1 = 180^\circ - 2\alpha = 144.48^\circ$

$\theta_1 = 144.48^\circ * \frac{\pi}{180^\circ} = 2.52rad$

Angle of contact on larger pulley (θ_2): $\theta_2 = 180^\circ + 2\alpha$

$\theta_2 = 180^\circ + 2\alpha = 215.52^\circ$

$\theta_2 = 215.52^\circ * \frac{\pi}{180^\circ} = 3.76rad$

When pulleys have different angles of contact (θ), then the design will refer to a pulley for which the value of $(\mu * \theta)$ is small. μ Coefficient of friction for belt material and balata material has 0.32 value.

$(\mu * \theta) = \mu * \theta_1 \cos ec\beta$

$(\mu * \theta) = \mu * \theta_1 \cos ec\beta = 0.32 * 2.52rad \cos ec18^\circ = 2.61$

For larger pulley

$(\mu * \theta) = \mu * \theta_2 \cos ec\beta = 0.32 * 3.76rad \cos ec18^\circ = 3.89$

Since $(\mu * \theta)$ is small for smaller pulley, therefore the design is based on smaller pulley.

Belt speed: $(V_b) = \frac{\pi * D * N_1}{60}$

$(V_b) = \frac{\pi * D * N_1}{60} = \frac{\pi * 0.042m * 1450}{60} = 1.015 m/s$

Mass of the belt per meter length will be

$$\text{Mass}(m_b) = Area(A) * centerdistance(X) * density(\rho_{bm})$$

Cross sectional area of the belt assumed $A = 750*10^{-6} m^2$

$$m_b = 750*10^{-6} m^2 * 0.3m * 1100 \, {Kg}/{m^3} = 0.2475 \, {Kg}/{m}$$

Now centrifugal tension

$$T_c = m_b V_b^{\,2} = 0.2475 \, {Kg}/{m} * \left(1.015 \, {m}/{s}\right)^2 = 2.55N$$

The maximum tension in belt; $T = \sigma * A$

$$T = \sigma * A = 4 \, {N}/{mm^2} * 750mm^2 = 3000N$$

Total tension in belt; $T = T_1 + T_c$

$$T = T_1 + T_c \Rightarrow T_1 = T - T_c = (3000 - 2.55)N = 2997.45N$$

According to Hannah and Stephens (1970), the power transmitted by belt is given by

$P = (T_1 - T_2)V_b$ But $V_b = \dfrac{(\pi DN)}{60}$ and also $2.3\log\left(\dfrac{T_1}{T_2}\right) = \mu * \theta \, \text{cosec}\beta$

β Groove semi-angle; θ is angle of lab

We know that

$$2.3\log\left(\frac{T_1}{T_2}\right) = \mu * \theta_1 \, \text{cosec}\beta = 2.61$$

$$\log\left(\frac{T_1}{T_2}\right) = \frac{2.61}{2.3} = 1.135 \Rightarrow T_2 = \frac{T_1}{anti\log(1.135)} = \frac{2997.45}{3.11} = 963.81N$$

Power transmitted per belt

$$P = (T_1 - T_2) * V_b = (2997.45 - 963.81)N * 1.015 \, {m}/{s} = 2064.14W = 2.0641kW$$

The number of belts used is 2 i.e. $n = 2$

B.5. Design of Shaft

Torque transmitted by driven or the shaft from V-belt design

$$T_t = \frac{60 * p}{2\pi * N_2} = \frac{60 * 3000W}{2 * \pi * 11.6rpm} = 2470.898Nm$$

$N_2 = 11.6rpm, T_1 = 2997.45N$, $T_2 = 963.81N$ and $R_2 = 0.1125m$ from V-belt design

Torque transmitted by driven or the shaft from V-belt design

$$T_t = \frac{60 * p}{2\pi * N_2} = \frac{60 * 3000W}{2 * \pi * 11.6rpm} = 2470.898Nm$$

Weight of flight is $W_f = {}^{50N}\!/_{1400mm} = 0.036\,{}^{N}\!/_{mm}$ and the weight of the pulley is

$W_p = 40N$

Vertical load on the pulley by belt and pulley (W_d) at d is from *Figure 4.12*

$$W_{df} = T_1 + T_2 + pulley(40N) = 2997.45 + 963.81 + 40 = 4001N$$

From equilibrium equation;

$$\sum F_y = 0$$

$$R_a - W_b + R_c - W_p + R_d = 0$$

$$R_a + R_c + R_d = 40.0252N$$

$R_a = 21.53N$, $R_c = 41.94N$ and $R_e = 26.94N$

Bending moment at point A and E is zero. i.e. $M_A = M_E = 0$ *Figure 4.12*.

Bending moment at b is $M_b = 6125.66Nmm$ at c $M_c = 5143.03Nmm$

Therefore, maximum bending moment is at point b and is $M = M_b = 6125.66Nmm$

According to maximum shear stress theory, equivalent twisting moment is given as;

$$T_e = \sqrt{(M)^2 + (T)^2} = \sqrt{(6125.66)^2 + (24070898)^2} = 2407088981Nmm$$

Now the equivalent twisting moment:

$$T_e = \frac{\pi}{16} * \tau * {d_s}^3 \Leftrightarrow {d_s}^3 = \frac{16T_e}{\pi(\tau)} = \frac{16 * 2407088981}{3.14 * 42\,{}^{N}\!/_{mm^2}} \Leftrightarrow d_s = 47.94mm$$

From standard shaft diameter the diameter of the shaft is selected to be $d_s = 50mm$

C.5. Design of pulley

Dimensions of pulleys

iii. The diameter of the pulley D may be obtained either from velocity ratio consideration or centrifugal stress consideration.

$$\sigma_t = \rho V^2{}_b = 2700^{Kg}\!/_{m^3} * (1.015^{m}\!/_{s})^2 = 2781.6Nm = 2.781kPa$$

iv. From width of the belt, the width of pulley or face width of the pulley (B) is :

The dimension of standard V-grooved pulley is selected from which we find that for D type belt.

$W = 20mm, d = 21mm, a = 8mm, c = 14mm, f = 18$ And $e = 30$

Now the face width of the pulley

$$B_p = (n-1)e + 2f = (2-1)*30 + 2*18 = 66mm$$

The following are the width of V-belt of aluminium pulleys in mm:
16,20,25,32,40,50,63,71,80,90,100,112,125,140,160,180,200,224,250,315,355,400,450,560 and 630.

So from standard width of the larger pulley is $(B_p) = 200$mm

v. The thickness of the pulley rim(t) varies:

$\frac{d}{300} + 2mm$ To $\frac{d}{200} + 3mm$ for single belt and $\frac{d}{200} + 6mm$ for double belt. The diameter of the pulley is $d = 225mm$

So thickness of the pulley

$\frac{205}{300} + 2mm$ To $\frac{205}{300} + 6mm \Rightarrow$ 2.683mm to 6.683mm

Since, single belt is used its thickness is 7mm.

B.6. Bearing selection

Using bore diameter from a text book of machine design by Khurmi and Gupta the following data is selected.

Outside diameter for bore diameter of d=25mm and d=30mm is 52mm and 62mm consecutively.

Bearing width for bore diameter of d=25mm and d=30mm is 15mm and 16mm consecutively.

Basic static (C_0) and dynamic (C) capacities of various types of radial ball bearings single row deep groove ball bearing using diameter of shaft (bore diameter of 25mm and 30mm) that have basic capacities of static $(C_o)=10kN$ and dynamic $(C)=19.5kN$ for bore diameter 30mm and $(C_o)=6.95kN$, $(C)=14kN$ for bore diameter of 25mm.

4. From shaft design we have a radial load $(W_R)=40N$
5. From belt design the speed $(N)=11.6rpm$
6. $K=3$, for ball bearing.

Using $(W)=W_R=40N$

Now the approximate rating (or service) life of a single row deep groove ball bearing is given as;

$$L=\left(\frac{C}{W}\right)^K *10^6 \text{ Revolution}$$

$$L=\left(\frac{C}{W}\right)^K *10^6=\left(\frac{19500}{40}\right)*10^6=487.5*10^6 \text{ Revolutions}$$

From $L=60N*L_H$ the life working hours: $L_H=\frac{L}{60N}=\frac{487.5*10^6}{60*11.6}=700431.035$ hours.

B.7. Screw feeder

$$A=\frac{1}{8}\left[\left(1-2\frac{0.003}{0.16}\right)^2-\left(\frac{0.05}{0.003}\right)^2\right]\left[\left(\frac{0.1}{0.16}-\frac{0.003}{0.16}\right)\right]=20.98$$

$$Q_t=A\omega D^3=20.98*0.2\,{}^{rad}\!/_{s}*0.16^3={}^{0.0172m^3}\!/_{s}$$

The actual volumetric throughput (material) of the screw conveyor Q_{act} is less than the theoretical and is quantified by volumetric efficiency and is given by: $\eta_v = \frac{Q_{act}}{Q_t}$

$$Q_{act} = Q_t \eta_v = 0.0172 m^3/s * 0.90 = 0.0155 m^3/s$$

B.8. Design of reactors

The outer volume of the cylindrical reactor would be as follows

$$V_o = \pi L_o r_o^{\,2} \Rightarrow \pi L_o r_o^{\,2} = 0.080 m^3$$

$L_o r_o^{\,2} = 0.0255$ And solving for one variable

$$r_o^{\,2} = 0.0255\left(\frac{1}{L_o}\right)$$

The inner volume of a cylindrical reactor would be as follows

$$V_i = \pi L_i r_i^{\,2} \Rightarrow \pi L_i r_i^{\,2} = 0.0281344 m^3$$

$$r_i^{\,2} = 0.008963\left(\frac{1}{L_i}\right)$$

Therefore, from the Mat lab result the maximum outer length of the reactor selected is 1.1m and the inner reactor length is 1.4m.

$$r_o^{\,2} = 0.0255\left(\frac{1}{L_o}\right) \Rightarrow r_o^{\,2} = 0.0255\left(\frac{1}{1.1}\right) = 0.0232 \Rightarrow r_o = 0.152 m \text{ And}$$

$$r_i^{\,2} = 0.008963\left(\frac{1}{L_i}\right) \Rightarrow r_i^{\,2} = 0.008963\left(\frac{1}{1.4}\right) = 0.006402 \Rightarrow r_i = 0.085 m$$

$$D_o = 2r_o = 2 * 0.152 m = 0.304511 m$$

$$D_i = 2r_i = 2 * 0.085 m = 0.17 m$$

The maximum volume of area for the gas is determined by the difference between the outer reactor volume and the inner reactor volume as follows.

$$V_{\max,gas} = \pi R^2{}_o L_o - \pi R_i{}^2 L_i = \pi(0.152m)^2 * 1.1m - \pi(0.085m)^2 * 1.4m = 0.048m^3$$

The maximum mass of flower waste occupied in the inner reactor is

$$M_{flower.Wast} = V_i * \rho_{dry} = 0.0281m^3 * 540 {kg}/{m^3} = 15.174kg$$

B. 9. Screw conveyor

For screw conveyors with screws having standard pitch helical flights the conveyor speed may be calculated by the formula.

$$V_{cs} = \frac{P_s n}{60} = \frac{0.1m * 11.6rpm}{60} = 0.0193 {m}/{s}$$

The effect of conveyor diameter to corresponding speeds is given by non-dimensional specific speed number by Revolutions per minute of screw:

$$N_s = \frac{\omega^2 R_o}{g} = \frac{N^2 D_o}{1789} = \frac{(11.6rpm)^2 * 0.305}{1789} = 0.023$$

The volumetric through put of screw conveyor is given by equation (4.42) similar to screw feeder.

Where $Q_t = A\omega D^3$

$$A = \frac{1}{8}\left[\left(1 - 2\frac{0.003}{0.16}\right)^2 - \left(\frac{0.05}{0.003}\right)^2\right]\left[\left(\frac{0.1}{0.16} - \frac{0.003}{0.16}\right)\right] = 20.98$$

Q_t= maximum theoretical volumetric throughput with conveyor running 100% full and the bulk material moving axially without rotation.

$$Q_t = 20.98 * 0.2 rad/s * (0.16m)^3 = 0.0172 m^3/s$$

The mass throughput- the influence of bulk density (ρ): the mass throughput of screw conveyor in kg/s is given by :

$$Q_m = \rho Q = Q_t \rho \eta_v$$

$$Q_m = 0.001242 m^3/s * 540 kg/m^3 * 0.75 = 0.05 kg/s$$

The flight height of the screw conveyor is

$$h = \frac{D_o - D_i}{2} = \frac{0.305 - 0.17}{2} = 0.0675m$$

B.10. cyclone

The inlet (H_c) of the cyclone is equal to the diameter of the internal reactor and is $H_c = 170mm$

Therefore the rest dimension of the cyclone will be determined as follows

$$H_c = \frac{D_c}{2} \Rightarrow D_c = 2H_c = 2*170mm = 340mm$$

Therefore diameter of cylindrical part and upper diameter of the cone of the cyclone. The vapours and gas exit diameter is calculated as follows

$$D_e = \frac{D_c}{2} = \frac{340mm}{2} = 170mm$$

The length of the cylindrical part

$$L_c = 1.25D_c = 1.25*340mm = 425mm$$

The depth of pipe

$$S_c = \frac{D_c}{8} = \frac{340mm}{8} = 42.5mm$$

The length of the hopper part

$$Z_c = 1.25D_c = 1.25*340mm = 425mm$$

The exit diameter of the Biochar

$$J_c = \frac{D_c}{4} = \frac{340mm}{4} = 85mm$$

The overall length of the cyclone is

$$L_{overalllength} = L_c + Z_c = 425mm + 425mm = 850mm$$

C. Proximate Analysis of flower waste lab test result

Geological Survey of Ethiopia
Geochemical Laboratory Directorate
Hydrocarbon Laboratory analysis report format:Form GD0006
File ID 2187/17pvt
Originator Geremew Nugusse.
Sample type:Flower Waste.
Number of Samples:1
Preparation required :60mesh
Element to be determined: (Moistur,Volatile matter, Fixed carbon and Ash) and Calorie.
Method of analysis:Proximate Analysis and Adiabatic Calorie Meter.

customer type:pvt
Date submitted 05/11/2009(07/12/2017)
Date completed 12/11/2009(07/20/2017)

Field No.	*Lab No.*	*Moisture %*	*Volatile Matter %*	*Fixedcarbon %*	*Ash %*	*Calorific Value cal/gm*	Bulck Dencity gm/cm^3
GN-001	*2187/17*	12.47	65.83	16.49	5.21	3712.11	0.52
GN-001	*2187/17Dup*	*12.40*	*65.83*	*16.73*	*5.04*	3761.50	0.55

Geological Survey of Ethiopia Central Geological Lab-Tratory

ANALYSTS:
Alemnesh
Haimanot Bayeh

CHECKED BY:
Alemnesh Abate

QUALITY CONTROL:
Awash Yerga

DATE REPORTED
13/11/2009(07/21/2017)

Page 1 of 1